5th Lecture:

Spintronics, Design, Magnetization Control I
---- Focusing to designs of magnetic anisotropy ---

Tatsuki Oda

Institute of Science and Engineering, Kanazawa University

Spintronics Design Course in CMD-WS47

2th September, 2025

(90 minutes: 10:30～12:10)

第５講義：スピントロニクス・デザイン・磁化制御Ｉ (磁気異方性のデザイン)
：90分　小田竜樹（金沢大理工）

検索：

計算ナノ科学

Email: oda@cphys.s.kanazawa-u.ac.jp
http://cphys.s.kanazawa-u.ac.jp/~oda-web/index.html

Contents in 5th lecture

(5-1) Magnetic moment: spin, orbital

(5-2) Zeeman energy, Spin-orbit interaction

(5-3) Interaction between magnetic carriers: magnetic dipole interaction

(5-4) Control of magnetization

(5-5) Magnetic anisotropy energy: magnet shape, electron orbital

(5-6) Summary of density functional approach on magnetic anisotropy energy

(5-7) Magnetic anisotropy, Voltage-controlled magnetic anisotropy

(5-8) Magnetic anisotropy of thin film

(5-9) Electric polarization revers effects on the interface of magnetic anisotropy

(5-10) Rashba parameter in the magnetic interface

(5-1) Magnetic moment: spin, orbital

Origin of magnetism Most of magnetism in materials comes from the contained electrons.

main orgin of magnetism

electron : spin angular momentum

like being supposed to rotate on its own axis

$$\frac{1}{2}\hbar$$

two different spin states
in an electron,
different energy levels
for external magnetic field

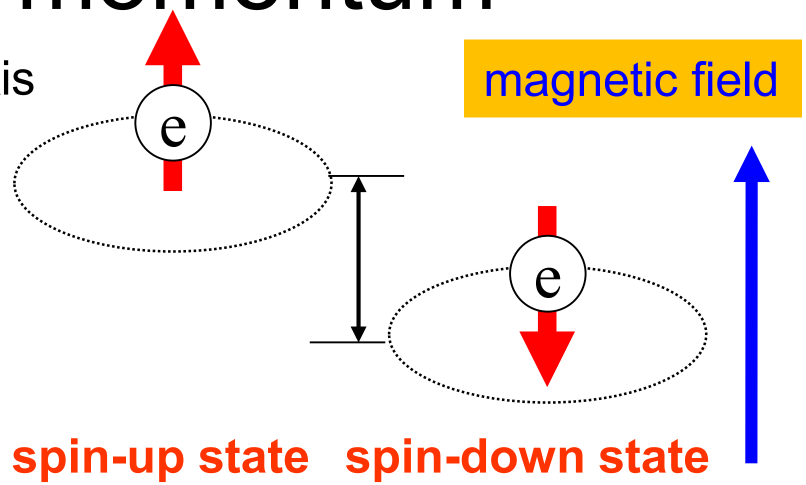

note) The orbital angular momentum appears from the orbit motion of electrons

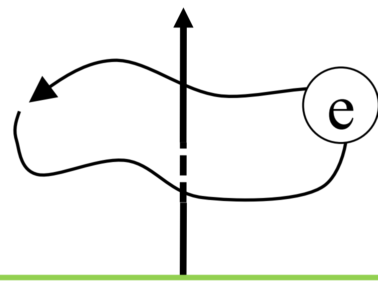

$$0, \hbar, 2\hbar, \ \ldots$$

(5-1-1) Orbital magnetic moment

An electron in a magnetic field along z-axis

Coulomb gauge
$\vec{\nabla}\cdot\vec{A}=0$

$$\mathcal{H}=\frac{1}{2m}\left(\vec{p}+\frac{e}{c}\vec{A}\right)^2+V(\vec{r}) \qquad \vec{p}=-i\hbar\vec{\nabla} \qquad \vec{A}=\frac{1}{2}H\left(-y\vec{e}_x+x\vec{e}_y\right)$$

$$\mathcal{H}=-\frac{\hbar^2}{2m}\nabla^2+\frac{e\hbar H}{2imc}\left(x\frac{\partial}{\partial y}-y\frac{\partial}{\partial x}\right)+\frac{e^2H^2}{8mc^2}\left(x^2+y^2\right)+V(\vec{r}) \qquad (e>0)$$

$$-\mu_{\mathrm{B}}\vec{\ell}\cdot\vec{H}=-\overrightarrow{\mu_\ell}\cdot\vec{H}$$

$$-\frac{\partial\mathcal{H}}{\partial H}=-\frac{e}{2mc}\left(x\frac{\hbar}{i}\frac{\partial}{\partial y}-y\frac{\hbar}{i}\frac{\partial}{\partial x}\right)-\frac{e^2H}{4mc^2}\left(x^2+y^2\right)$$

$$\overrightarrow{\mu_\ell}=-\frac{e\hbar}{2mc}\vec{\ell}=-\mu_{\mathrm{B}}\vec{\ell}$$

orbital magnetic moment

$$\frac{\ell}{\hbar}\rightarrow\ell$$

$$\mu_d=-\frac{e^2H}{4mc^2}\left(x^2+y^2\right)$$

$$\mu_d=-\frac{e^2H}{4mc^2}\left\langle x^2+y^2\right\rangle=-\frac{e^2H}{6mc^2}\left\langle r^2\right\rangle$$

diamagnetic moment

(5-1-2) Spin magnetic moment

Spin angular momentum

Stern-Gerlach, anomalous Zeeman's effect,

Doublet of the D-line in sodium

Zeeman's energy term in Dirac equation

$$\frac{\hbar e}{2mc}\vec{\sigma}\cdot\vec{H} = \mu_{\mathrm{B}} 2\vec{s}\cdot\vec{H} = g\mu_{\mathrm{B}}\vec{s}\cdot\vec{H}$$

spin angular momentum $\vec{\mu}_s = -g\mu_B\vec{s}$ $\quad \frac{s}{\hbar} \rightarrow s$

$$s_z|m_s\rangle = \begin{cases} \frac{\hbar}{2}|m_s\rangle & m_s = \frac{\hbar}{2} \\ -\frac{\hbar}{2}|m_s\rangle & m_s = -\frac{\hbar}{2} \end{cases}$$

$$(\vec{s})^2 = s(s+1)$$

Contribution from the *i*'th electron $\vec{\mu}_i = -(2\vec{s}_i + \vec{\ell}_i)\mu_{\mathrm{B}}$

Dirac equation (as a reference, see Appendix 4)

$$\left\{ p_0 + \frac{e}{c} A_0 - \rho_1 \left(\vec{\sigma}, \vec{p} + \frac{e}{c} \vec{A} \right) - \rho_3 mc \right\} \Psi = 0$$

$$p_0 = i\hbar \frac{\partial}{\partial (ct)}$$

ρ_1, ρ_3, σ **4 × 4 matrixes**

$$\sigma_1 = \begin{pmatrix} \sigma_x & 0 \\ 0 & \sigma_x \end{pmatrix} \quad \sigma_2 = \begin{pmatrix} \sigma_y & 0 \\ 0 & \sigma_y \end{pmatrix} \quad \sigma_3 = \begin{pmatrix} \sigma_z & 0 \\ 0 & \sigma_z \end{pmatrix}$$

$$\vec{p} = -i\hbar \frac{\partial}{\partial \vec{r}}$$

$$\rho_1 = \begin{pmatrix} 0 & 1 \\ 1 & 0 \end{pmatrix} \quad \rho_2 = \begin{pmatrix} 0 & i \\ i & 0 \end{pmatrix} \quad \rho_3 = \begin{pmatrix} 1 & 0 \\ 0 & -1 \end{pmatrix}$$

$$-eA_0 \ (\equiv V(\vec{r}))$$

mixing term between L and S

A_0 **scalar potential**

$\vec{A}$ **vector potential**

$$\Psi = \begin{pmatrix} \varphi_1 \\ \varphi_2 \\ \varphi_3 \\ \varphi_4 \end{pmatrix} = \begin{pmatrix} \varphi_L \\ \varphi_S \end{pmatrix} \qquad \varphi_L = \begin{pmatrix} \varphi_1 \\ \varphi_2 \end{pmatrix} \qquad \varphi_S = \begin{pmatrix} \varphi_3 \\ \varphi_4 \end{pmatrix}$$

(5-2) Zeeman energy, spin-orbit interaction

$$\left[\frac{1}{2m}\left(\vec{p}+\frac{e}{c}\vec{A}\right)^2 + V + \frac{\hbar e}{2mc}\vec{\sigma}\cdot\vec{H}\right. \qquad \vec{H} = \vec{\nabla}\times\vec{A}$$

Non-relativistic

Zeeman energy

$$+\frac{\hbar}{4m^2c^2}\vec{\sigma}\cdot\left\{\left(\mathrm{grad}\,V\right)\times\left(\vec{p}+\frac{e}{c}\vec{A}\right)\right\} \qquad \boxed{\frac{\hbar}{4m^2c^2}\vec{\sigma}\cdot\left(\mathrm{grad}\,V\times\vec{p}\right)}$$

Spin-orbit interaction

$$\left.+\frac{\hbar^2}{8m^2c^2}\mathrm{div}\left(\mathrm{grad}\,V\right)\right]\varphi_L = \left(\varepsilon - mc^2\right)\varphi_L$$

Darwin term

+ **Coulomb interaction and its relativistic correction**

(Two electron terms)

$$\varphi_L = \begin{pmatrix}\varphi_1\\ \varphi_2\end{pmatrix}$$

Wave function of 2-component spinor

(5-3) Interaction between magnetic carriers: magnetic dipole interaction

Magnetic dipole term in Breit's interaction

$$E_{\text{Breit}}^{\text{magnetic dipole}} = \frac{e^2}{4m^2c^2}\frac{\vec{\sigma}_1 \cdot \vec{\sigma}_2 - 3(\vec{\sigma}_1 \cdot \hat{\mathrm{r}}_{12})(\vec{\sigma}_2 \cdot \hat{\mathrm{r}}_{12})}{r_{12}^3}$$

Interaction between atomic magnetic moments

$$E_{ij}^{\text{dipole}} = \frac{e^2}{4m^2c^2}\frac{\vec{\mu}_i \cdot \vec{\mu}_j - 3(\vec{\mu}_i \cdot \hat{\mathrm{R}}_{ij})(\vec{\mu}_j \cdot \hat{\mathrm{R}}_{ij})}{R_{ij}^3}$$

(5-4) Control of magnetization

- ➢Dynamical control
- ➢Statistical control

Tunnel magnetoresistance (TMR)

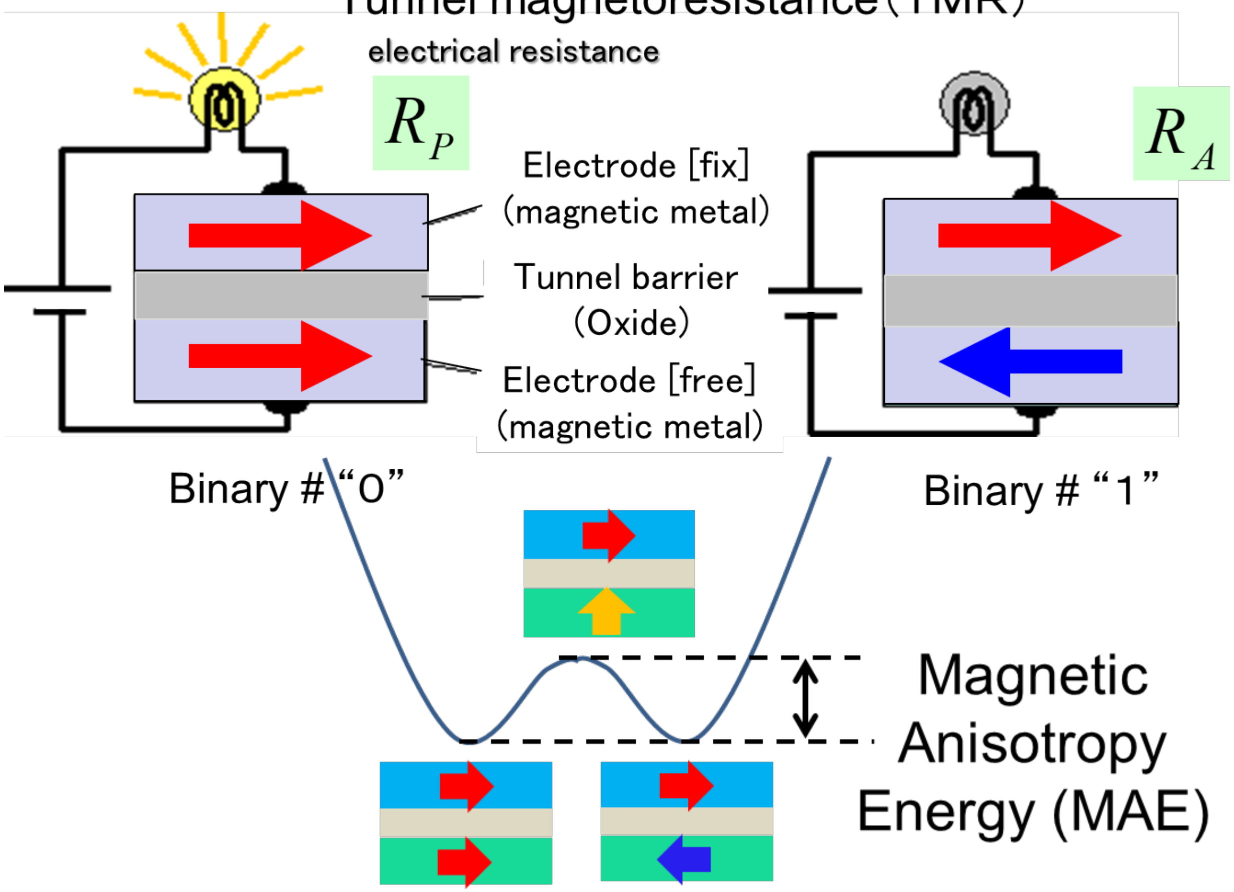

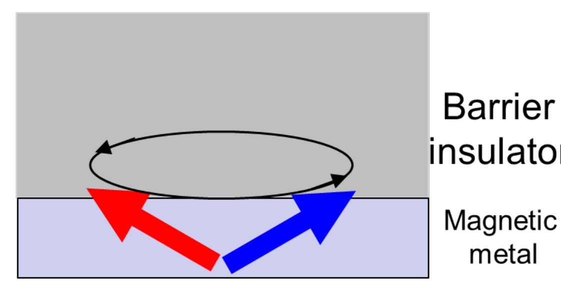

Driving forces in dynamical control of magnetization

External magnetic field (by current)

Injection of spin polarized current

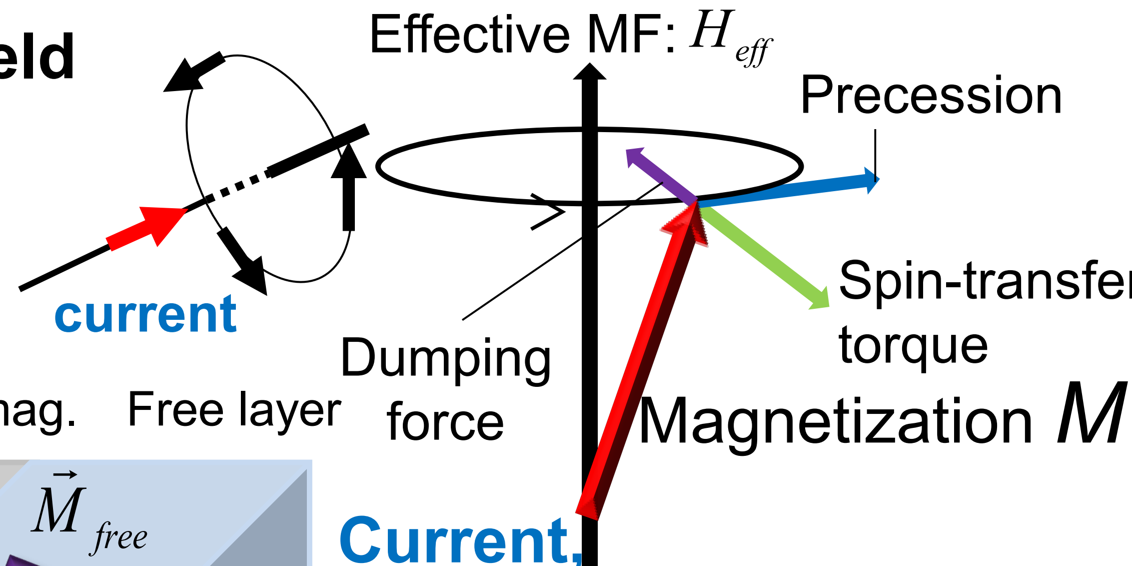

Fixed layer   Non-mag.   Free layer

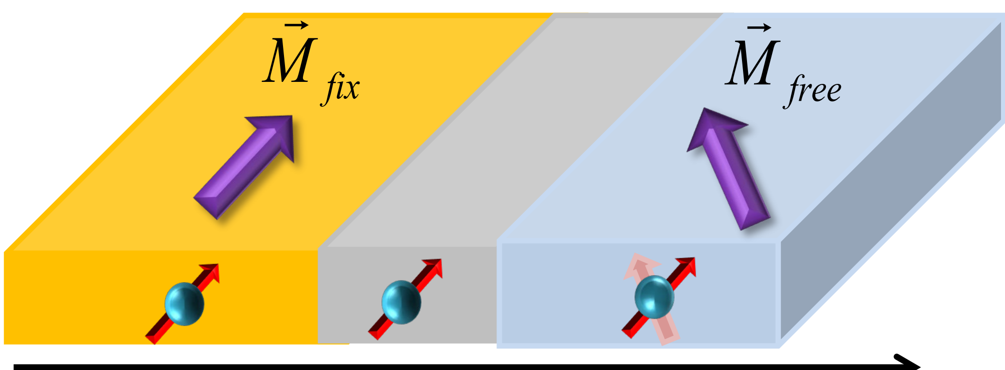

Spin polarized current

Conservation law of (spin) angular momenta

Current, Spin polarized current

Problem: Disturbing compactness, energy consumption, Joule heating, etc.

↓

Electric field (Voltage)

$$\vec{H}_{eff} = \vec{H}_{ext} + \vec{H}_{stt} + \vec{H}_{shape} + \vec{H}_{aniso}$$

Expectation: ultra-low energy consumption, non-volatile property, compactness(high density memory), enough high speed in reading&writing

Landau–Lifshitz–Gilbert equation (LLG-equation)

$$\frac{d\vec{M}}{dt} = -\gamma\left(\vec{M} \times \vec{H}_{\mathrm{eff}}\right) + \frac{\alpha}{M_s}\vec{M} \times \frac{d\vec{M}}{dt} - \eta(\theta)\frac{\mu_{\mathrm{B}} I}{eV}\frac{\vec{M}}{M_s} \times \left(\frac{\vec{M}}{M_s} \times \frac{\vec{M}_{\mathrm{fix}}}{M_{\mathrm{fix}}}\right)$$

precessional term dumping term spin transfer torque

$\vec{M}$:Magnetization vector at free layer

α :Gilbert magnetic damping factor

γ :gyromagnetic factor

$\vec{M}_{fix}$:Magnetization vector at fixed layer

$\eta(\theta)$:spin transfer efficiency

$$\vec{H}_{\mathrm{eff}} = \vec{H} + \vec{H}_{\mathrm{shape}} + \vec{H}_{\mathrm{cry-aniso}}$$

J. C. Slonczewski, Journal of Magnetism and Magnetic Materials 159 (1996) L1-L7

(5-5) Magnetic anisotropy energy: magnet shape, electron orbital

Shape magnetic anisotropy (SMA)

in-plane contribution

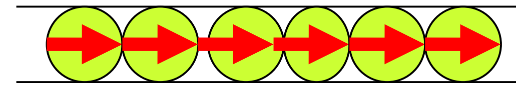

Magnetostatic contribution

$$E_{\text{d-d}} = \frac{1}{c^2} \sum_{\vec{R}_i, \vec{R}_j}^{i \neq j} \left\{ \frac{\vec{m}(\vec{R}_i) \cdot \vec{m}(\vec{R}_j)}{R_{ij}^3} - 3 \frac{\left[\vec{m}(\vec{R}_i) \cdot (\vec{R}_i - \vec{R}_j)\right]\left[\vec{m}(\vec{R}_j) \cdot (\vec{R}_i - \vec{R}_j)\right]}{R_{ij}^5} \right\}$$

2D square lat.

Shape aniso.

This depends on the arrangement of magnetic atoms, not so depend on electric field.

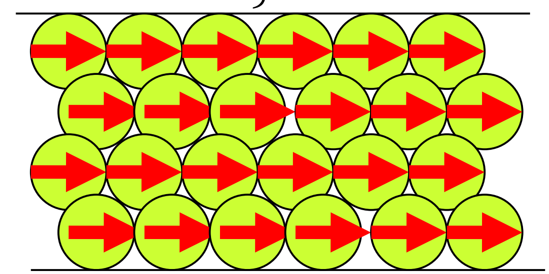

Electronic structure contribution

perturbation of spin-orbit interaction,

MA appears from an anisotropy of orbitals

$$H_{\text{SOI}} = \xi \vec{\ell} \cdot \vec{\sigma}$$

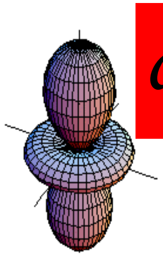

$d_{3z^2-r^2}$

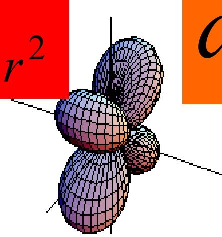

d_{zx}

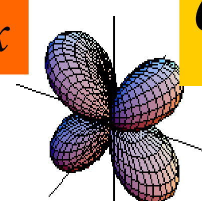

d_{yz}

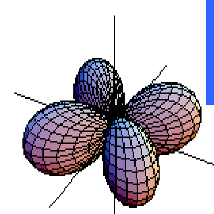

d_{xy}

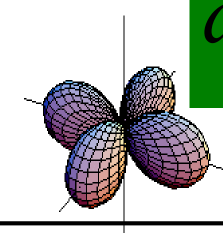

$d_{x^2-y^2}$

It is important to see the behavior of each angular orbitals.
Anisotropic occupation of electrons leads to MA.

Magnetocrystalline anisotropy (MCA)

Origin of MCAE in electronic structure

$$H_{SOI} = \xi \vec{\ell} \cdot \vec{\sigma}$$

•**spin-orbit coupling contribution from band electrons**

(A) 2nd perturbative contributions

$$\mathrm{MCAE} = E_x - E_z \approx (\xi)^2 \sum_{o,u} \frac{\left|\langle o_\downarrow | \ell_z | u_\downarrow \rangle\right|^2 - \left|\langle o_\downarrow | \ell_x | u_\downarrow \rangle\right|^2}{\varepsilon_u^\downarrow - \varepsilon_o^\downarrow}$$

matrix element

z	$\langle xz\|\ell_z\|yz\rangle = 1$ $\langle x^2-y^2\|\ell_z\|xy\rangle = 2$
x	$\langle 3z^2-r^2\|\ell_x\|yz\rangle = \sqrt{3}$ $\langle xy\|\ell_x\|xz\rangle = 1$ $\langle x^2-y^2\|\ell_x\|yz\rangle = 1$
y	$\langle 3z^2-r^2\|\ell_y\|xz\rangle = \sqrt{3}$ $\langle xy\|\ell_y\|yz\rangle = 1$ $\langle x^2-y^2\|\ell_y\|xz\rangle = 1$

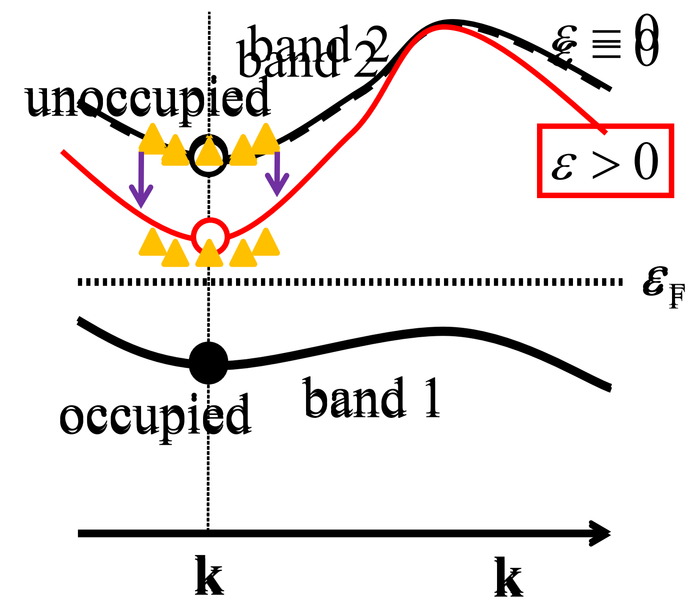

In the case of Fe element

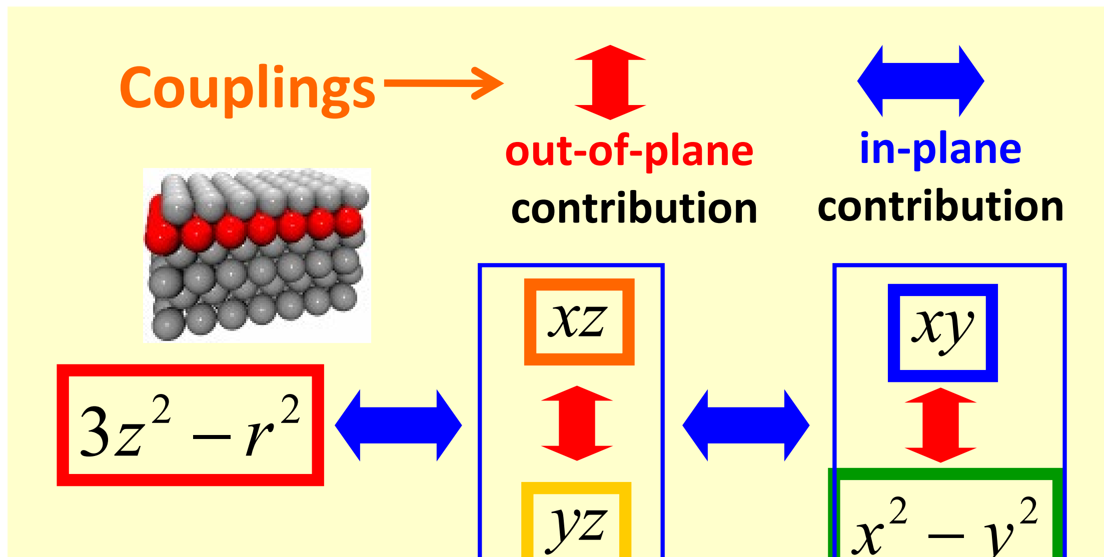

(B) Existence of partly-occupied degenerate levels

$\xi m \cos\theta$

Low dimentional system **D. S. Wang, R. Wu, and A. J. Freeman, Phys. Rev. B 47,14932 (1993).**

2nd perturbative contributions (more general)

No spin flip:

$$\mathrm{MCAE} \approx (\xi)^2 \sum_{o,u} \frac{\left|\langle o_\downarrow | \ell_z | u_\downarrow \rangle\right|^2 - \left|\langle o_\downarrow | \ell_x | u_\downarrow \rangle\right|^2}{\varepsilon_u^\downarrow - \varepsilon_o^\downarrow} + (\xi)^2 \sum_{o,u} \frac{\left|\langle o_\uparrow | \ell_z | u_\uparrow \rangle\right|^2 - \left|\langle o_\uparrow | \ell_x | u_\uparrow \rangle\right|^2}{\varepsilon_u^\uparrow - \varepsilon_o^\uparrow}$$

Spin flip terms:

$$- (\xi)^2 \sum_{o,u} \frac{\left|\langle o_\uparrow | \ell_z | u_\downarrow \rangle\right|^2 - \left|\langle o_\uparrow | \ell_x | u_\downarrow \rangle\right|^2}{\varepsilon_u^\downarrow - \varepsilon_o^\uparrow} - (\xi)^2 \sum_{o,u} \frac{\left|\langle o_\downarrow | \ell_z | u_\uparrow \rangle\right|^2 - \left|\langle o_\downarrow | \ell_x | u_\uparrow \rangle\right|^2}{\varepsilon_u^\uparrow - \varepsilon_o^\downarrow}$$

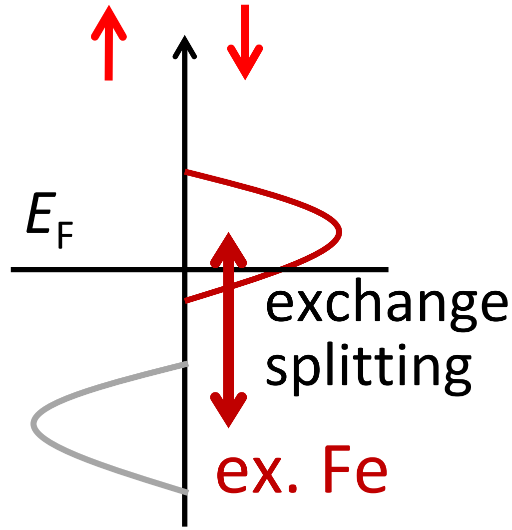

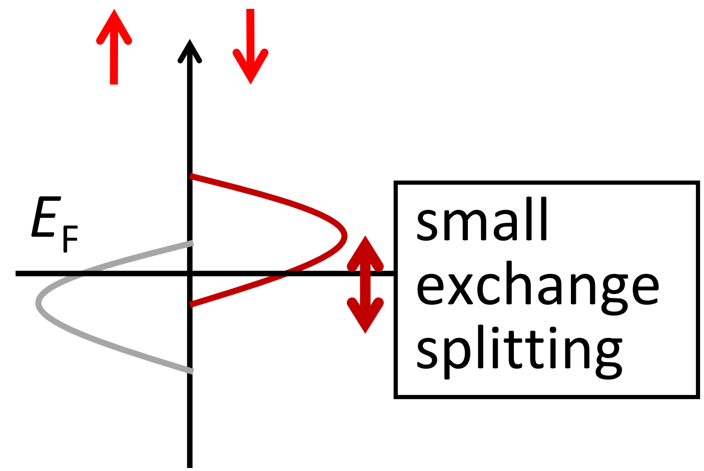

These contributions can be expected in Pd and Pt systems.

(5-6) Summary of density functional approach on magnetic anisotropy energy

Magnetocrystalline anisotropy (MCA)

Force theorem approach

↓

Grand canonical force theorem approach

Shape magnetic anisotropy (SMA)

Atomic magnetic moment

↓

Spin-density

Density functional theory(DFT)with MDI

$m = \hbar = e = 1$ **(Atomic unit)**

$$E[n(\mathbf{r})] = \sum_{i,\mathbf{k}} \int d\mathbf{r}\, \psi^*_{i\mathbf{k}}(\mathbf{r}) \left(-\frac{1}{2}\nabla^2 \right) \psi_{i\mathbf{k}}(\mathbf{r})$$

kinetic energy

$$+ \frac{1}{2} \iint d\mathbf{r} d\mathbf{r}' \frac{n(\mathbf{r}) n(\mathbf{r}')}{|\mathbf{r} - \mathbf{r}'|} + \int d\mathbf{r} v(\mathbf{r}) n(\mathbf{r}) + E_{\mathrm{XC}}\left[n(\mathbf{r}), \mathbf{m}(\mathbf{r}) \right]$$

classical electronic static energy

external potential

exchange-correlation energy

$$+ \boxed{E^{\mathrm{MDI}}_{\mathrm{SDM}}}$$

Magnetic dipole-dipole energy

Kohn-Sham equation ➡

$$\left(-\frac{\hbar^2}{2m}\nabla^2 + V_{\mathrm{eff}} + \boxed{V^{\mathrm{MDI}}} \right) \psi_i = \varepsilon_i \psi_i$$

Potential except magnetic dipole-dipole effect

Magnetic dipole-dipole potential

MDI energy through spin density

$$E_{\mathrm{SDM}}^{\mathrm{MDI}} = \frac{1}{8c^2} \iint d\mathbf{r} d\mathbf{r}' \left[\frac{\mathbf{m}(\mathbf{r}) \cdot \mathbf{m}(\mathbf{r}')}{|\mathbf{r}-\mathbf{r}'|^3} - 3 \frac{\{\mathbf{m}(\mathbf{r}) \cdot (\mathbf{r}-\mathbf{r}')\}\{\mathbf{m}(\mathbf{r}') \cdot (\mathbf{r}-\mathbf{r}')\}}{|\mathbf{r}-\mathbf{r}'|^5} \right]$$

$$E_{\mathrm{SDM}}^{\mathrm{MDI}} = - \int d\mathbf{r}\, \mathbf{m}(\mathbf{r}) \cdot \mathbf{H}(\mathbf{r}).$$

$$V_{\mathrm{KS}}^{\mathrm{MDI}}(\mathbf{r}) = -\mathbf{H}(\mathbf{r}) \cdot \boldsymbol{\sigma}$$

$\left(\sigma_x, \sigma_y, \sigma_z\right)$ Pauli matrix

Self-consistent procedure

This estimation is based on spin density:

Spin Density Model (SDM)

Magnetic field $\mathbf{H}(\mathbf{r})$

Macro magnet

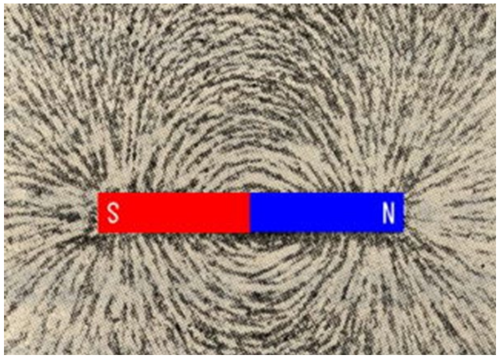

Magnetic field lines

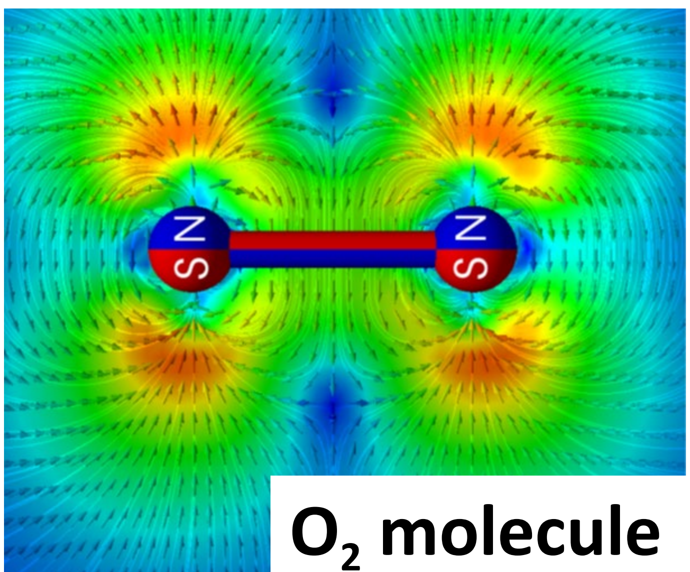

O_2 molecule

Fe square alignment

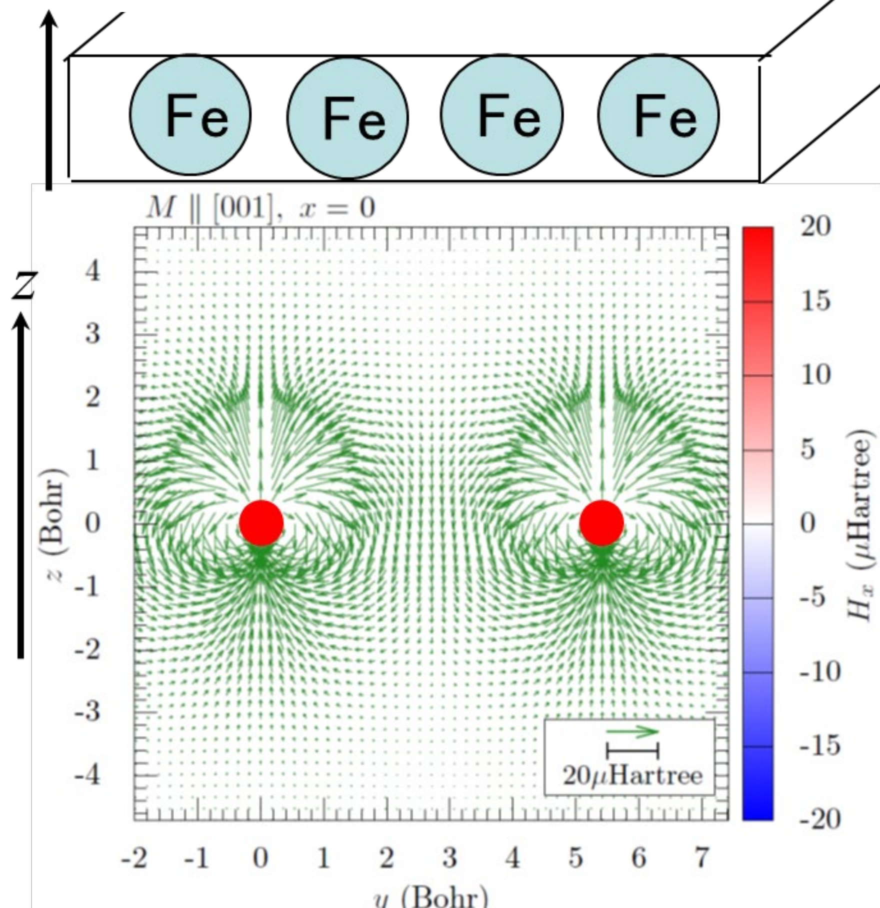

Shape Magnetic Anisotropy Energy (SMAE)

From magnetic dipole interaction(MDI)

$$\mathbf{SMAE} = \boldsymbol{E}_{\mathbf{MDI}}^{[\mathbf{001}]} - \boldsymbol{E}_{\mathbf{MDI}}^{[\mathbf{100}]}$$

Continuum approach (CA)

$$\mathrm{MAE} = E_{\mathrm{MDI}}^{[001]} - E_{\mathrm{MDI}}^{[100]} = \frac{1}{2}\mu_0 \frac{M^2}{\Omega}$$

M : Total magnetization

Ω : Volume of magnetic material

μ_0 : Permeability of vacuum

Discrete approach (DA) [1,2]

$\mathbf{m}(\mathbf{R}_i)$: Atomic magnetic moment

$$E_{\mathrm{MDI}}^{\mathbf{m}} = \frac{e^2}{4m^2c^2} \sum_{\mathbf{R}_i,\mathbf{R}_j}^{i \neq j} \left[\frac{\mathbf{m}(\mathbf{R}_i) \cdot \mathbf{m}(\mathbf{R}_j)}{{R_{ij}}^3} - 3\frac{\mathbf{m}(\mathbf{R}_i) \cdot (\mathbf{R}_i - \mathbf{R}_j)\mathbf{m}(\mathbf{R}_i) \cdot (\mathbf{R}_i - \mathbf{R}_j)}{{R_{ij}}^5} \right]$$

Spin density approach (SDA) [3]

$$E_{\mathrm{MDI}}^{\mathbf{m}} = \frac{e^2}{4m^2c^2} \iint d\mathbf{r}_1 d\mathbf{r}_2 \left[\frac{\mathbf{m}(\mathbf{r}_1) \cdot \mathbf{m}(\mathbf{r}_2)}{|\mathbf{r}_1 - \mathbf{r}_2|^3} - 3\frac{\mathbf{m}(\mathbf{r}_1) \cdot (\mathbf{r}_1 - \mathbf{r}_2)\, \mathbf{m}(\mathbf{r}_2) \cdot (\mathbf{r}_1 - \mathbf{r}_2)}{|\mathbf{r}_1 - \mathbf{r}_2|^5} \right]$$

- High precision shape magnetic anisotropy from spin density distribution: magnetic interface/surface

[1] H. J. G. Draaisma and W. J. M. de Jonge, J. Appl. Phys. 64, 1988.
[2] L. Szunyogh et al, Phys. Rev. B 51, 9552, 1995.
[3] T. Oda and M. Obata, J. Phys. Soc. Jpn. 87, 064803, 2018.

Magnetic anisotropy energy (MAE)

MAE=SMAE + MCAE

$$\mathrm{SMAE}{=}E_{\mathrm{MDI}}[100]-E_{\mathrm{MDI}}[001] \qquad \mathrm{MCAE}{=}E_{\mathrm{SDFT}}[100]-E_{\mathrm{SDFT}}[001]$$

Total Energy(Energy Functional: SDFT)

$$E_{\mathrm{tot}}[n(\mathbf{r}),\mathbf{m}(\mathbf{r})] = E_{\mathrm{MDI}}[\mathbf{m}(\mathbf{r})]+E_{\mathrm{SDFT}}[n(\mathbf{r}),\mathbf{m}(\mathbf{r})]$$

Kohn-Sham equation

$$\left[-\frac{1}{2}\nabla^2+V_{\mathrm{eff}}^{\mathrm{SDFT}}(\mathbf{r})+V_{\mathrm{MDI}}^{\mathrm{SDI}}(\mathbf{r})\right]\Phi_i(\mathbf{r})=\varepsilon_i\Phi_i(\mathbf{r})$$

Grand-canonical force theorem (GCFT) for MCAE

$$\delta E_{\mathrm{SDFT}}^{\mathbf{m},\mathrm{GCFT}} = \sum_{\mathbf{k}}\sum_{\ell}\delta\varepsilon_{\ell\mathbf{k}}^{\mathbf{m},\mathrm{GCFT}}$$

$$\delta\varepsilon_{\ell\mathbf{k}}^{\mathbf{m},\mathrm{GCFT}} = f_{\ell\mathbf{k}}^{\mathbf{m}}(\varepsilon_{\ell\mathbf{k}}^{\mathbf{m},\mathrm{GCFT}}-\mu_0)-f_{\ell\mathbf{k}}^{0}(\varepsilon_{\ell\mathbf{k}}^{0}-\mu_0)$$

MCAE

- Atom-resolved
- ***k***-resolved

$f_{\ell\mathbf{k}}^{\mathbf{m}}, f_{\ell\mathbf{k}}^{0}$: Fermi function

SAME: Shape magnetic anisotropy energy

MCAE: Magnetocrystalline anisotropy energy

GCFT: D. Li et al., Phys. Rev. B 88, 214413 (2013);
I. Pardede et al., J. Magn. Magn. Mater., 500, 166357 (2020).

Interactions and eigenvalues

- Hamiltonian $$H = -\frac{1}{2}\nabla^2 + V_{\mathrm{eff}}^{\mathrm{SDFT}}(\mathbf{r}) + V_{\mathrm{MDI}}^{\mathrm{SDI}}(\mathbf{r})$$

$$V_{\mathrm{eff}}^{\mathrm{SDFT}}(\mathbf{r}) = V_{\mathrm{ion}}^{0}(\mathbf{r}) + V_{\mathrm{ion}}^{\mathrm{SOI}}(\mathbf{r}) + V_{\mathrm{H}}(\mathbf{r}) + V_{\mathrm{XC}}^{\mathrm{N}}(\mathbf{r})\sigma_0 + V_{\mathrm{XC}}^{\mathrm{M}}(\mathbf{r})\frac{\mathbf{m}\cdot\boldsymbol{\sigma}}{m}$$

$$V_{\mathrm{ion}}^{\mathrm{SOI}}(\mathbf{r}) = \sum_I \xi_I \mathbf{L}_I \cdot \boldsymbol{\sigma}$$

Spin-orbit int.

$$V_{\mathrm{MDI}}^{\mathrm{SDI}}(\mathbf{r}) = \mathbf{H}^{\mathrm{dip}}(\mathbf{r}) \cdot \boldsymbol{\sigma}$$

Dipole field

Exchange int.

Depend on only **relative angle** between spins (parallel spin)

- Eigenvalues for a given potential

$$\varepsilon_{\ell\mathbf{k}}^{\mathbf{m},\mathrm{GCFT}} \qquad \left[-\frac{1}{2}\nabla^2 + V_{\mathrm{eff}}^{\mathrm{SDFT}}(\mathbf{r}) + V_{\mathrm{MDI}}^{\mathrm{SDI}}(\mathbf{r})\right]\Phi_i(\mathbf{r}) = \varepsilon_i \Phi_i(\mathbf{r})$$

$\mathbf{m}$: a given magnetization direction (non-collinear with SOI)

$$\varepsilon_{\ell\mathbf{k}}^{0} \qquad \left[-\frac{1}{2}\nabla^2 + V_{\mathrm{eff}}^{\mathrm{SDFT}}(\mathbf{r}) + V_{\mathrm{MDI}}^{\mathrm{SDI}}(\mathbf{r})\right]\Phi_i(\mathbf{r}) = \varepsilon_i \Phi_i(\mathbf{r})$$

m : magnetization (collinear cal. Without SOI)

MagnetoCrystalline anisotropy energy (MCAE)

➢ *k*-resolved MCAE

$$E_{\text{SDFT}}^{\mathbf{m},\text{GCFT}}\left(\mathbf{k}\right)=\sum_{\ell} f_{\ell\mathbf{k}}^{\mathbf{m}}\left(\varepsilon_{\ell\mathbf{k}}^{\mathbf{m},\text{GCFT}}-\mu\right)$$

$f_{\ell\mathbf{k}}^{\mathbf{m}}$: Fermi function

➢ Atom-resolved MCAE

$$E_{\text{SDFT}}^{\mathbf{m},\text{GCFT}}\left(I\right)=\sum_{\ell,\mathbf{k},a} f_{\ell\mathbf{k}}^{\mathbf{m}}\left(\varepsilon_{\ell\mathbf{k}}^{\mathbf{m},\text{GCFT}}-\mu\right)\left|\left\langle \chi_{Ia} \middle| \Phi_{\ell\mathbf{k}}\right\rangle\right|^2$$

➢ Atom-resolved and *k*-resolved MCAE

$$E_{\text{SDFT}}^{\mathbf{m},\text{GCFT}}\left(I,\mathbf{k}\right)=\sum_{\ell,a} f_{\ell\mathbf{k}}^{\mathbf{m}}\left(\varepsilon_{\ell\mathbf{k}}^{\mathbf{m},\text{GCFT}}-\mu\right)\left|\left\langle \chi_{Ia} \middle| \Phi_{\ell\mathbf{k}}\right\rangle\right|^2$$

I. Pardede et al., J. Magn. Magn. Mater., 500, 166357 (2020).

Magnetic Anisotropy Energy (MAE)

For ferromagnets

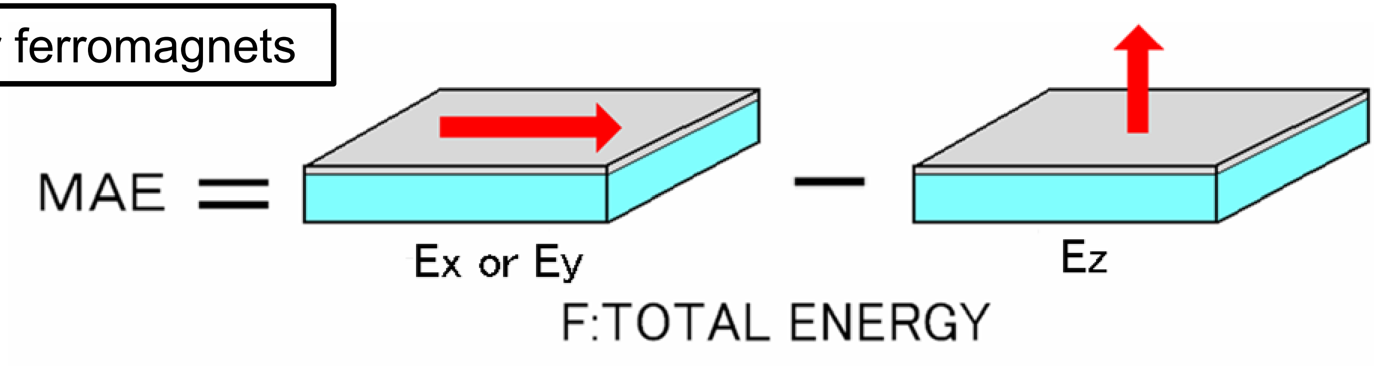

$$\mathrm{MAE} = E[100] - E[001]$$

MAE > 0 : perpendicular anisotropy

For antiferromagnets

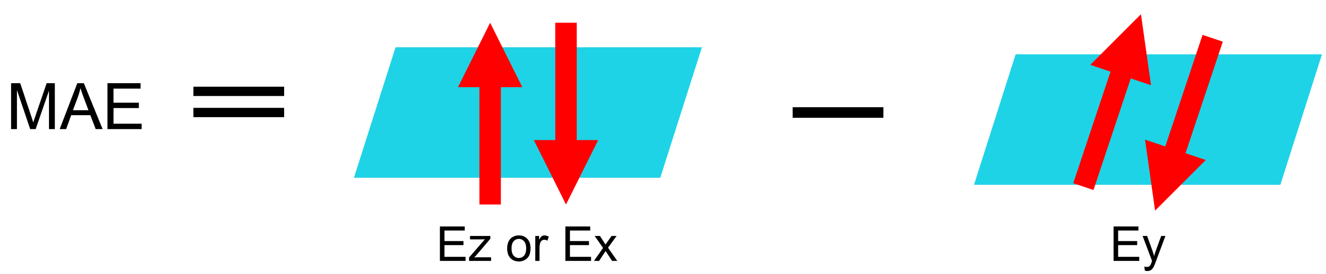

MAE from d-d interaction for Fe-multilayers

In-plane lattice constant
MgO 4.21Å

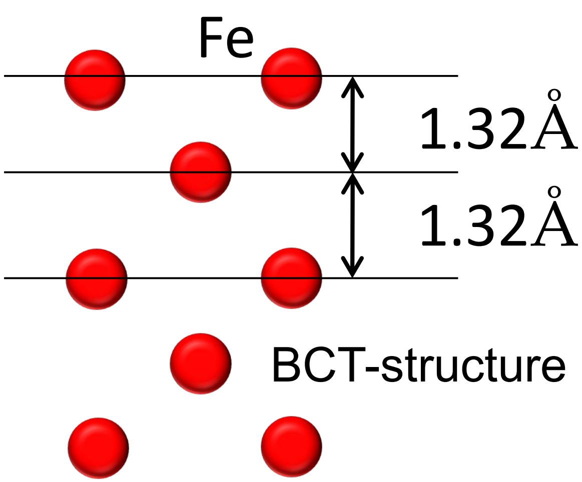

Fe: 2.96 μ_B(interface)
2.63 μ_B(inside)

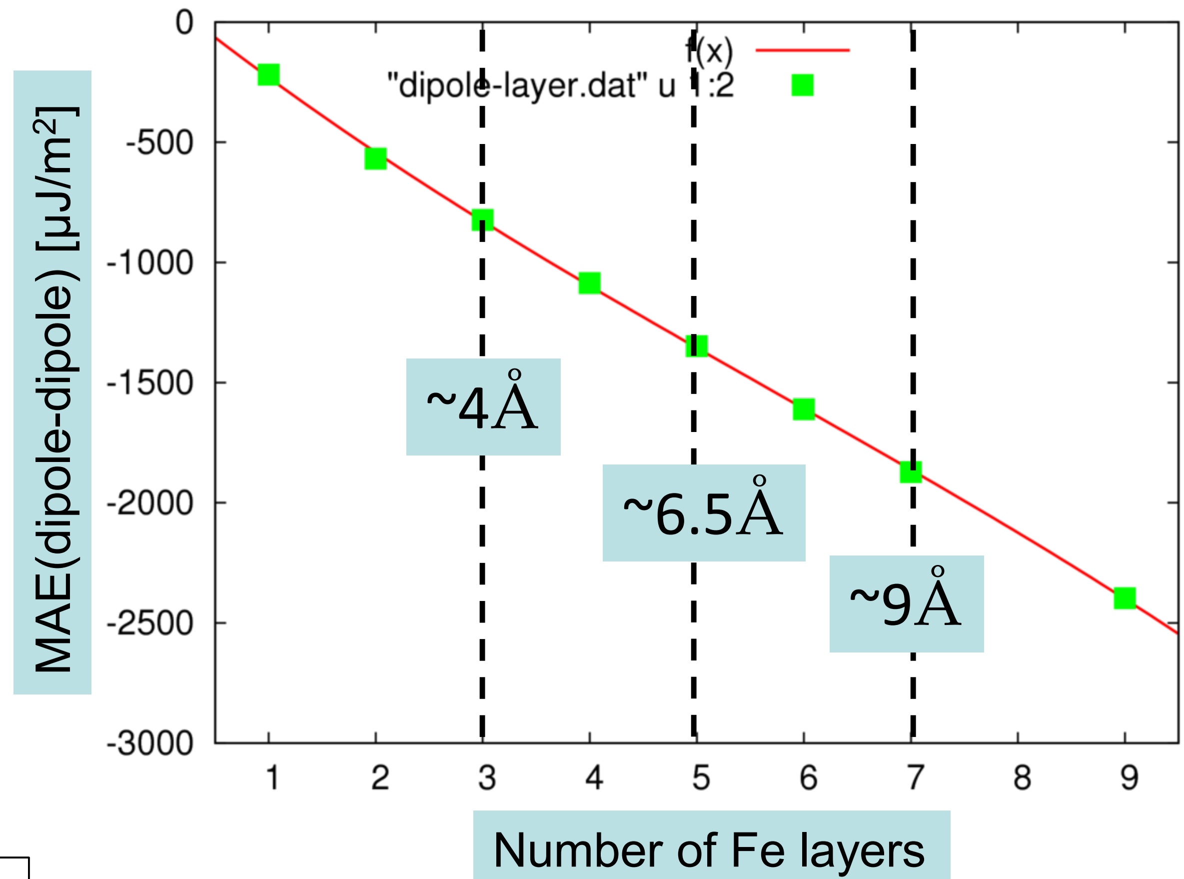

FeCo layer
> 6.3Å in-plane
< 6.3Å out-of-plane
Y. Shiota et. al., Appl. Phys. Exp., **4**, 043305(2011).

In-plane MAE increases by 250-300μJ/m^2 per Fe-layer

Ref.)L. Szunyogh et al., Phys. Rev. B, **51**, 9552, (1995)

Magnetic anisotropy: MCA, in-plane, perpendicular

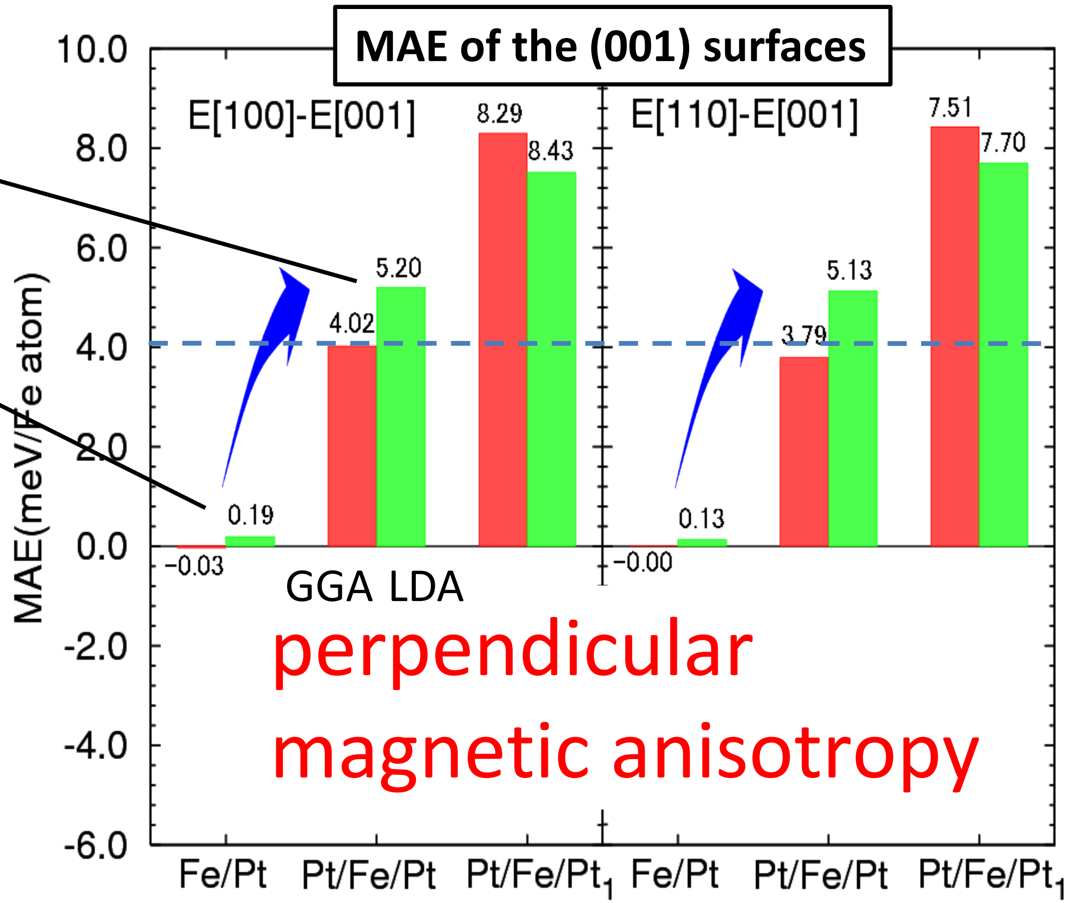

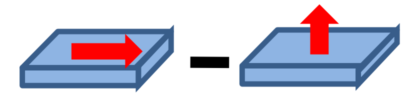

$11 mJ/m^2$

$0.40 mJ/m^2$

- **Pt capping layer drastically enhances the MCAE.**

$L1_0$-FePt regular alloy(LDA) MAE
2.61meV[a]、
2.724meV[b]

[a]P. Ravindran *et.al*, (2001).
[b]TO *et.al*, (2005).

Tsujikawa et al. (2008, 2009)

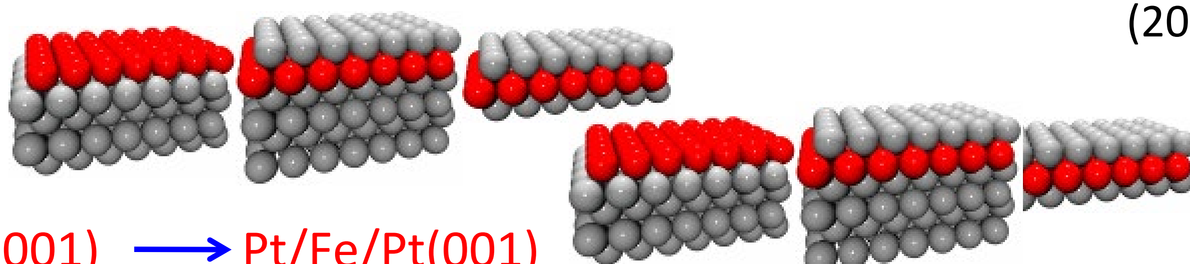

Fe/Pt(001) → Pt/Fe/Pt(001)

dipole: $-0.32 mJ/m^2$

(5-7) Magnetic Anisotropy (MA), Voltage-Controlled Magnetic Anisotropy (VCMA):

- **Fe/MgO interface**

Typical interface Fe/MgO on Magnetic anisotropy and its electric field effect

Let us learn the electronic structure for getting the knowledge of MCA.

Starting from the Fe monolayer, …

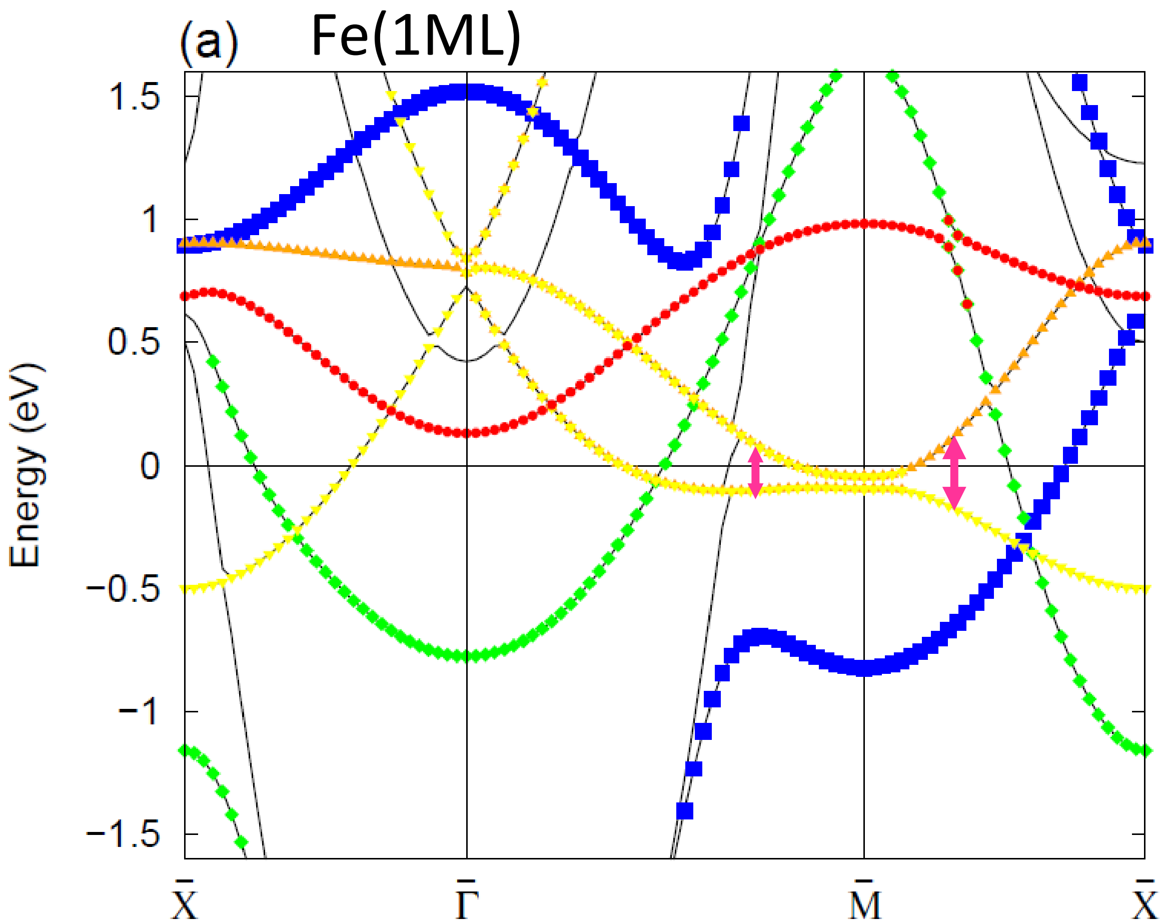

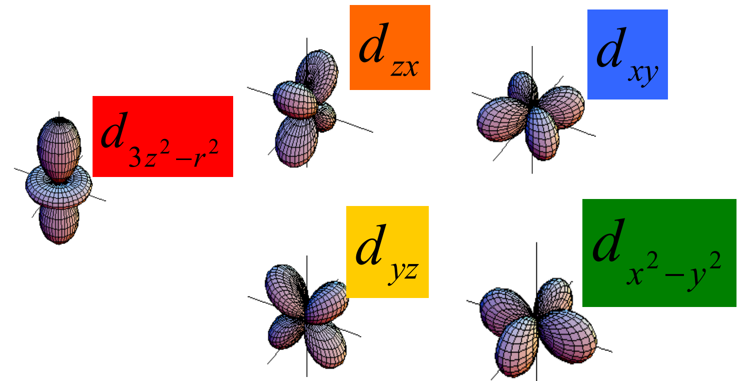

d_{zx} ↕ d_{yz}: Perpendicular (out-of-plane) Near M-bar

$d_{3z^2-r^2}$ band are above the Fermi level

No in-plan contribution

MAE= 1.23mJ/m^2 (= 1.51 -0.28), slope rate= 12fJ/Vm

Tsujikawa and Oda

Electronic structure of the interface Fe/MgO: Band

Ex. Fe(5ML)/MgO(5ML)

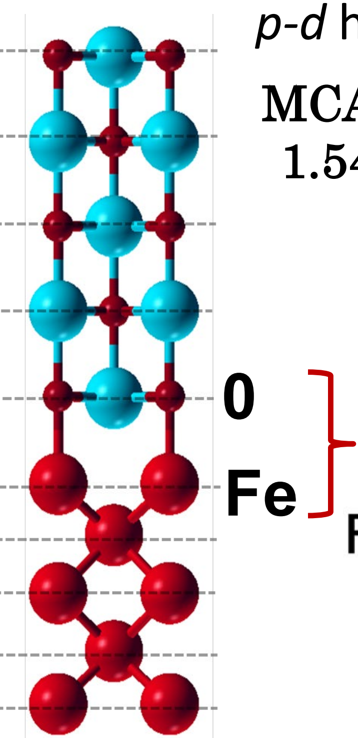

p-d hybridization

MCAE= 1.54 mJ/m²

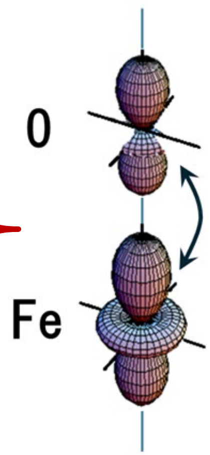

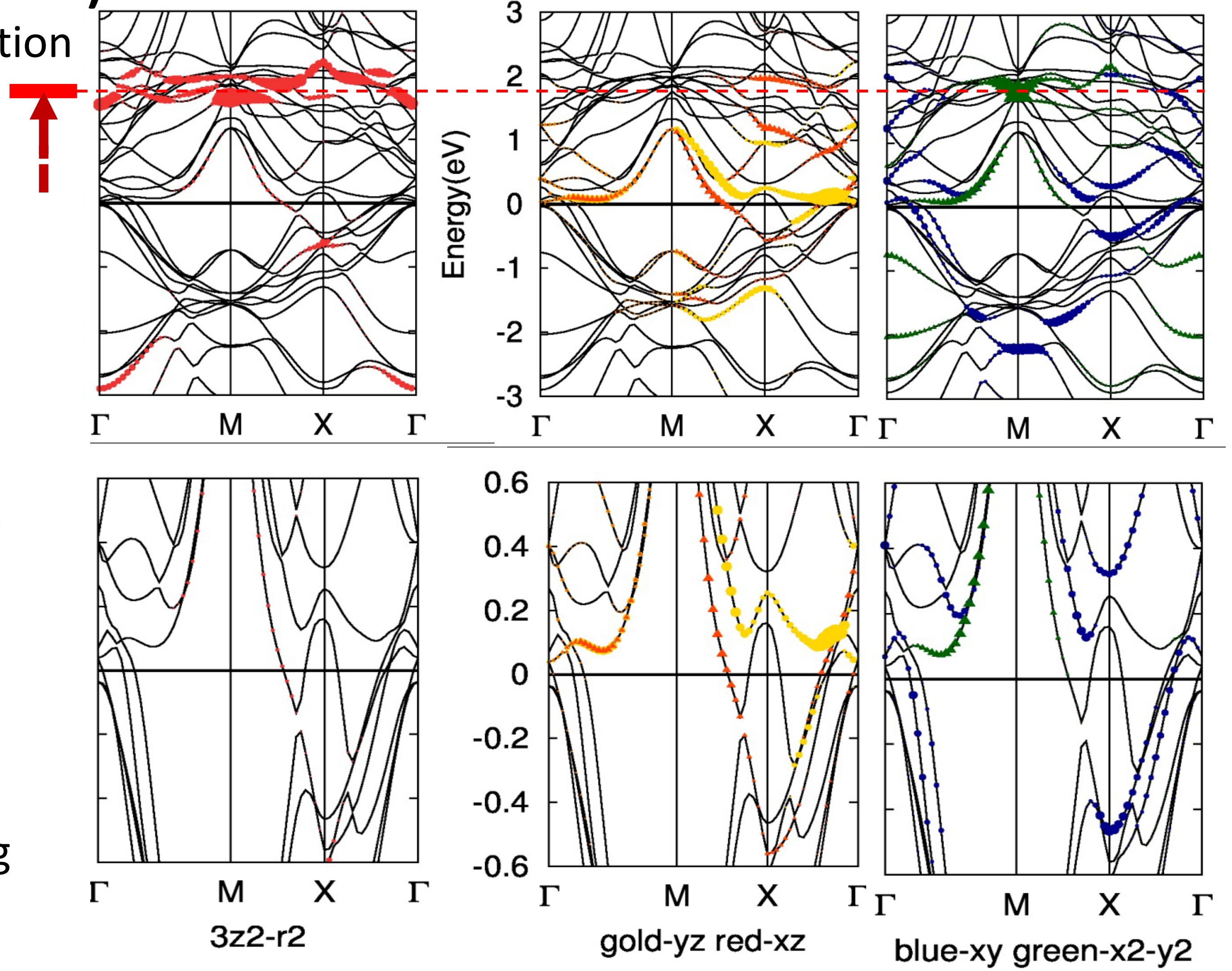

The *p-d* hybridization pushed up the energy level of $3z^2$-r^2, vanishing its component at the Fermi level.

Such electronic structure kept the large **out-of-plane MCA**.

Electronic structure of the interface Fe/MgO: DOS

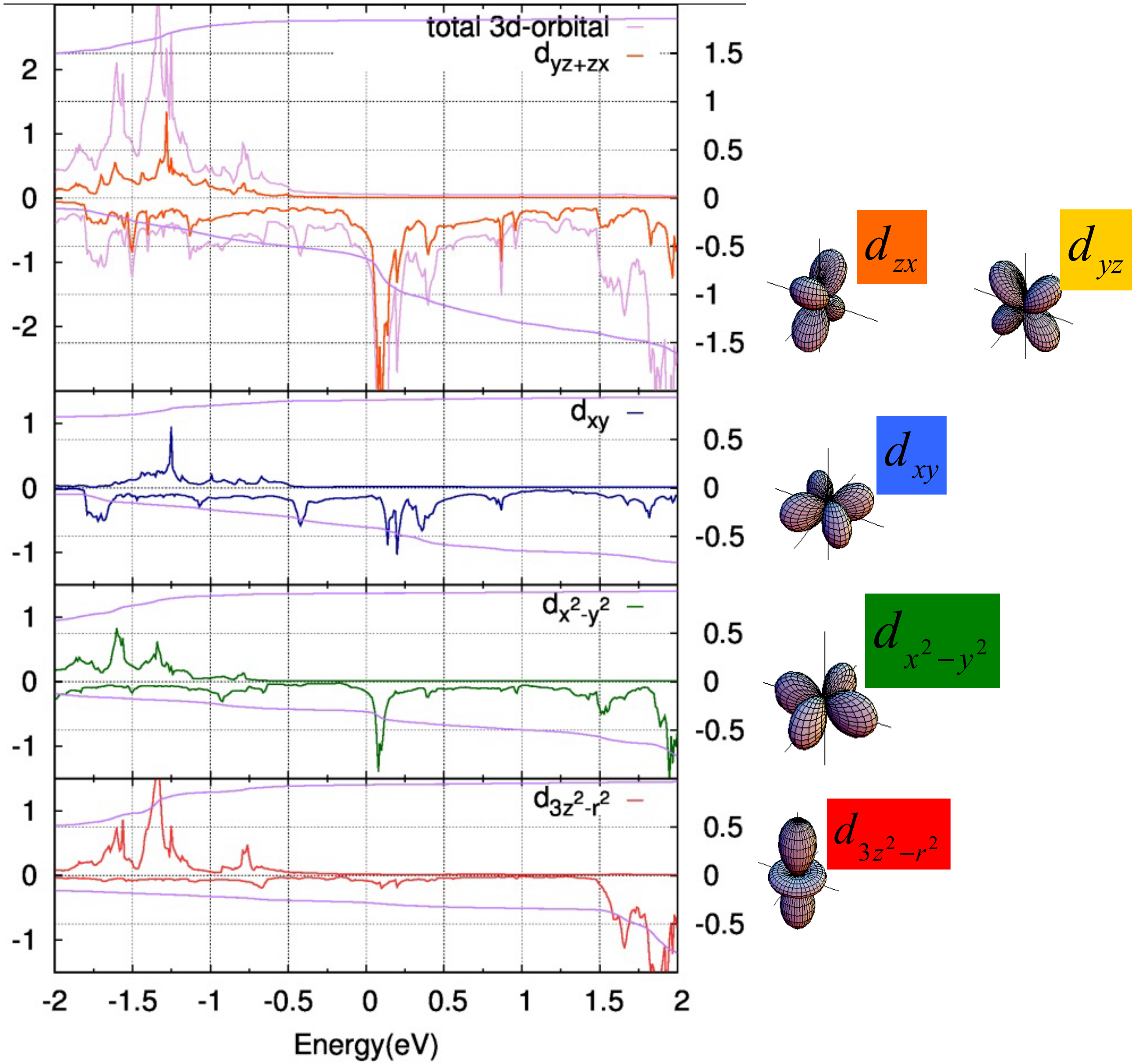

MAE and VCMA in Fe/MgO interface (Exp.)

Fe/MgO interface was found as a multi-functional one:

- **High TMR ratio**
- **Large perpendicular magnetic anisotropy (PMA)**
- **Large voltage-controlled magnetic anisotropy (VCMA)**

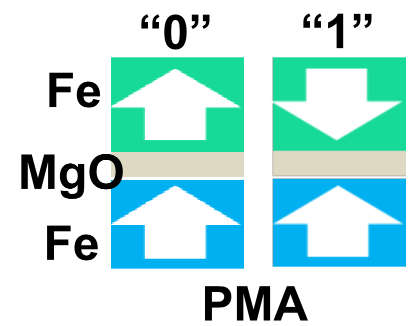

Cr/Fe/MgO

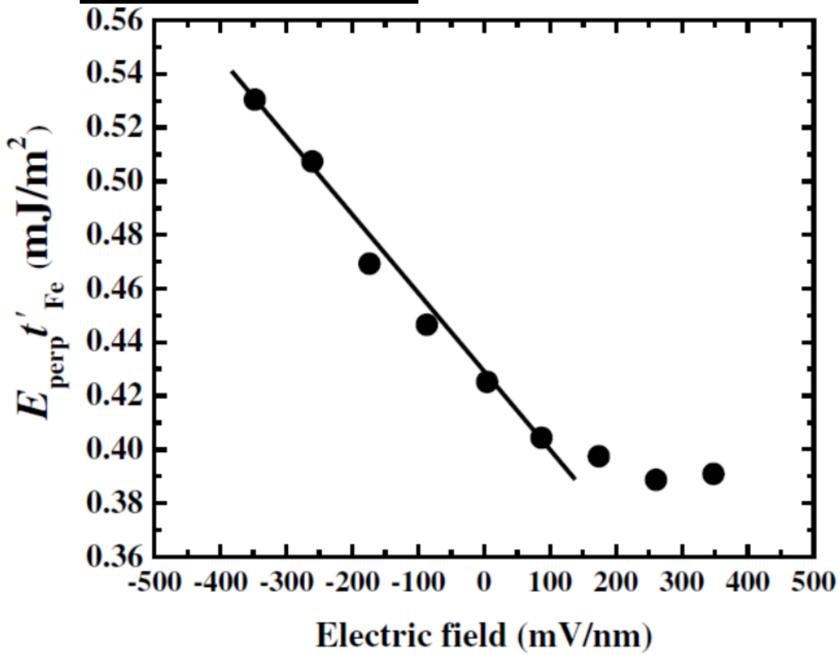

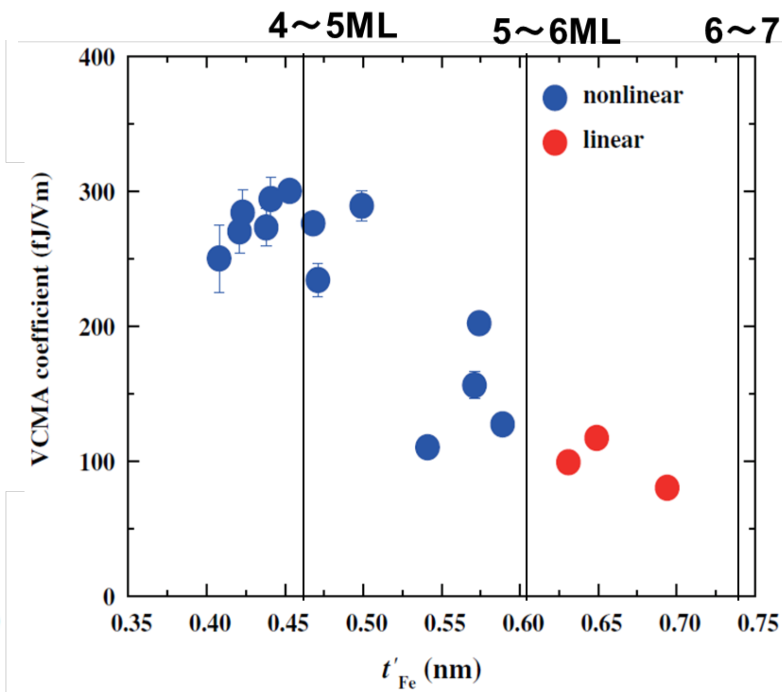

T. Nozaki *et al.*, Phys. Rev. Appl. 5, 044006 (2016)

MAE: Interface Cr/Fe/MgO

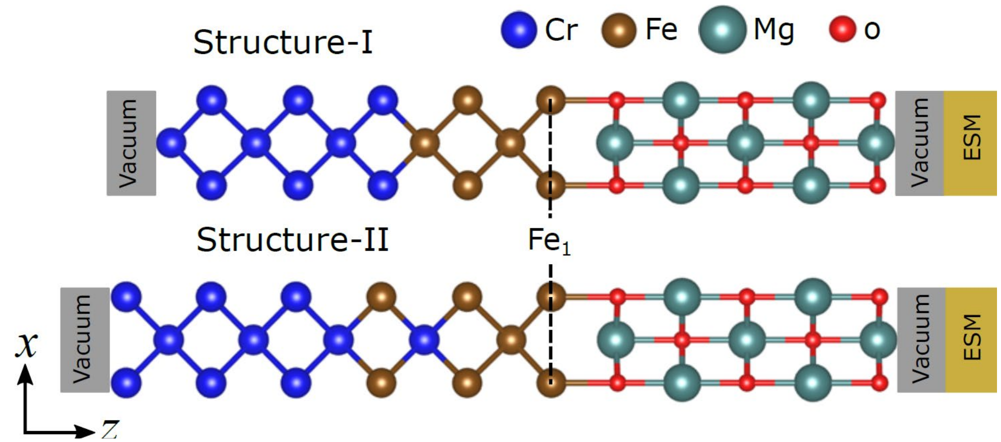

Alloying effect was investigated.

Structure	a (Å) (a_{Cr})	VCMA (fJ/Vm)	MCAE (SOI) (mJ/m^2)	SMAE (mJ/m^2)		MAE (MCAE+SMAE) (mJ/m^2)	
				DA	SDA	SOI + DA	SOI + SDA
Structure-I [1]	2.88	85	**0.586**	−1.353	**−1.336**	−0.763	**−0.750**
Structure-II [1]	2.88	89	**1.280**	−1.097	**−1.053**	0.183	**0.227**
Exp. [2]	2.88	~300	–	–	–	0.651	**~ 0.500**

[1] I. Pardede et al., Crystals 10, 1118 (2020)
I. Pardede et al., IEEE Trans. Magn. 55, 2860581 (2018)
[2] T. Nozaki et al., Phys. Rev. Appl., 5, 044006 (2016)

Interface Fe/MgO (Structure-II) : MCA

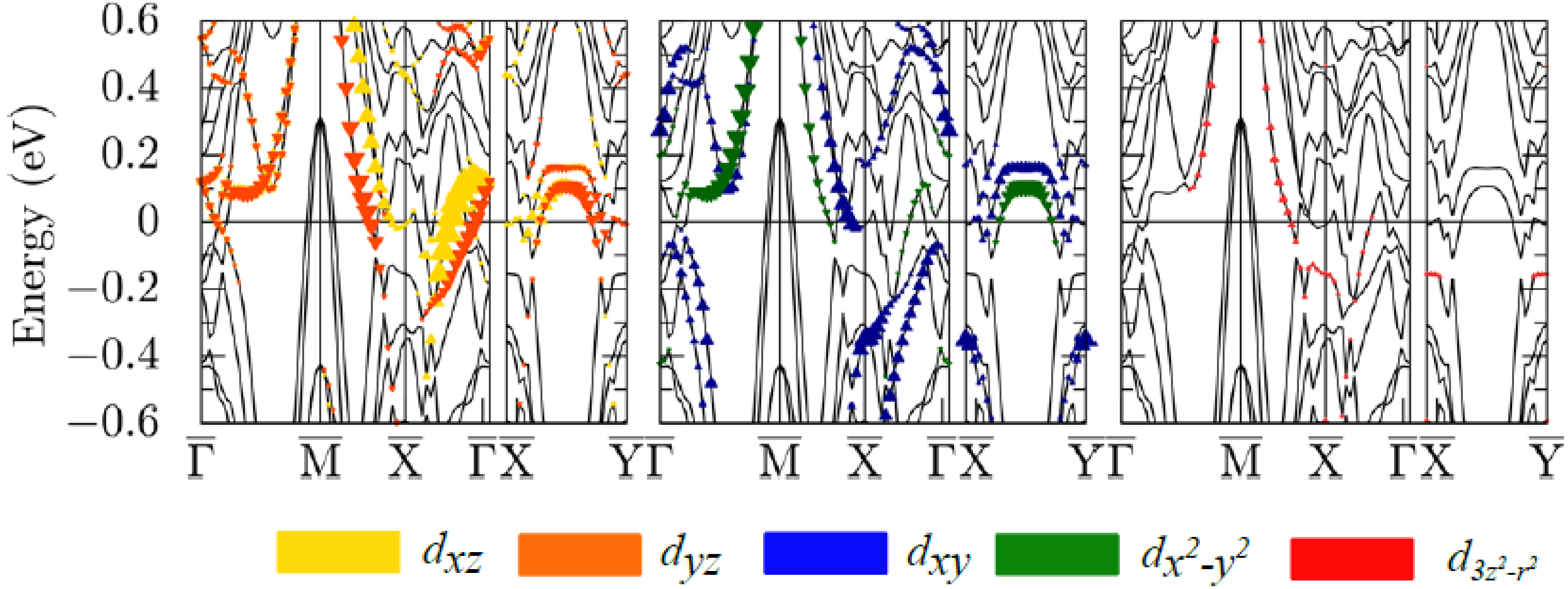

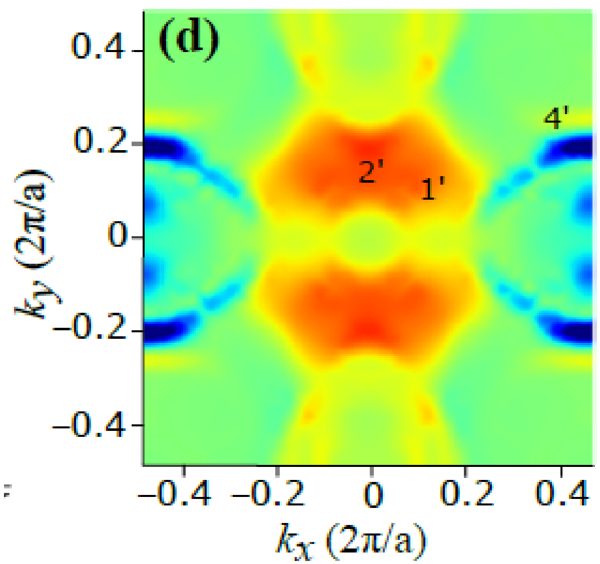

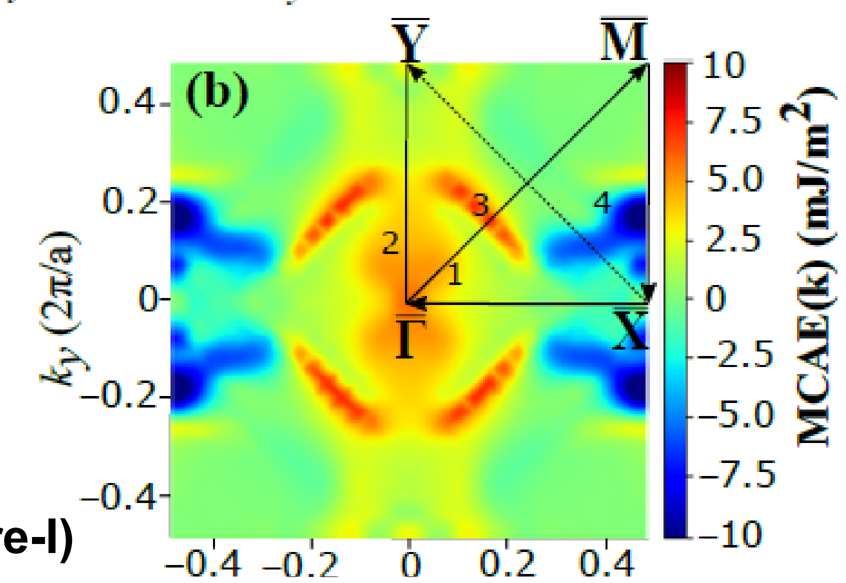

(Structure-I)

Interface Fe/MgO (Structure-II) : SMA

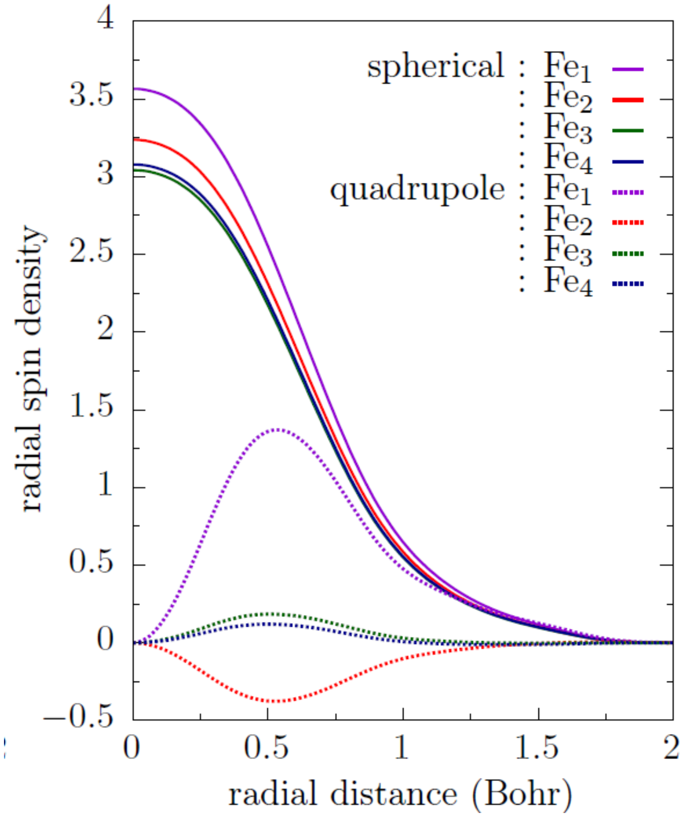

Fe_1

prolate

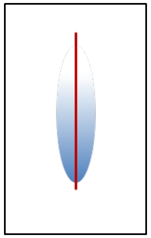

Structure	SMAE (mJ/m^2)	
	DA	SDA
Structure-I	−1.353	**−1.336**
Structure-II	−1.097	**−1.053**

Reduction is not so much in this case.

I. Pardede et al., Crystals 10, 1118 (2020)

Strain effect on MAE and VCMA in Fe/MgO interface

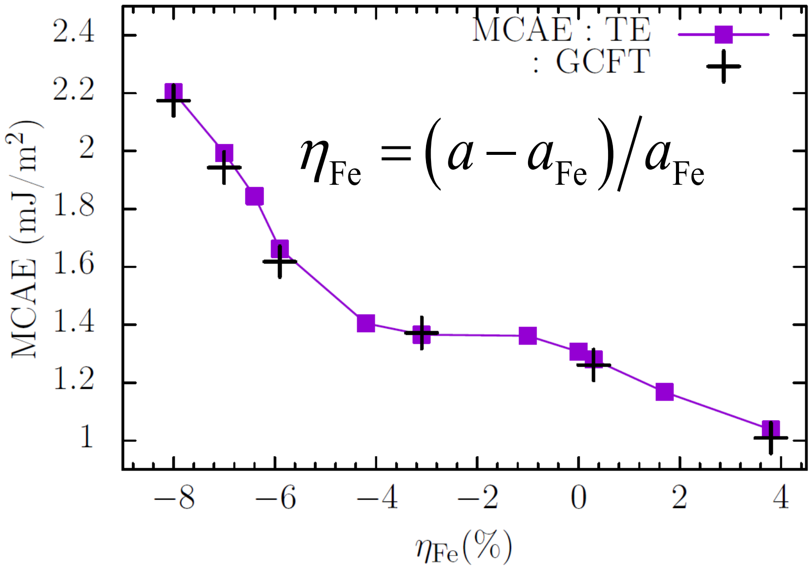

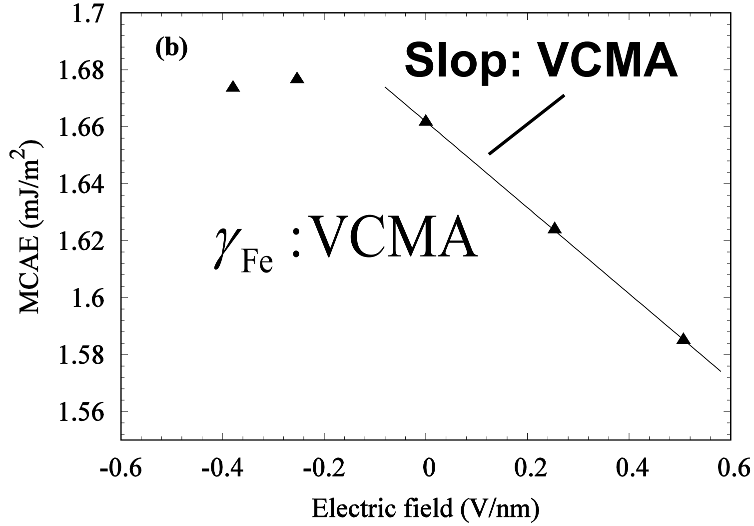

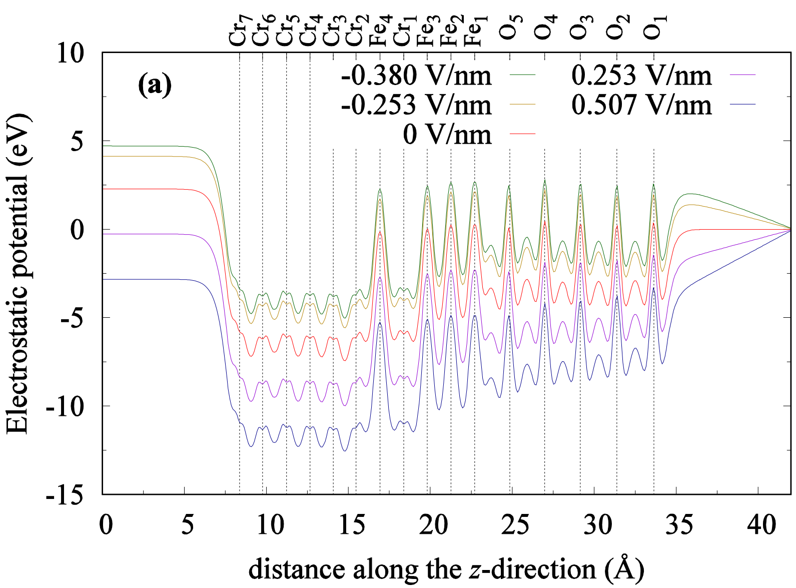

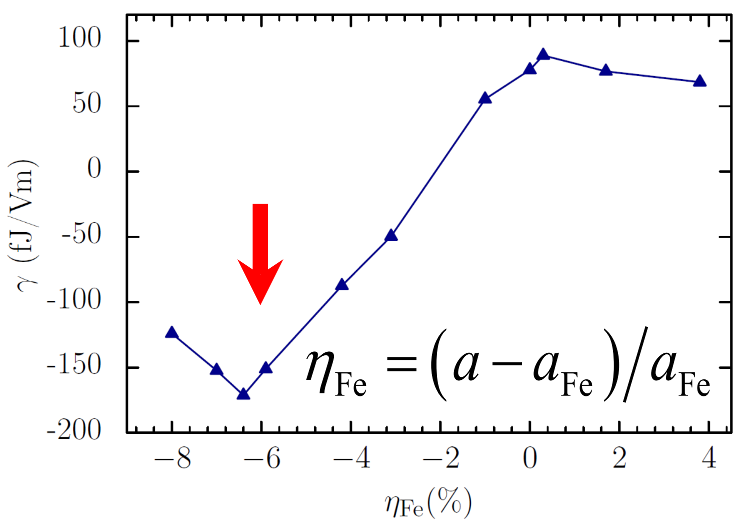

I. Pardede et al., Crystals 10, 1118 (2020)

Strain effect in the Fe-Cr mixing system

The system different from the previous page

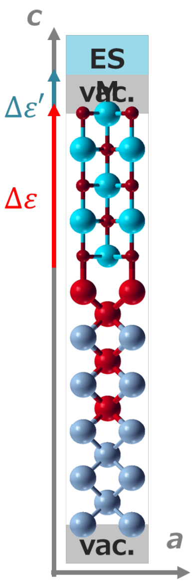

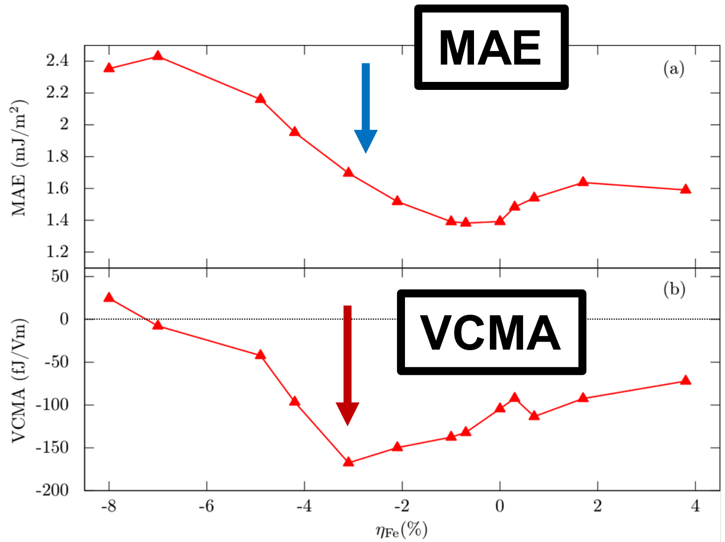

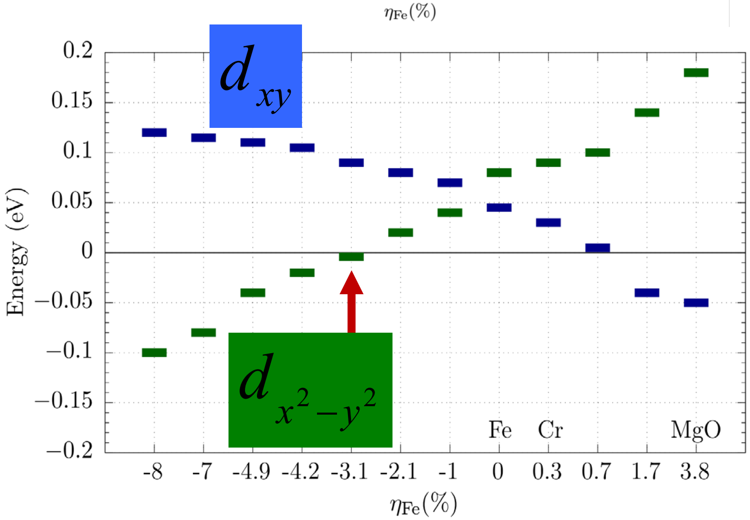

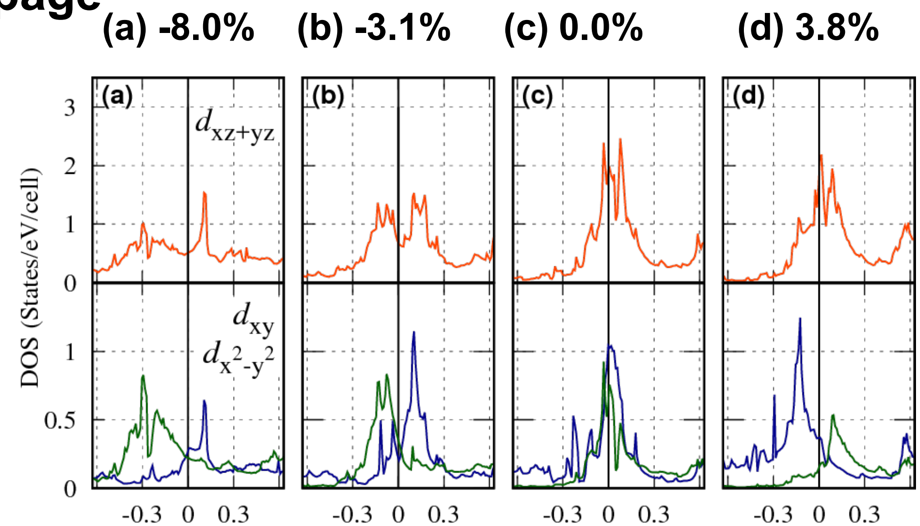

MAE: k-resolved map at -3.1%

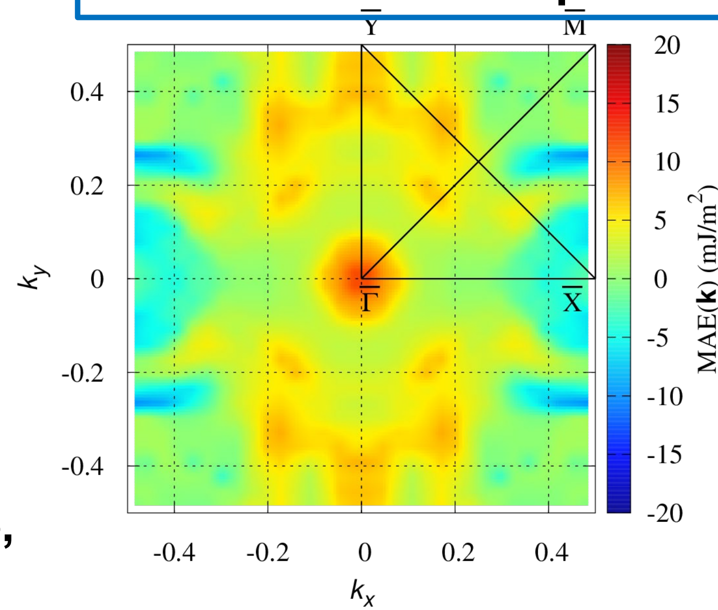

I. Pardede et al., IEEE Trans. Magn. 55, 2860581 (2018).

VCMA at the compressive strain (-3.1%)

MAE: Layer resolved

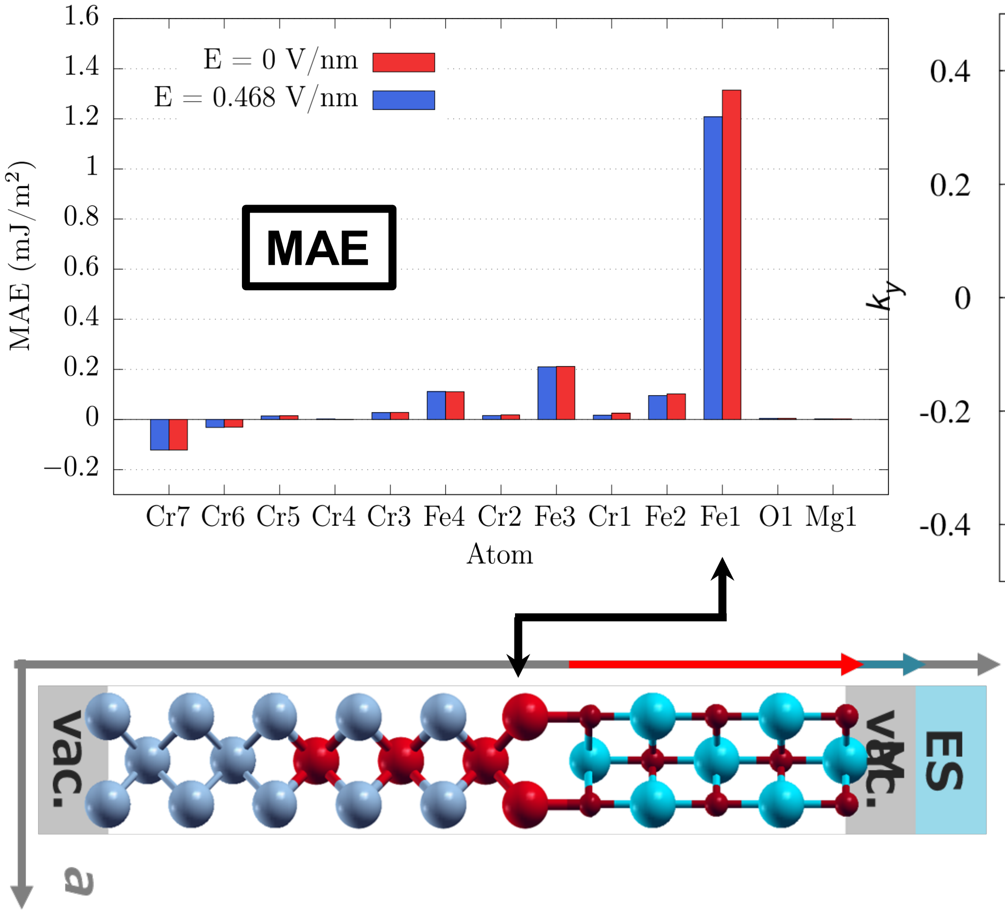

VCMA: k-resolved (k-map)

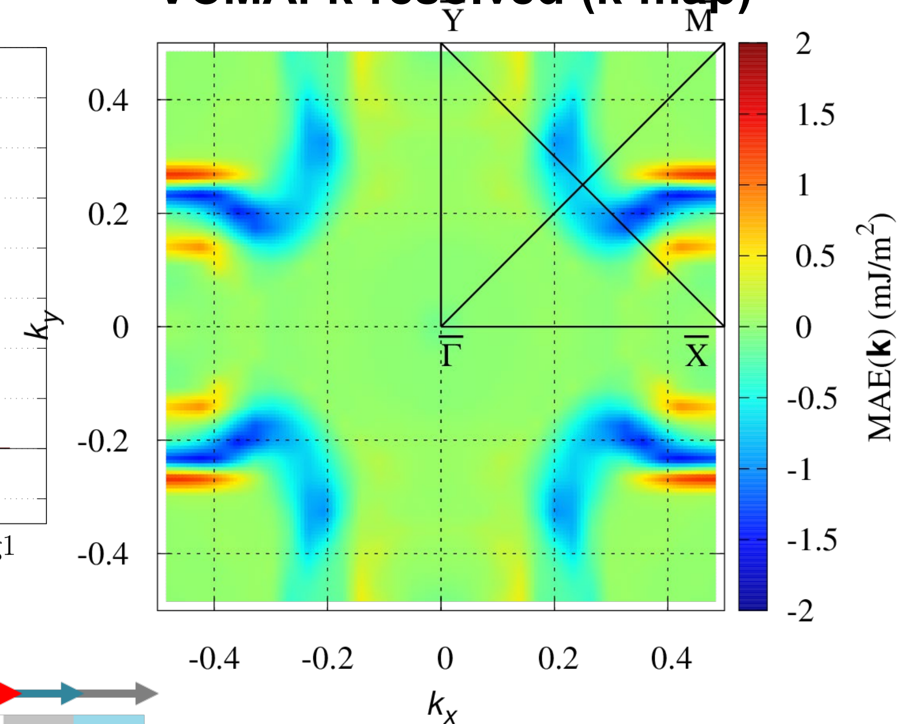

(5-8) Magnetic anisotropy of thin film: Ni/Co/Ni multilayer

I. Pardede et al., J. Magn. Magn. Mater., **500**, 166357 (2020).

Large PMA   Ni/Co/Ni layer

Potential for STT-MRAM

- ❑ **High PMA**
- ❑ **High spin polarization**
- ❑ **Low damping constant**

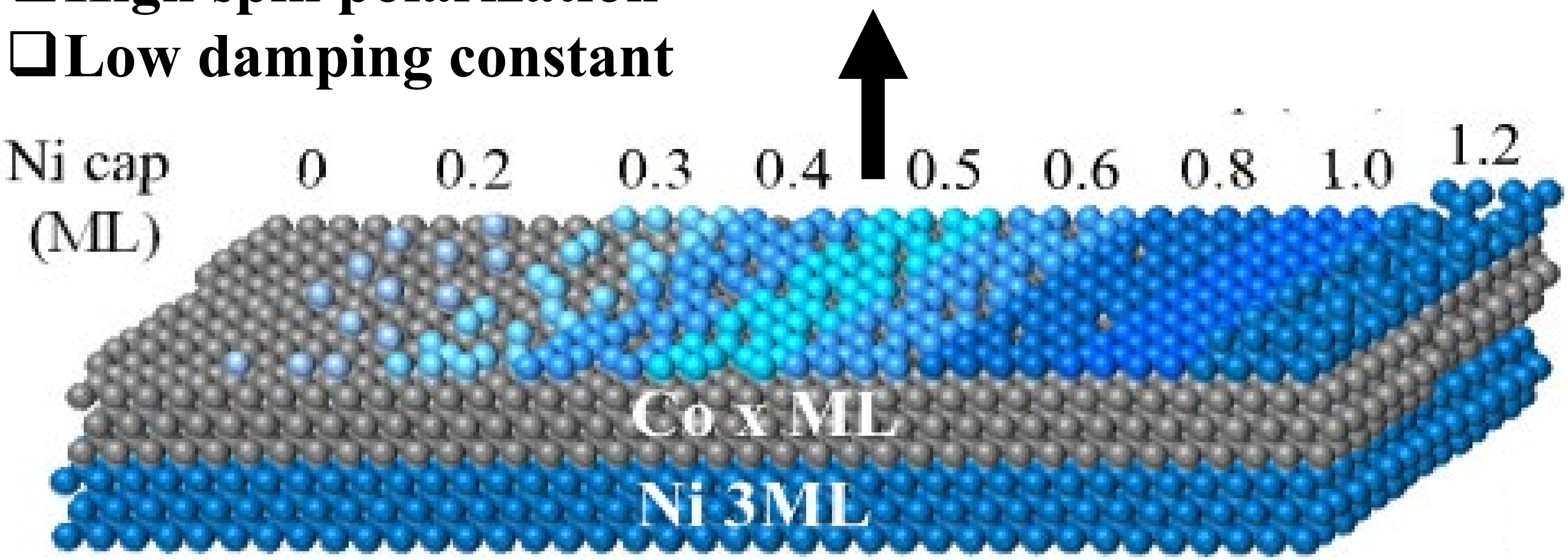

Co/Ni multilayer

S. Andrieu et al, Phys. Rev. Matt., 2:064410 (2018).

Ni/Co/Ni layer

Experimental systems

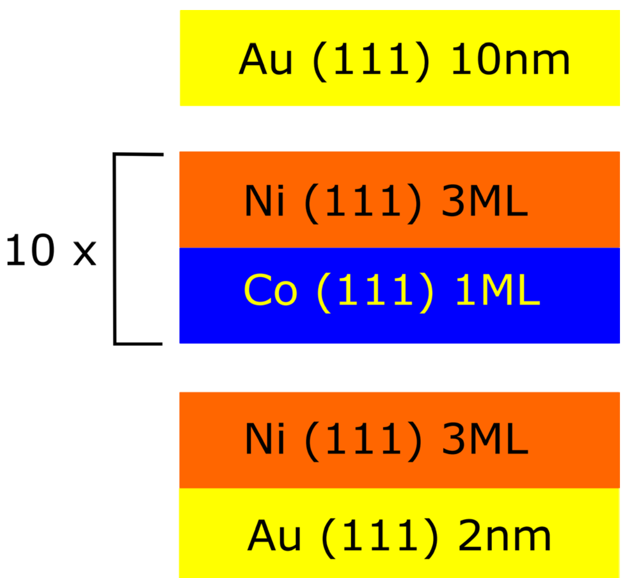

The structural models of SDFT approach

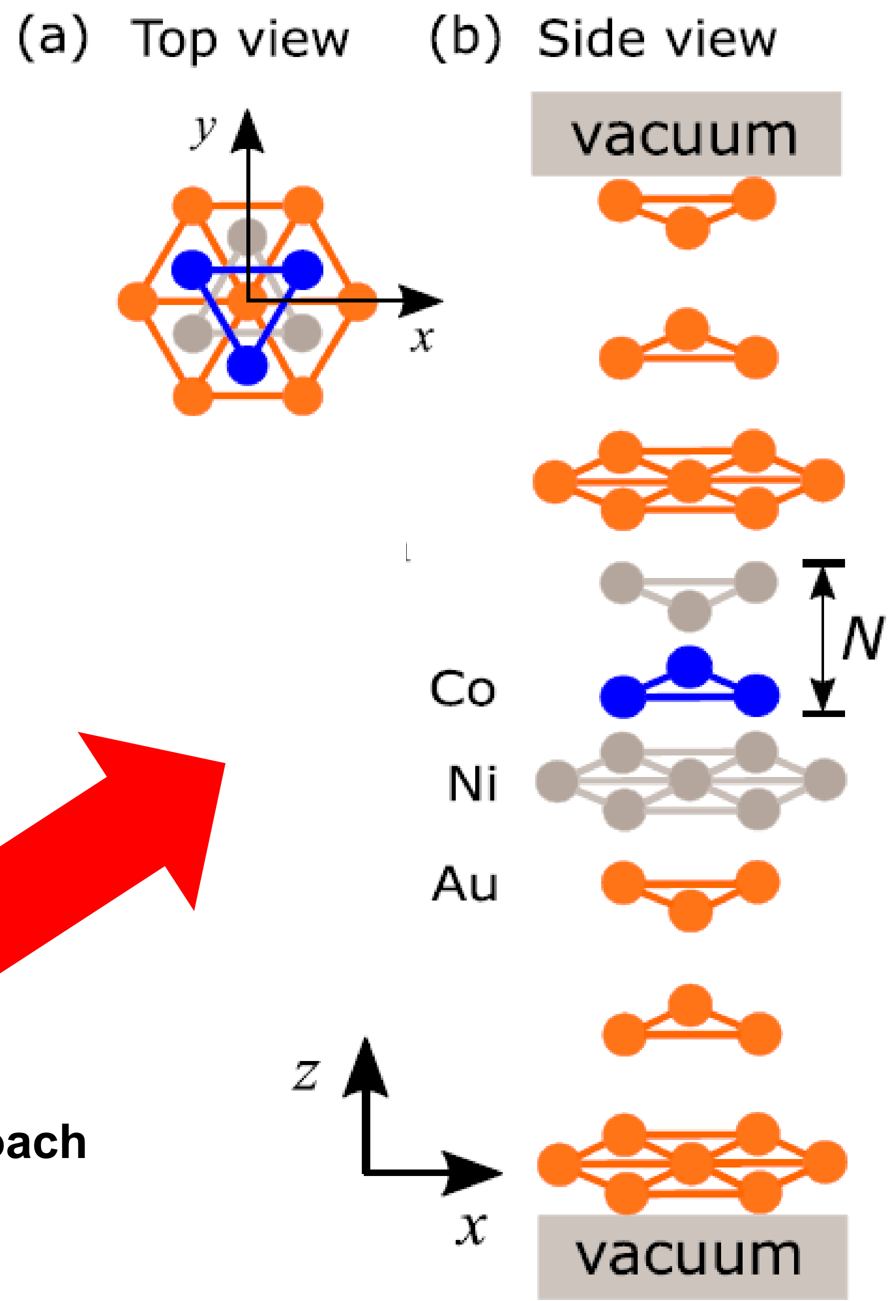

Atom- and $\boldsymbol{k}$-resolved MCAE: Au/[Ni(t_{Ni})/Co(1ML)]$_N$/Ni(t_{Ni})/Au

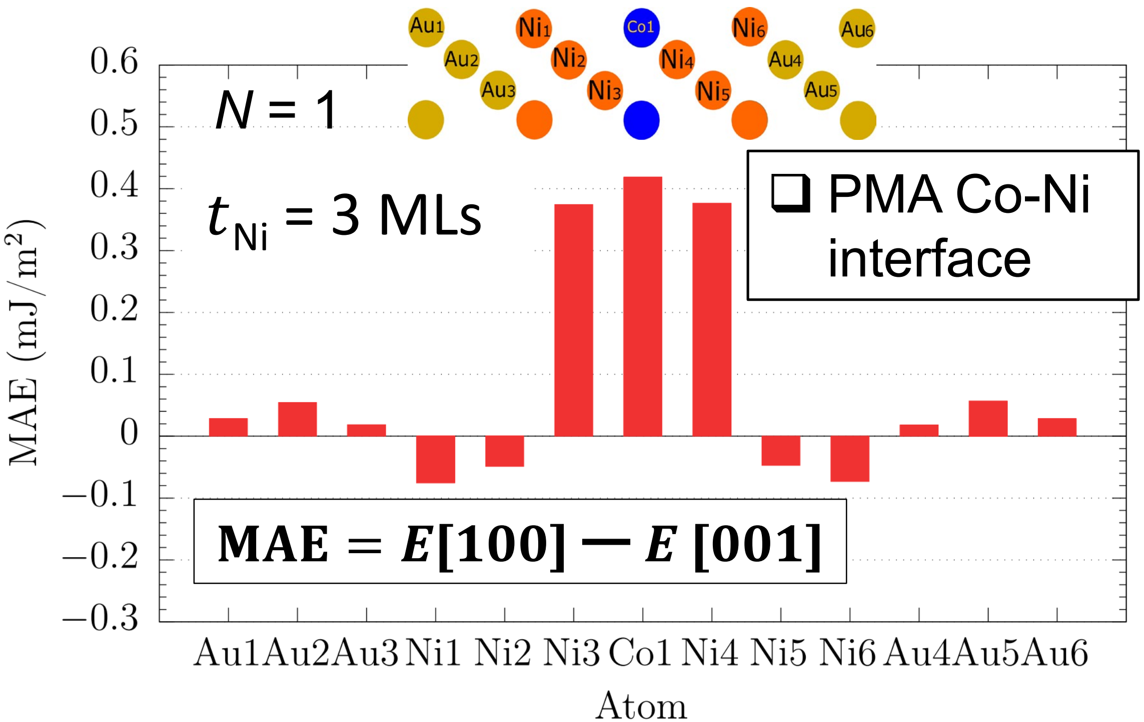

MAE = E[010] — E[001]

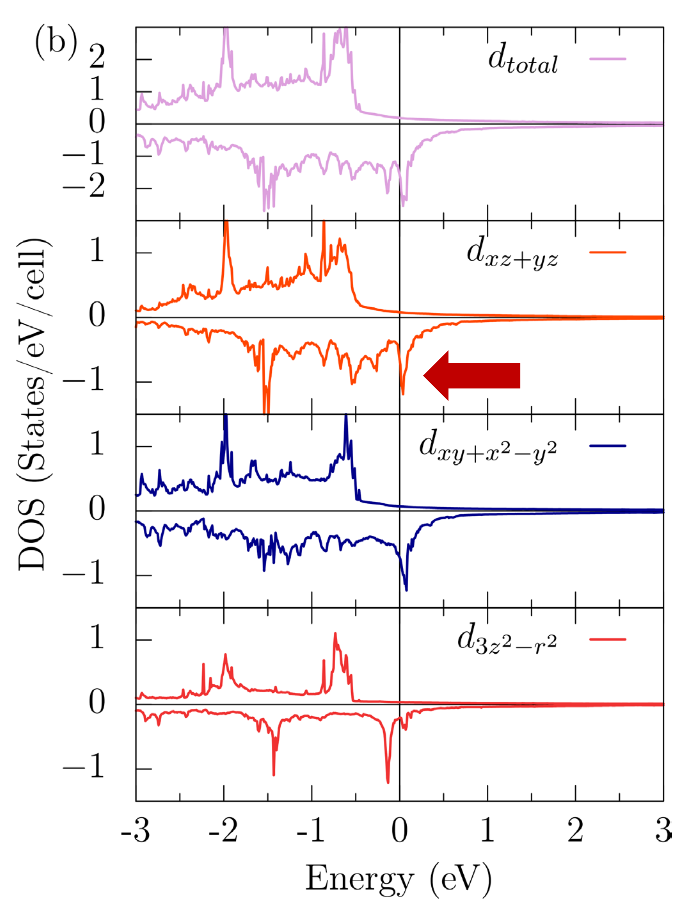

Not-symmetrized (Bare)

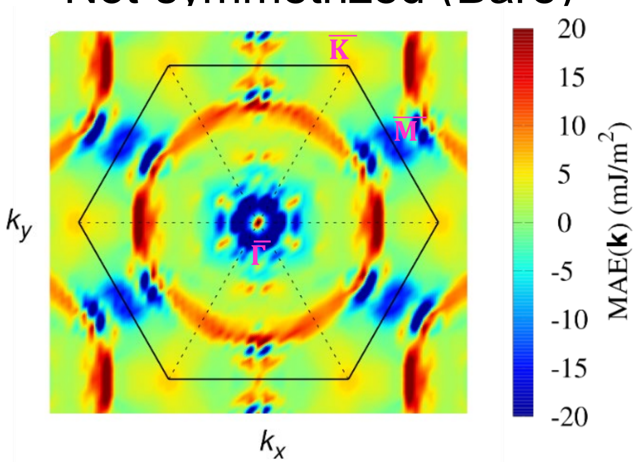

- ❑ Positive: along the $\bar{\Gamma}$-$\bar{K}$ line
- ❑ Negative: $\bar{\Gamma}$ and $\bar{M}$ points

I. Pardede et al., J. Magn. Magn. Mater., **500**, 166357 (2020).

High spin polarization **70 %**

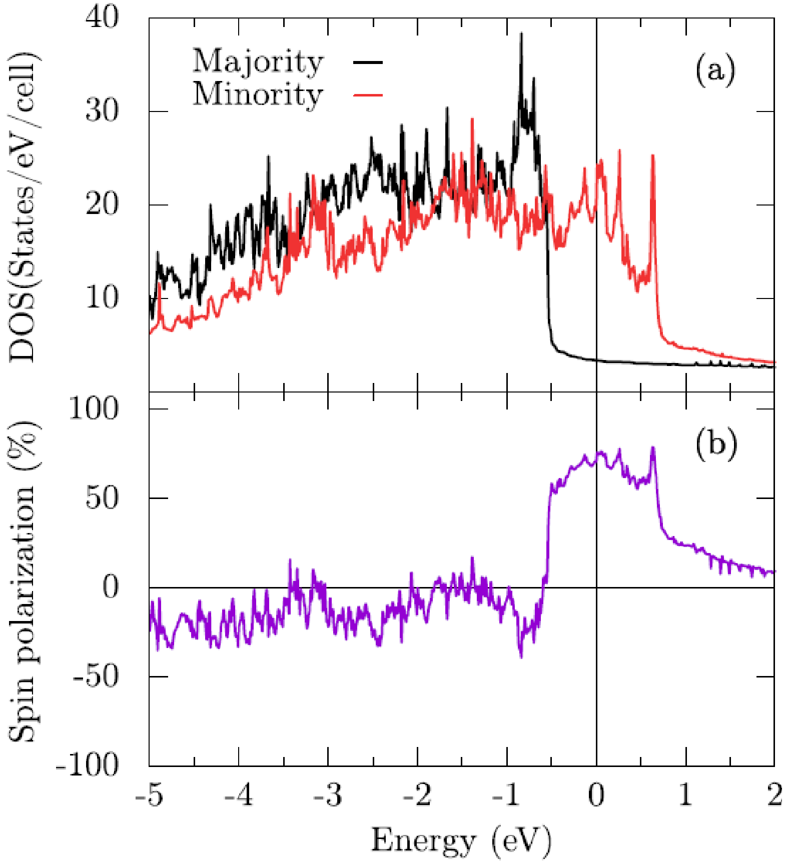

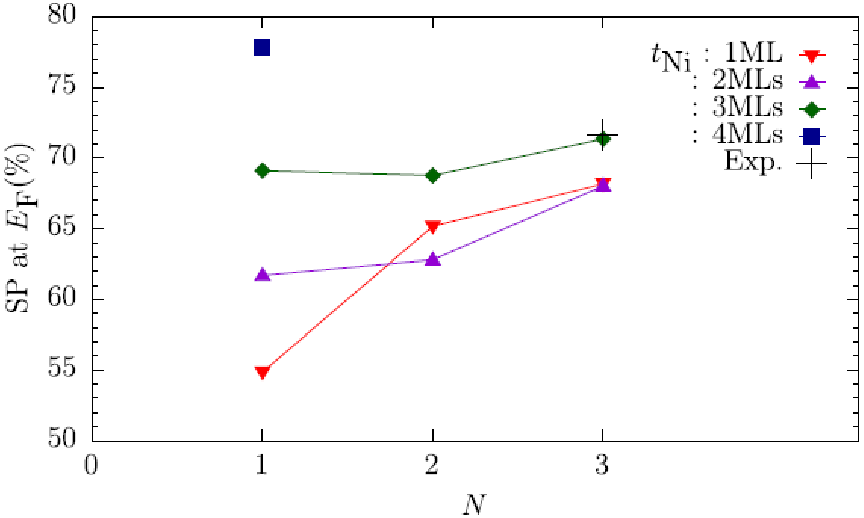

TE(total energy) and GCFT on MCAE

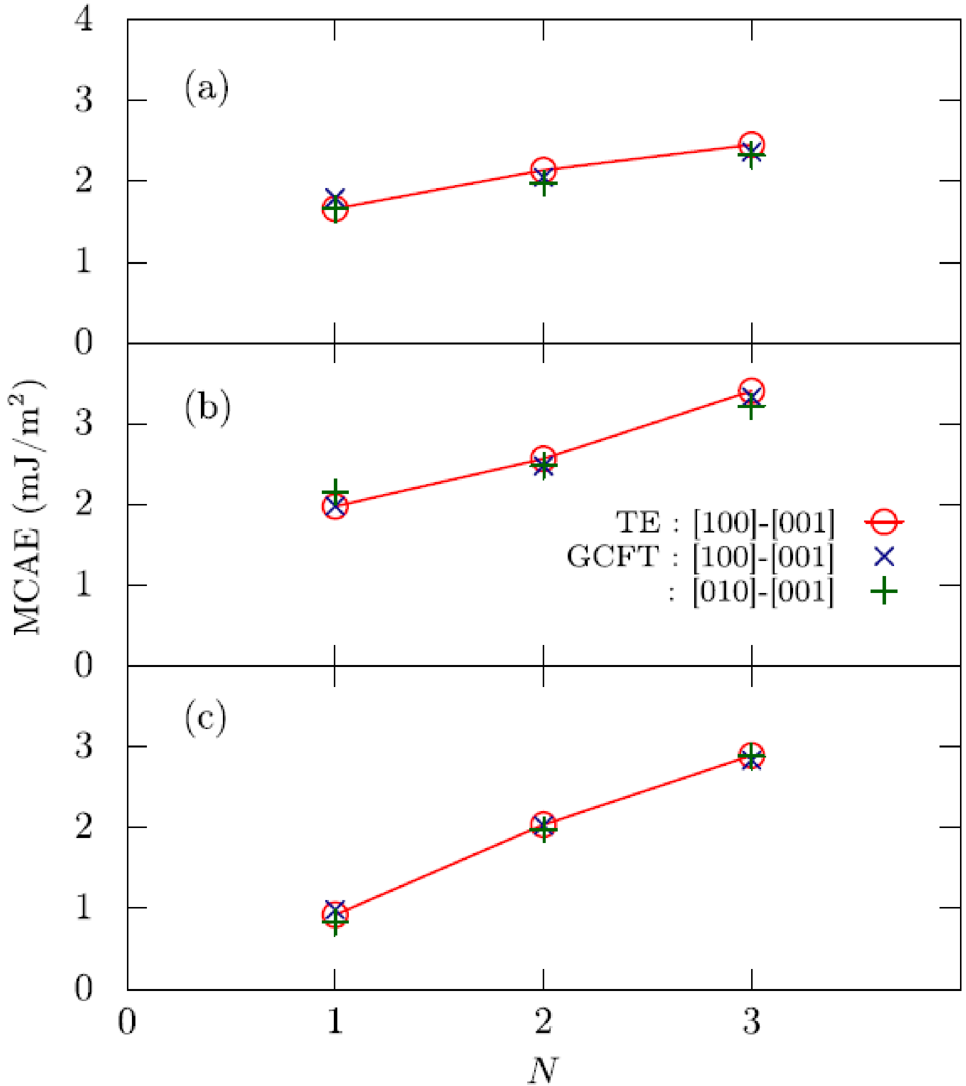

Both methods provide similar value on MCAE.

MDI contribution to SMAE

Empty symbols: Spin density approach (SDA)

Filled symbols: Discrete approach(DA)

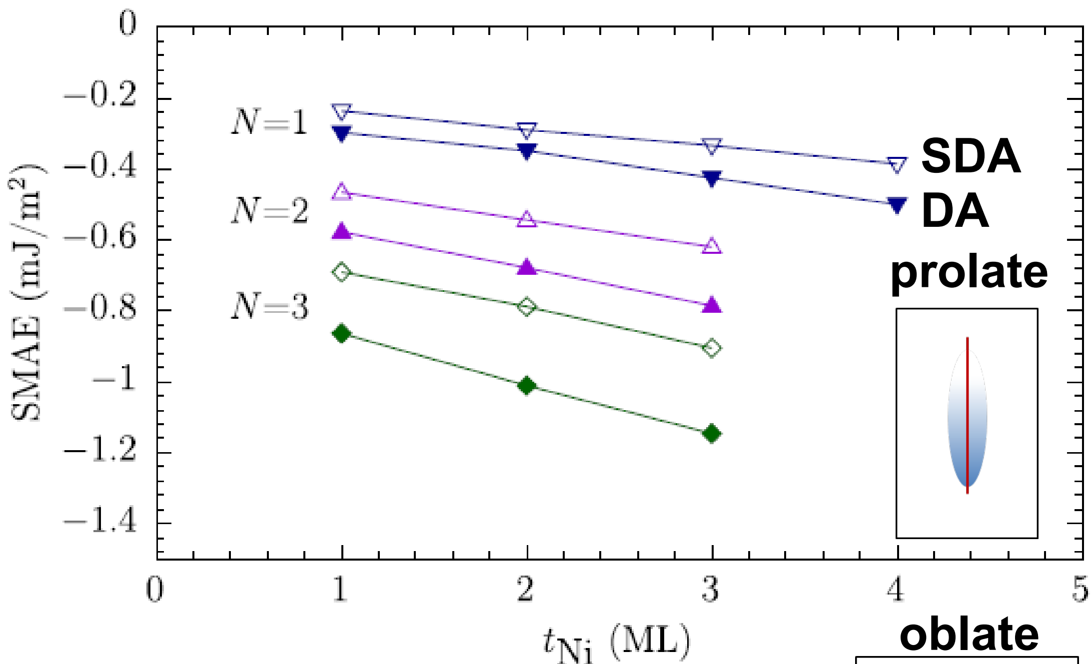

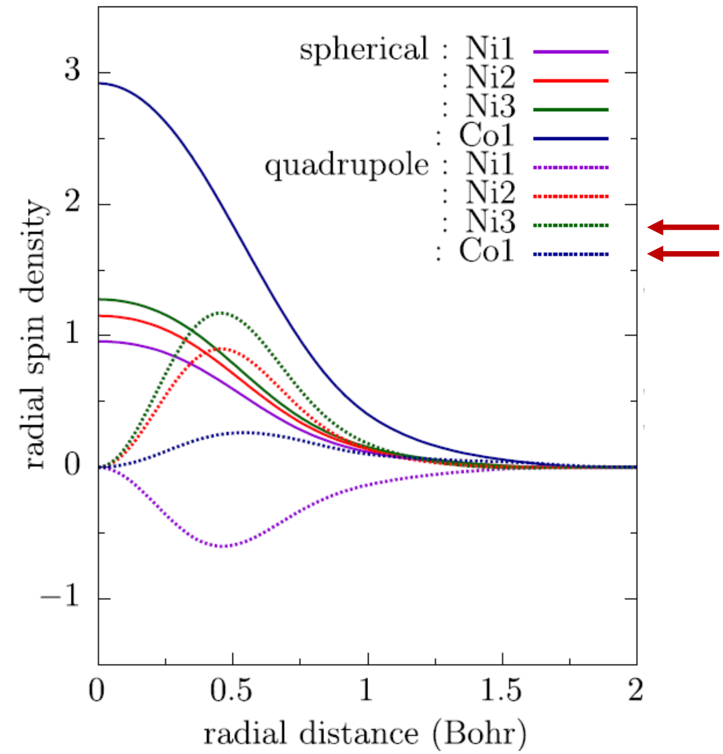

oblate

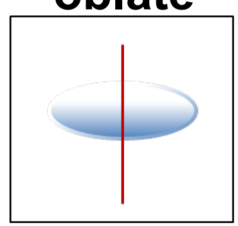

Larger difference between SDA and DA

There are quadrupole contribution to SMAE.

The prolate (oblate) shape of spin density leads a decrease (an increase) of the in-plane anisotropy

Total magnetic anisotropy (MAE): Au/Ni/Co/Ni/Au

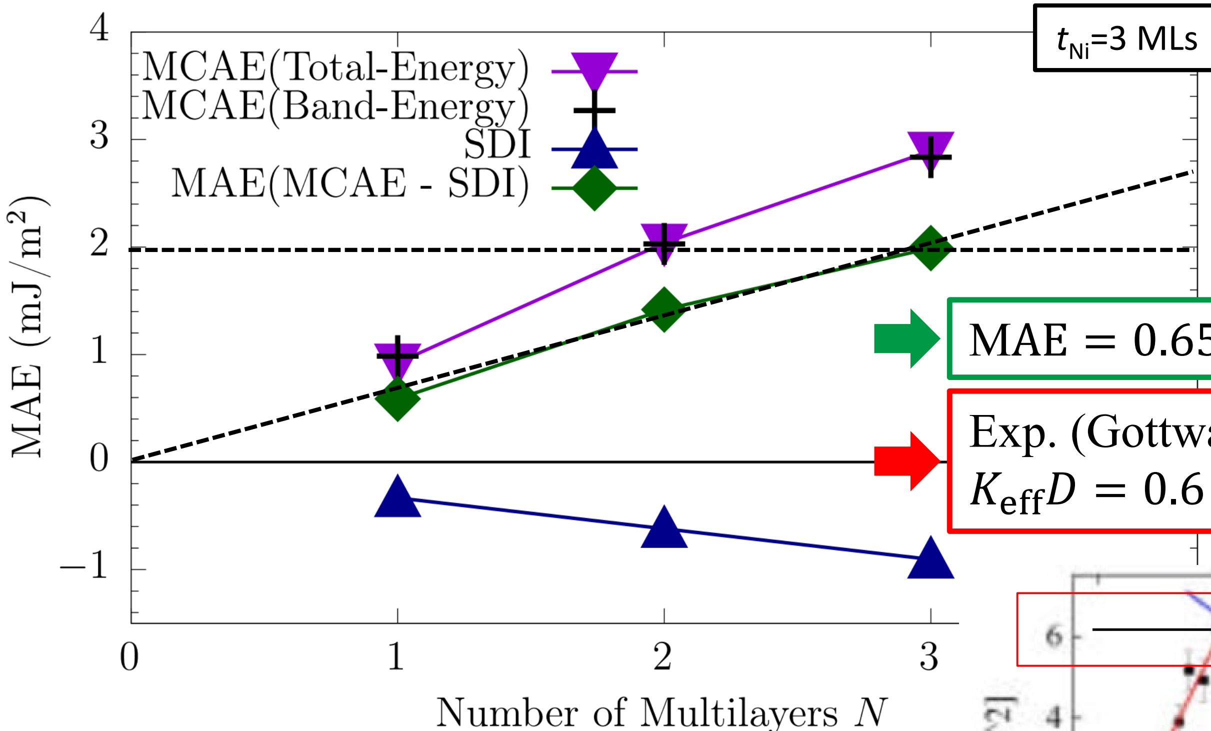

MAE=
MCAE +
SMAE

$\text{MAE} = 0.65\ \text{mJ/m}^2/N$

Exp. (Gottwald et al.)
$K_{\text{eff}}D = 0.6\ \text{mJ/m}^2/N$

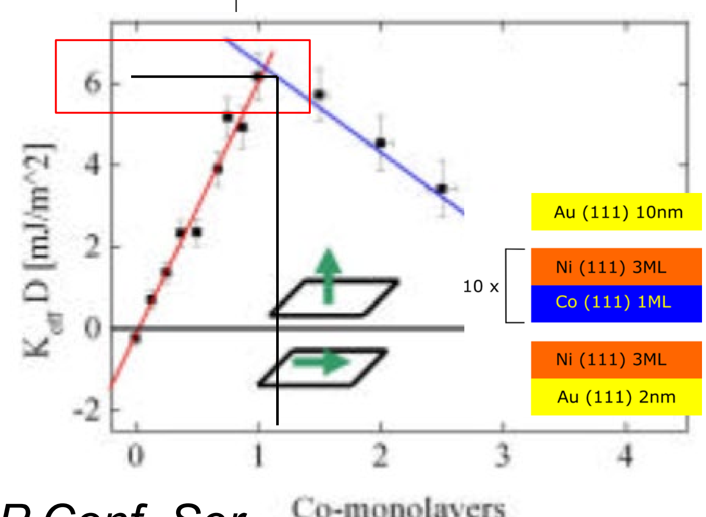

- ❑ Positive MAE indicates a PMA.
- ❑ For N = 3, the MAE reaches to the value of 2 mJ/m².

M. Gottwald *et al*, *IOP Conf. Ser. Mater. Sci. Eng* **12**, 012018, (2010).

Layer resolved MCAE

$$\mathbf{MAE} = \boldsymbol{E}[\mathbf{010}] - \boldsymbol{E}[\mathbf{001}]$$

$$\vec{M} \propto [010]$$
$$\vec{E} \propto [001]$$

Rashba potential induced

The potential of spin-orbit coupling (SOC)

$$H_{\mathrm{SOI}} = \frac{\hbar}{4m^2c^2}\vec{\sigma}\cdot\left(\mathrm{grad}\, V(\vec{r})\times\vec{p}\right) \propto \vec{M}\cdot\left(\vec{E}\times\vec{k}\right)$$

$$\Delta_{\mathrm{SOI}}\left(\vec{k}\right) \propto \vec{M}\cdot\left(\underline{\vec{E}}\times\vec{k}\right)$$

$$\Delta_{\mathrm{SOI}}\left(\vec{k}\right) \propto k_x$$

$$\propto \left(\vec{e}_y \times \underline{\vec{e}_z}\right)\bullet\vec{k} \propto k_x$$

Energy splitting of SOC is proportional to the linear Term.

$$\varepsilon\left(\vec{k}\right) = \varepsilon_0\left(\vec{k}\right) + \alpha_{\mathrm{SOI}}\left(\vec{k}\right)k_x$$

$$\frac{1}{2}\left\{\varepsilon\left(k_x\right) + \varepsilon\left(-k_x\right)\right\} = \varepsilon_0\left(\vec{k}\right)$$

Using $E_{\mathrm{SDFT}}^{\mathbf{m},\mathrm{GCFT}}\left(I,\mathbf{k}\right)$

Non-symmetrized **Symmetrized**

$$\frac{1}{2}\left\{\mathrm{MCAE}\left(k_x\right) + \mathrm{MCAE}\left(-k_x\right)\right\} = \mathrm{sym}(\mathrm{MCAE})\left(\vec{k}\right)$$

As shown in the next pages,

t_{Ni}=2 MLs, N = 1

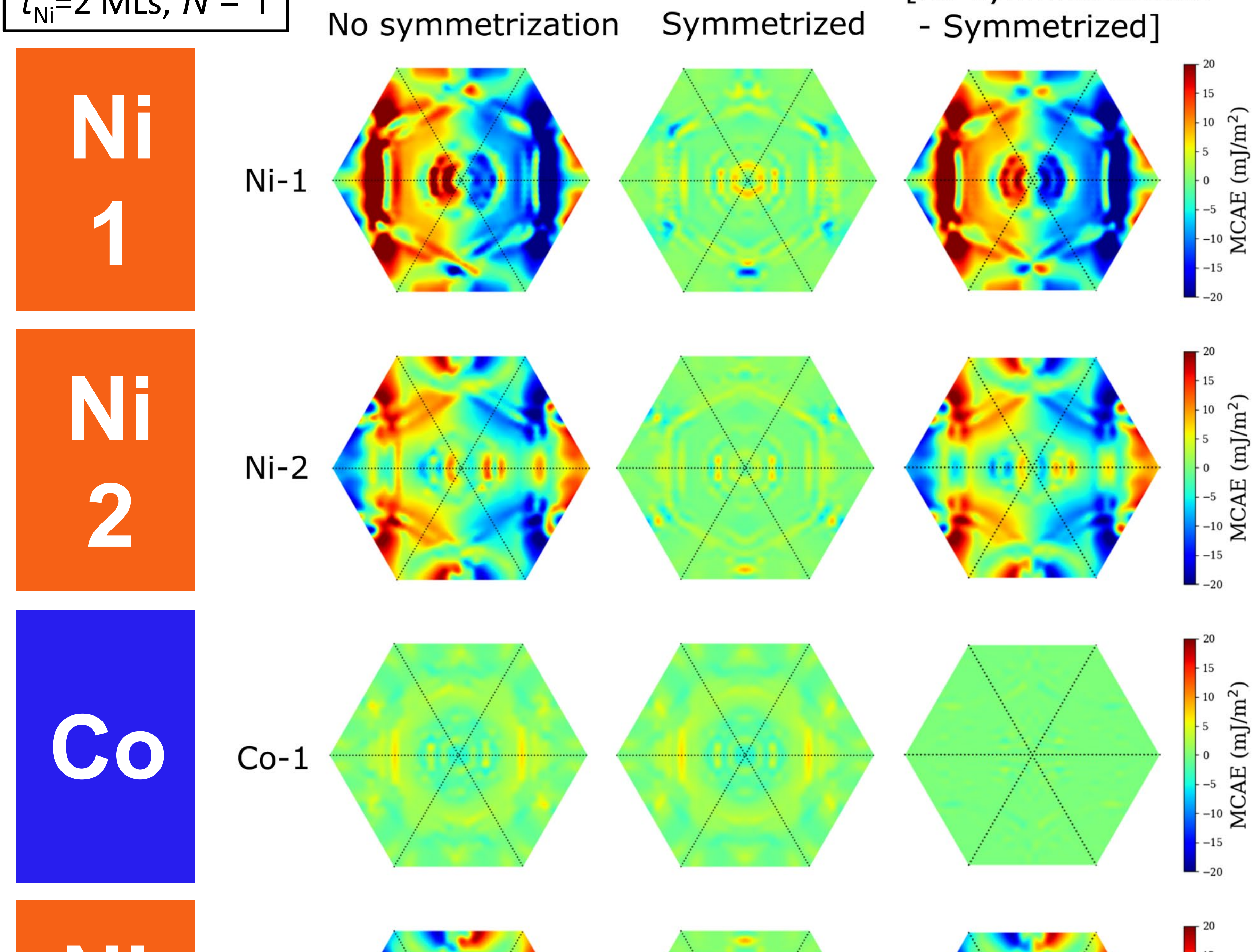

Ni 1
Ni 2
Co
No symmetrization
Symmetrized
[No symmetrization - Symmetrized]
Ni-1
Ni-2
Co-1
MCAE (mJ/m²)
20
15
10
5
0
−5
−10
−15
−20

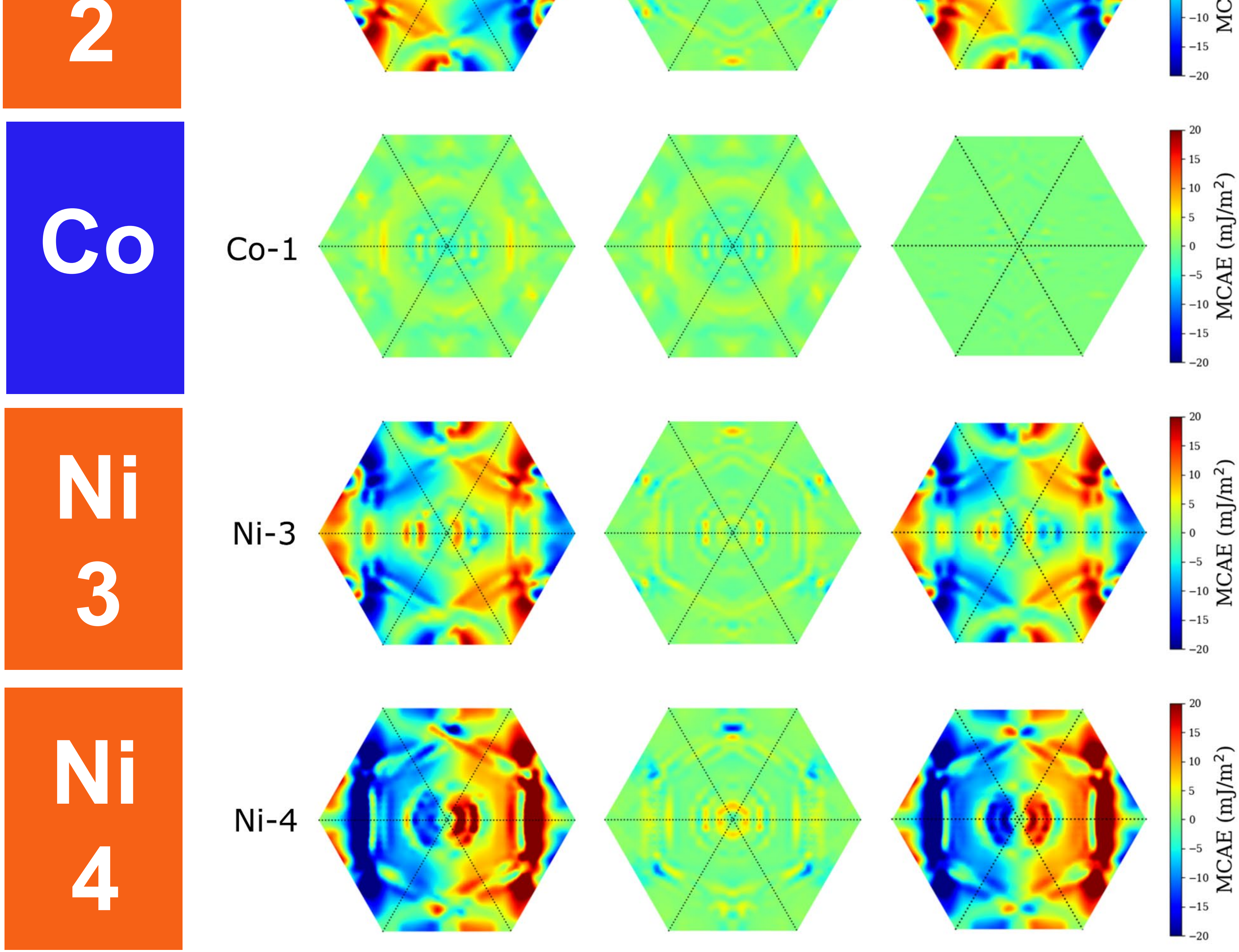
2
Co
Co-1
Ni
3
Ni-3
Ni
4
Ni-4
20
15
10
5
0
−5
−10
−15
−20
MCAE (mJ/m²)

(5-9) Electric polarization revers effects on the interface of magnetic anisotropy

- **Pt/CoO/ZnO interface**

Interface: magnetic metal and dielectric insulator (Exp.) magnetic anisotropy change by electric polarization switching

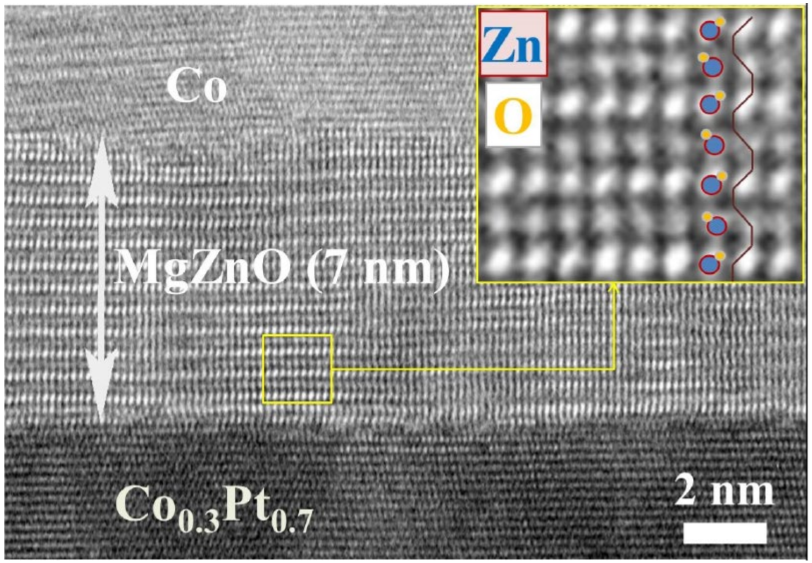

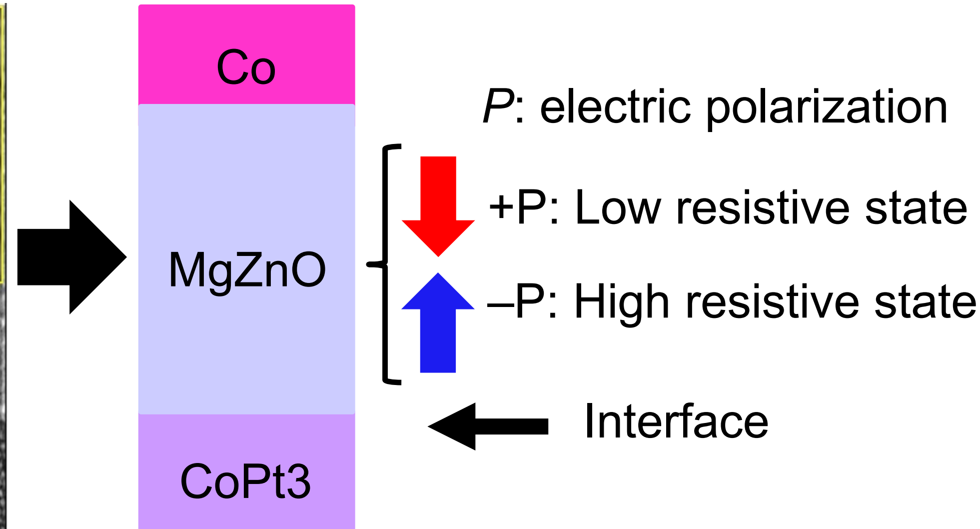

- ➢Theory: "Multi-ferroic-like"
- ➢Experiment: "New type MTJ"

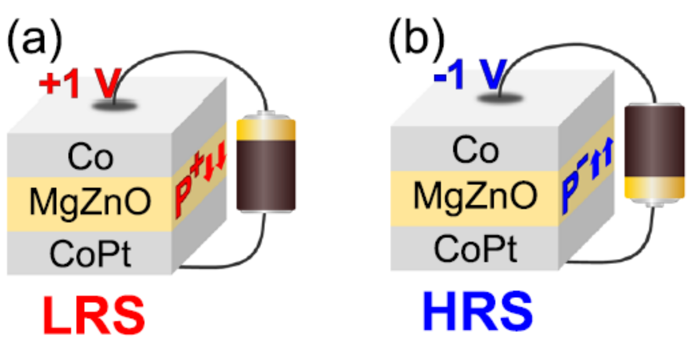

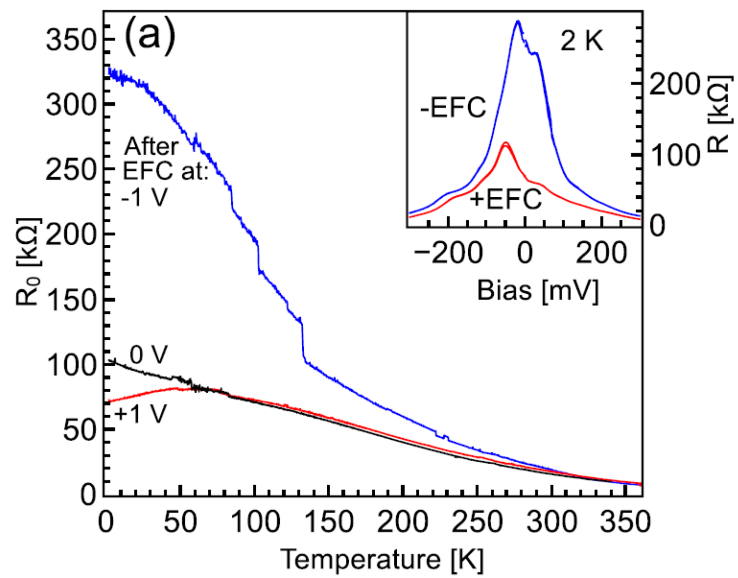

M. Belmoubarik et al., Appl. Phys. Lett.**109**, 054423(2016).

Interface: magnetic metal and dielectric insulator (DFT)

Low resistive state(LRS)

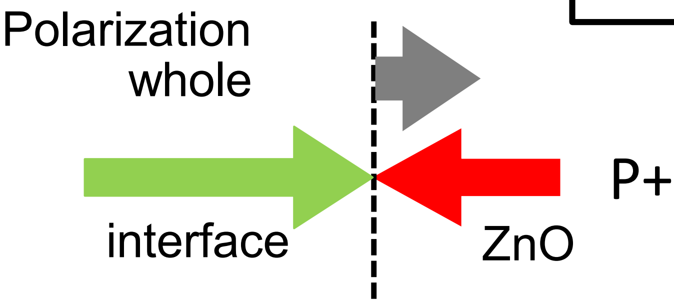

High resistive state(HRS)

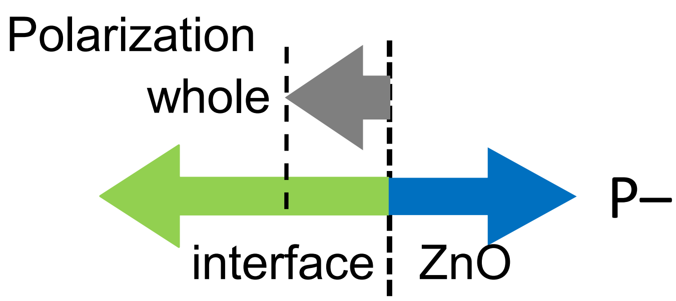

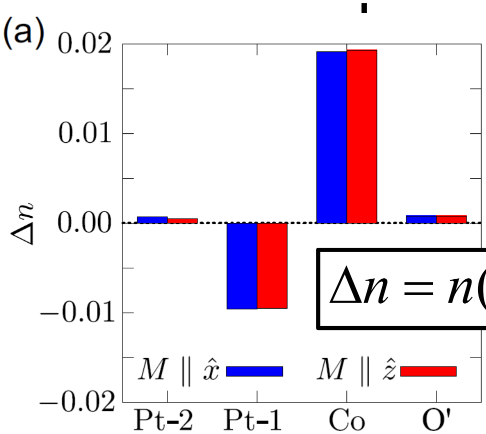

$$\Delta n = n(\mathrm{P}-) - n(\mathrm{P}+)$$

PtCoO/(ZnO)n-IcZnO

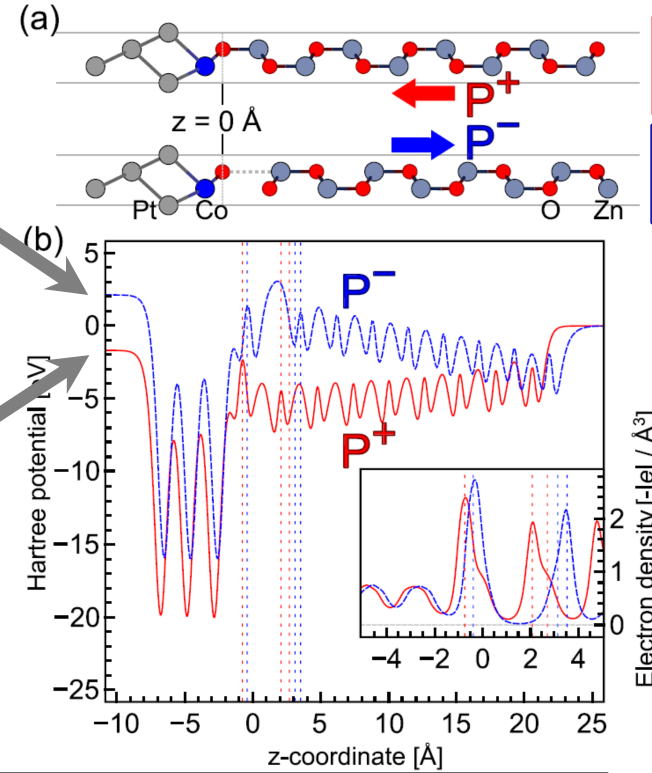

$$\mathbf{D}(z) = \varepsilon_0 \mathbf{E}(z) + \mathbf{P}(z)$$

MAE(SOI, int)

0.25 meV/cell

0.44 mJ/m²

-2.16 mJ/m²

-1.23 meV/cell

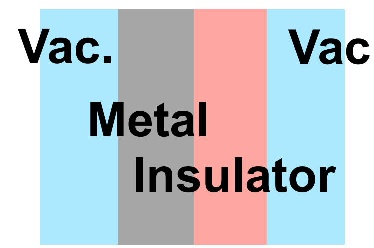

Throughout the slab

$$\mathbf{D}(z) = \mathbf{0}$$

For each layer

$$\mathbf{P}(z) = -\varepsilon_0 \mathbf{E}(z)$$

M. Al-Mahdawi et al., Phys. Rev. B **100**, 054423 (2019).

Density of states (DOS)

P+ P−

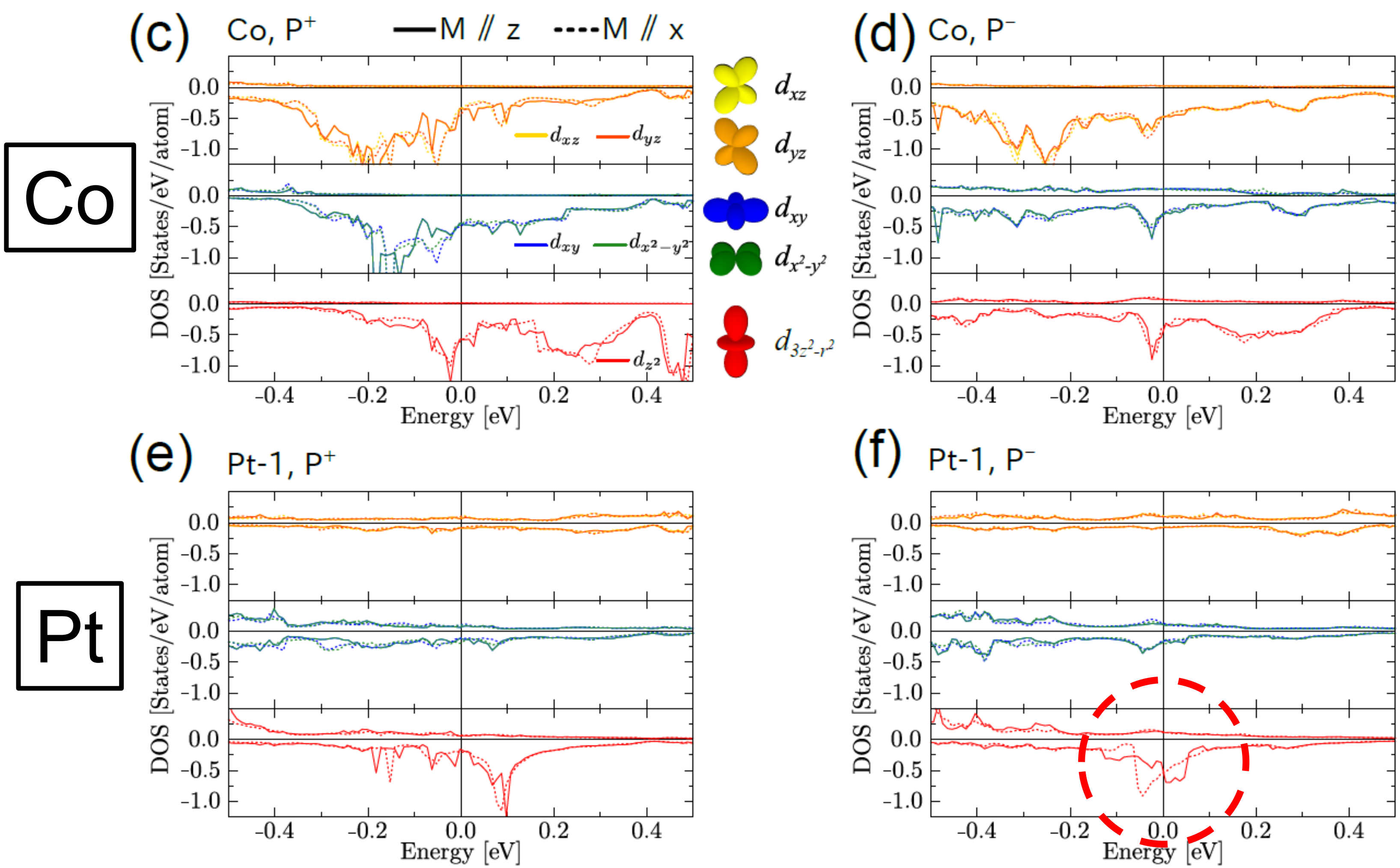

(5-10) Rashba parameter in the magnetic interface

Properties of Rashba type in the magnetic interface

Previous formula

$$H_{\mathrm{SOI}} = \frac{\hbar}{4m^2c^2}\vec{\sigma}\cdot\left(\mathrm{grad}\,V(\vec{r})\times\vec{p}\right) \propto \vec{M}\cdot\left(\vec{E}\times\vec{k}\right)$$

Rashba Hamiltonian

$$H_{\mathrm{R}} = \vec{\alpha}_R\cdot\left(\vec{k}\times\vec{\sigma}\right) = -\alpha_{\mathrm{R}}k_y\sigma_x$$

$$\begin{cases} \vec{E} \approx \alpha_R \vec{e}_z \\ \alpha_R = \dfrac{\hbar^2}{4m^2c^2}E \end{cases}$$

Using the GCFT formula,

$$\langle M_S\alpha_R\rangle = -\frac{1}{N_{\mathbf{k}}}\sum_{\mathbf{k}}\frac{\left[\sum_n \delta\varepsilon_{n\mathbf{k}}^{\hat{\mathbf{m}},\mathrm{GCFT}}\right]_{\mathrm{asym}}}{k_y}$$

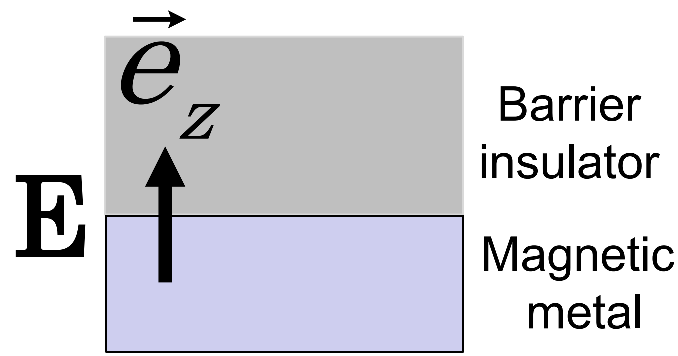

$$\alpha_R^I = \frac{\langle M_S\alpha_R\rangle_I}{m_S^I}$$

M_S **: Spin moment in Bohr magneton (mu_B)**

m_S^I **: Spin moment at *I*'th atom**

Averaged Rashba parameter in the magnetic interface

Fe(*n*ML)/MgO(5ML)

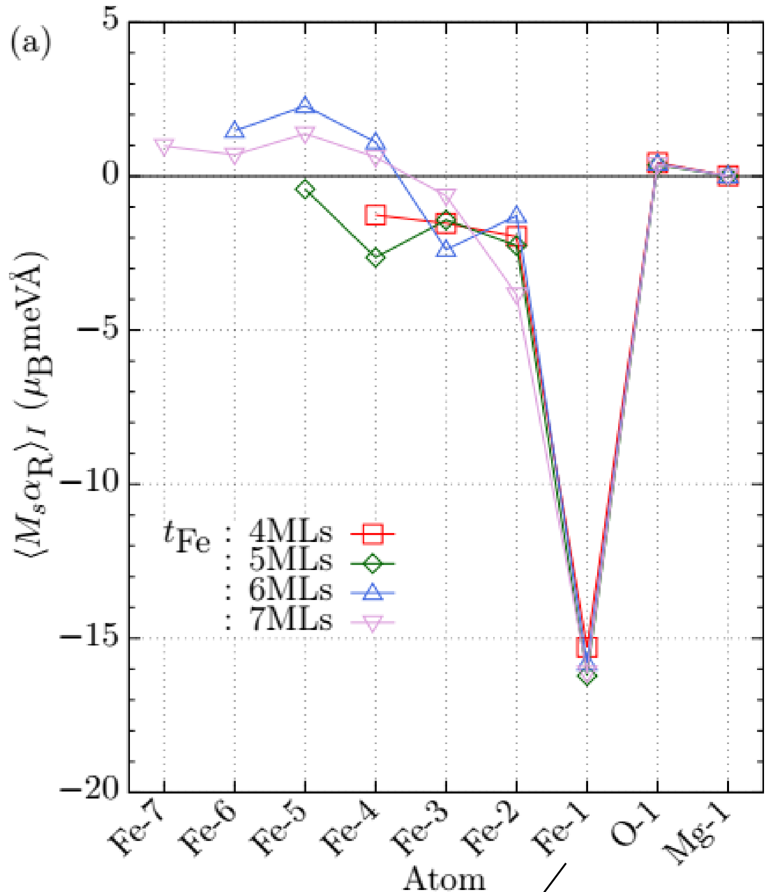

α_R (Fe1)	−5.6 meVÅ

PtCoO/(ZnO)n-lcZnO

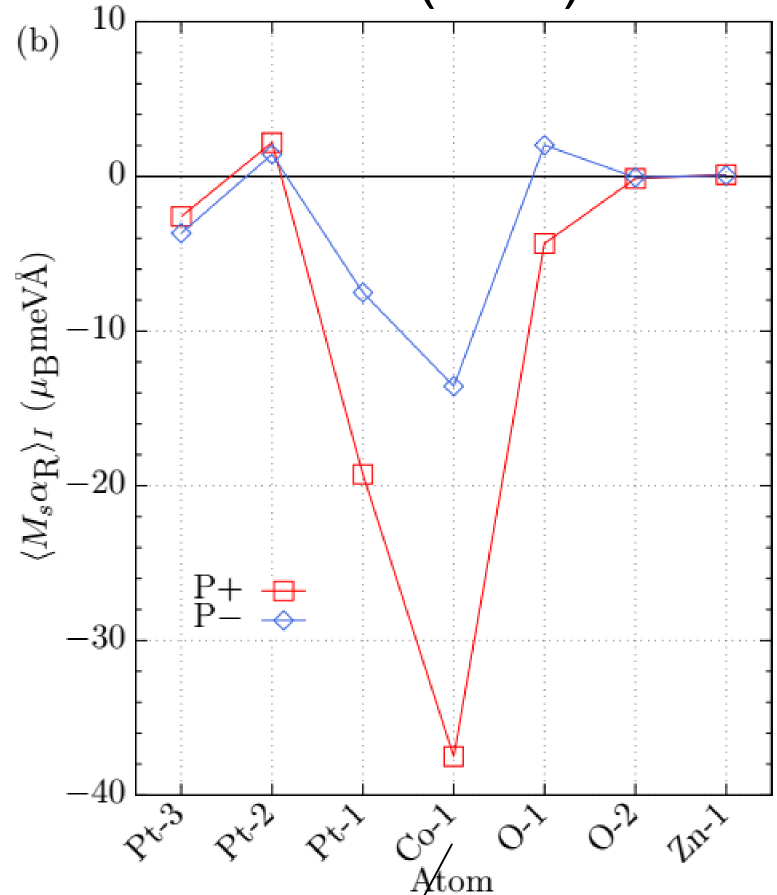

α_R(Co,P+)	−15.5 meVÅ
α_R(Co,P-)	−5.7 meVÅ

Summary

(5-1) Magnetic moment: spin, orbital, localized and itinerant
(5-2) Zeeman energy, Spin-orbit interaction
(5-3) Interaction between magnetic carriers: magnetic dipole interaction
(5-4) Control of magnetization
(5-5) Magnetic anisotropy energy: electron orbital, magnet shape
(5-6) Summary of density functional approach on magnetic anisotropy energy
(5-7) Magnetic anisotropy, Voltage-controlled magnetic anisotropy
(5-8) Magnetic anisotropy of thin film
(5-9) Electric polarization revers effects on the interface of magnetic anisotropy
(5-10) Rashba parameter in the magnetic interface

(Appendix 1)
Imposing the electric field perpendicular to surface/interface

A1-1. Imposing electric field

ESM (effective screening medium) method
(M.Otani and O.Sugino,Phys.Rev.B**73**,115407,2006)

Energy functional

$$E[n_e, V] = K[n_e] + E_{xc}[n_e] - \int d\vec{r}\,\frac{\varepsilon(\vec{r})}{8\pi}\left|\nabla V(\vec{r})\right|^2 + \int d\vec{r}\,[n_e(\vec{r}) + n_I(\vec{r})]V(\vec{r})$$

variation with the to static potential

variation with the orbital

Poisson equation

$$\nabla\cdot[\varepsilon(\vec{r})\nabla]V(\vec{r}) = -4\pi n_{tot}(\vec{r})$$

$$\nabla\cdot[\varepsilon(\vec{r})\nabla]G(\vec{r}) = -4\pi\delta(\vec{r}-\vec{r}\,')$$

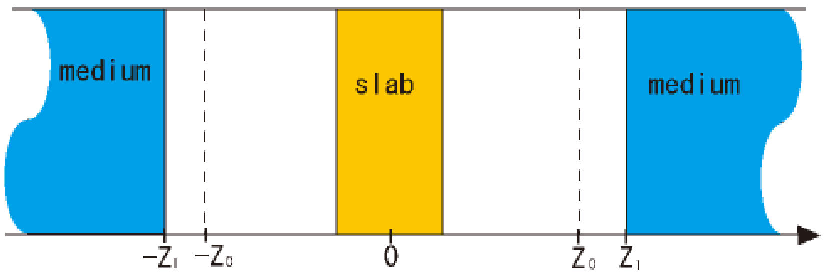

$$V(r) = \int d\vec{r}\,' G(\vec{r}, \vec{r}\,') n_{tot}(\vec{r}\,')$$

Kohn-Sham equation

$$\left[-\frac{1}{2}\nabla^2 + V(\vec{r}) + \hat{V}_{NL} + V_{xc}(\vec{r})\right]\phi_\alpha(\vec{r}) = \varepsilon_\alpha \phi_\alpha(\vec{r})$$

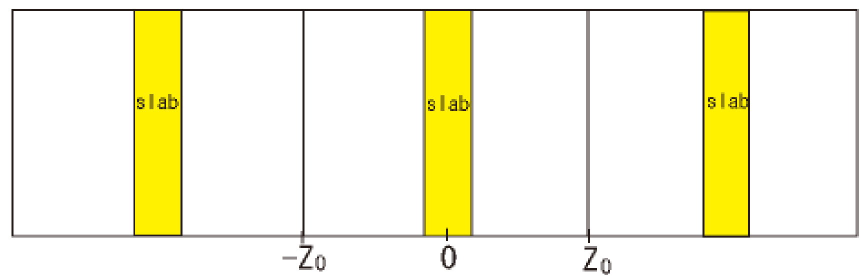

periodic boundary condition

Total energy representation by the Green's function

$$E[n_e] = K[n_e] + E_{xc}[n_e] + \frac{1}{2}\iint d\vec{r}\,d\vec{r}\,' n_e(\vec{r})G(\vec{r}, \vec{r}\,')n_e(\vec{r}\,')$$

$$+ \iint d\vec{r}\,d\vec{r}\,' n_e(\vec{r})G(\vec{r}, \vec{r}\,')n_I(\vec{r}\,') + \frac{1}{2}\iint n_I(\vec{r})G(\vec{r}, \vec{r}\,')n_I(\vec{r}\,')$$

A1-2.
Usual first-principles approach

Electrostatic potential (solution of Poisson's equation) ;

$$V_H(\vec{r}) = \int G(\vec{r},\vec{r}')n(\vec{r}')d\vec{r}'$$

$$G(\vec{r},\vec{r}') = \frac{1}{|\vec{r}-\vec{r}'|}$$

In practical, the above is calculated with the Fourier transformation

$$V_H(\vec{r}) = \sum_{\vec{g}(\neq 0)} \frac{4\pi}{\vec{g}^2} n(\vec{G})\, e^{i\vec{g}\cdot\vec{r}}$$

This procedure can not be applied for the system on which the electric field is imposed because of the breaking for the periodic boundary condition.

Imposing the electric field on a slab

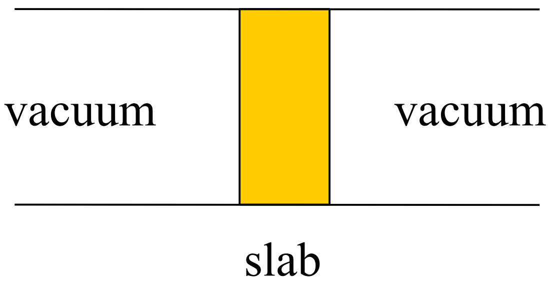

$$G(\vec{g}_{\parallel}, z, z') = \frac{4\pi}{2g_{\parallel}} e^{-g_{\parallel}|z-z'|}$$

$$V_H(\vec{g}_{\parallel}, z) = \int_{z_1}^{z_2} dz' G(\vec{g}_{\parallel}, z, z')\tilde{n}(\vec{g}_{\parallel}, z')$$

For small $g_{\parallel}$

$$G(\vec{g}_{\parallel}, z, z') = \frac{4\pi}{2g_{\parallel}} - 2\pi|z-z'|$$

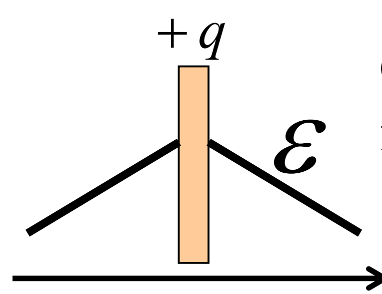

Green's function for a charged sheet

A1-3. ESM method (when the electrode is placed at one side of the cell.)

(M.Otani and O.Sugino,Phys.Rev.B73,115407,2006)

electrostatic potential $V(r) = \int d\vec{r}' G(\vec{r},\vec{r}') n_{tot}(\vec{r}')$

boundary condition $\begin{cases} V_H(\mathbf{g}_{\parallel}, z)\big|_{z=z_1} = 0 \\ \frac{\partial}{\partial z} V_H(\mathbf{g}_{\parallel}, z)\big|_{z=-\infty} = 0 \end{cases}$ $\varepsilon(z) = \begin{cases} 1 \text{ if } z \le z_1 \\ \infty \text{ if } z \ge z_1 \end{cases}$

$$G(\mathbf{g}_{\parallel}, z, z') = \frac{4\pi}{2g_{\parallel}} e^{-g_{\parallel}|z-z'|} - \frac{4\pi}{2g_{\parallel}} e^{-g_{\parallel}(2z_1 - z - z')}$$

the contribution from mirror image charge

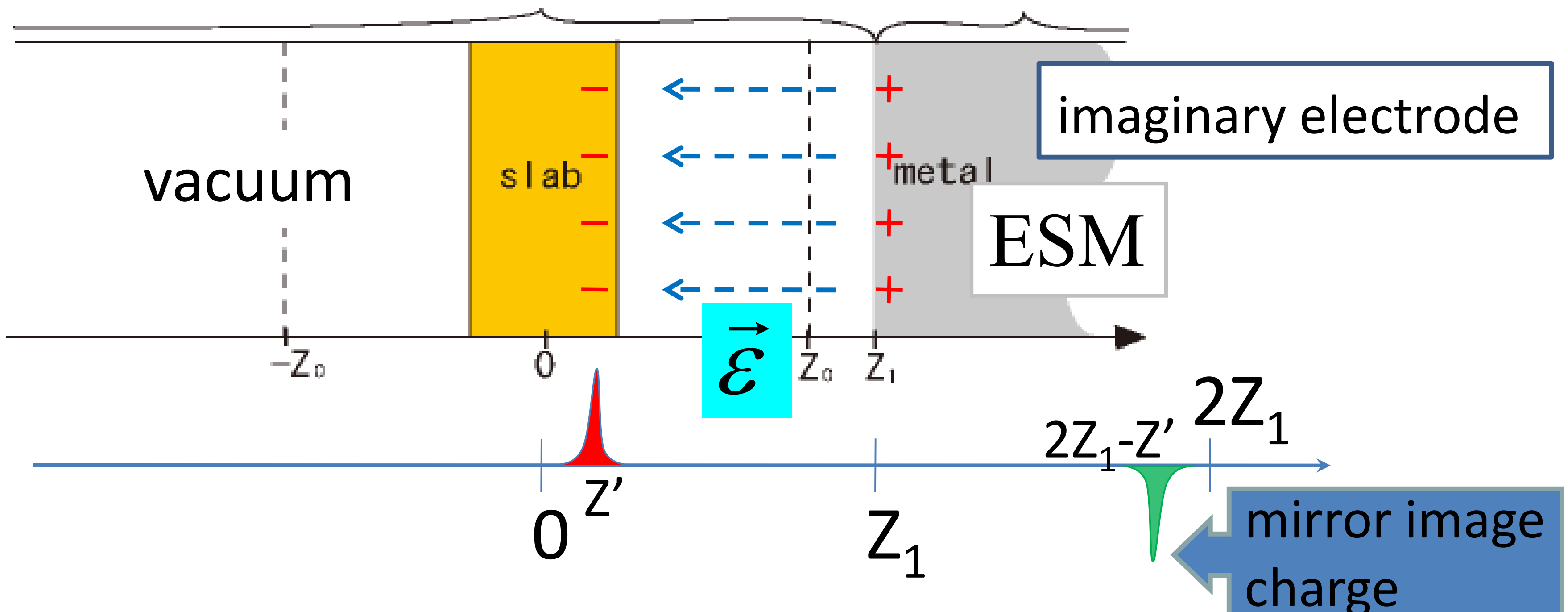

A1-4. Electric filed induced in scanning tunnel microscope (STM)

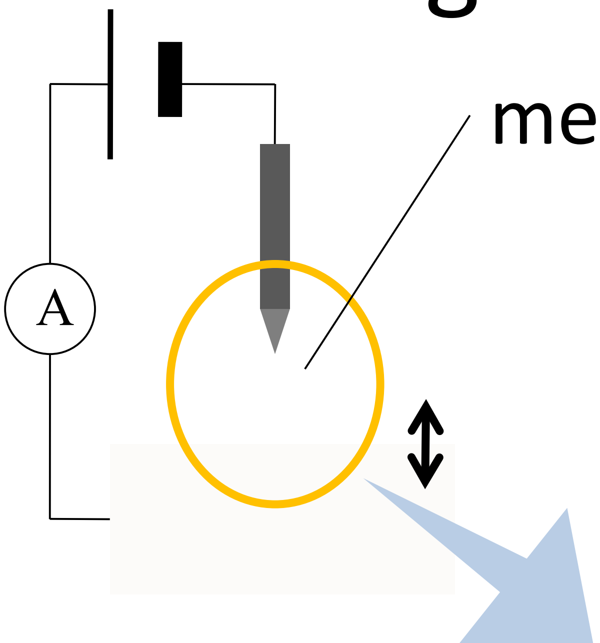

measure the tunnel current

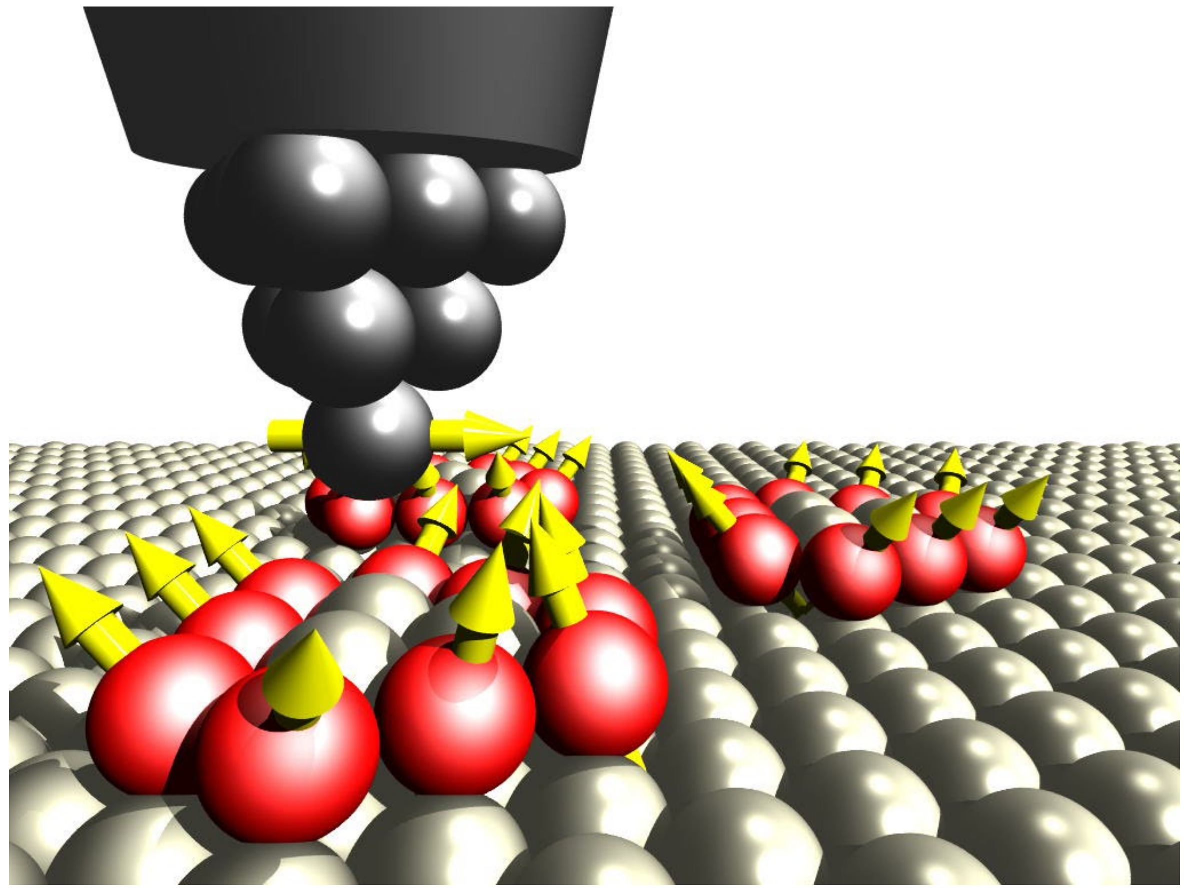

Scale of electric field

$$\approx 10^{8} - 10^{10}\,\mathrm{V/m}$$

(Appendix 2)
Single spin-state valley in the surface states of Tl/Si(111) and Tl/Si(110)

Tl/Si(111)-1×1 surface

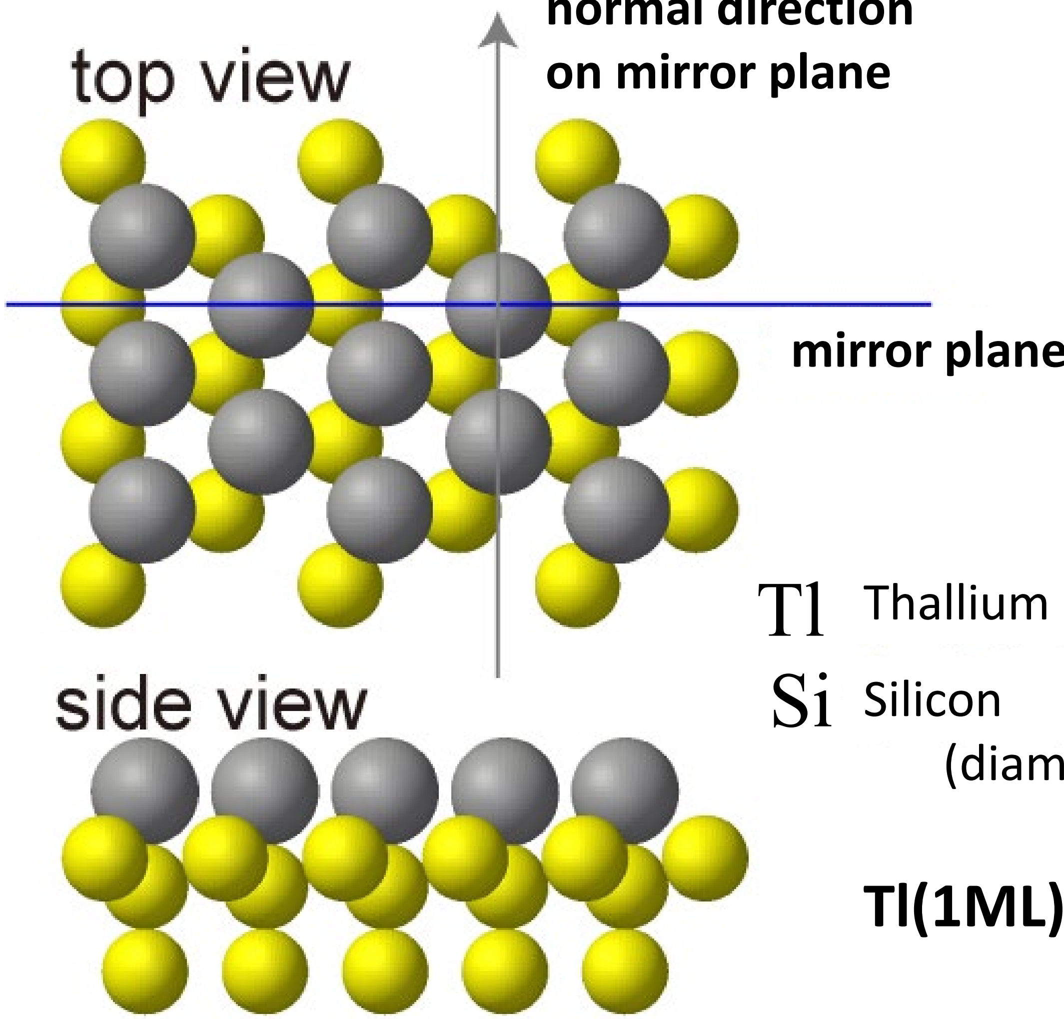

C_{3V}

Tl Thallium (adsorption atom)

Si Silicon
(diamond structure)

Tl(1ML)/Si(24ML)/H(1ML)

Sakamoto, Oda, Kimura *et al.*, Phys.Rev. Lett., 102 (2009) 096805.

Full spin-orbit interaction other than the Rashba term

$$H_{SOI} = \frac{\hbar}{4m^2c^2}\vec{\sigma}\cdot\left(\text{grad } V(\vec{r})\times\vec{p}\right)$$

$$\left(\varphi_{\vec{k}}\middle|H_{\text{SOI}}\middle|\varphi_{\vec{k}}\right)$$

$$\left(H_{\text{SOI}}\right) = \underbrace{\vec{\sigma}\cdot\left\{\vec{\alpha}_n(\vec{k})\times\vec{k}\right\}}_{\text{Rashba term}} + \underbrace{\vec{\sigma}\cdot\vec{B}_n(\vec{k})}_{\text{(Zeeman term)}}$$

$$\varphi_{n\vec{k}}(\vec{r}) = \frac{1}{\sqrt{\Omega}}\exp(i\vec{k}\cdot\vec{r})\underline{u_{n\vec{k}}(\vec{r})}$$

$$\vec{\alpha}_n = \frac{\hbar^2 N}{4m_e^2c^2\Omega}\int_{cell} d\vec{r}\left|u_{n\vec{k}}(\vec{r})\right|^2\vec{\nabla}V(\vec{r}) \longrightarrow \vec{\alpha}_n = \alpha\,\vec{e}_z$$

$$\vec{B}_n(\vec{k}) \approx \frac{\hbar^2 N}{4m_e^2c^2\Omega}\int_{cell} d\vec{r}\,\frac{1}{r}\frac{dV}{dr}\left\{u^*_{n\vec{k}}(\vec{r})(\vec{\ell})u_{n\vec{k}}(\vec{r})\right\}$$

Sakamoto, Oda, Kimura *et al.*, Phys.Rev. Lett., 102 (2009) 096805.

Surface band structure in Tl/Si(111)

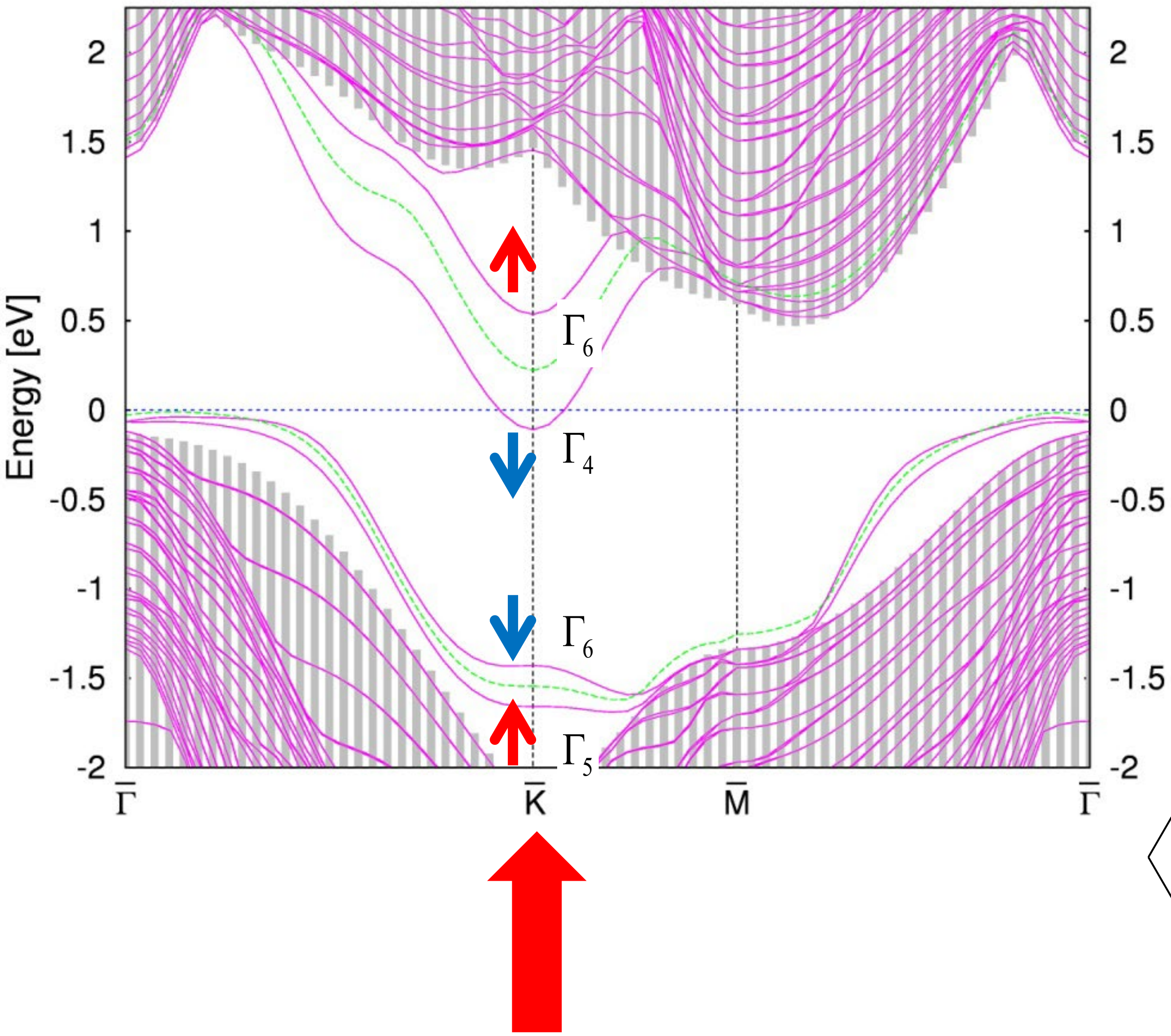

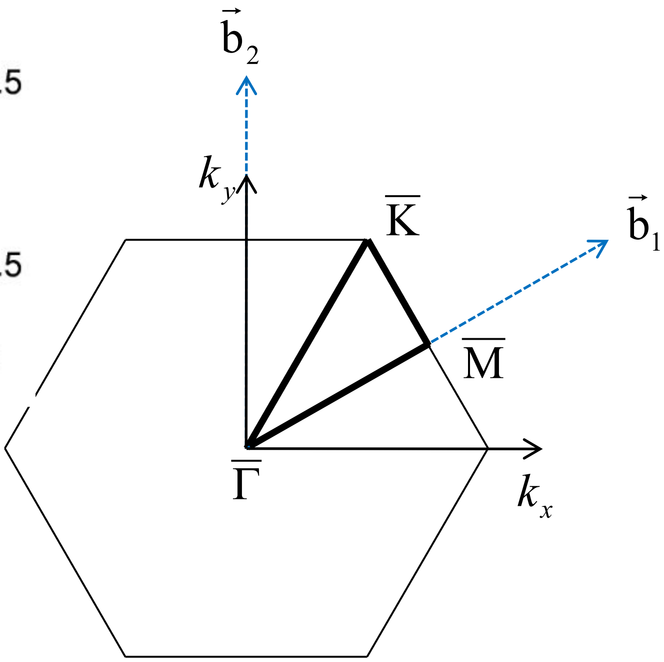

Spin splitting of Tl/Si(111)1×1 surface band

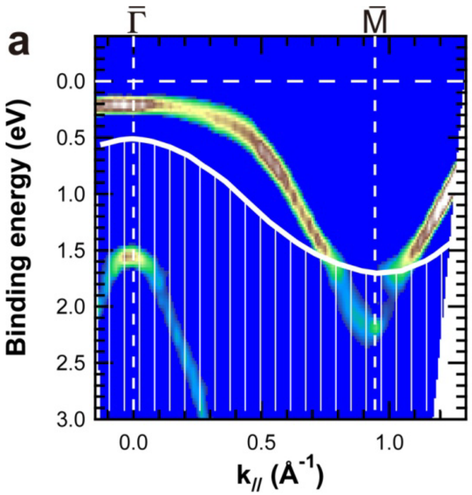

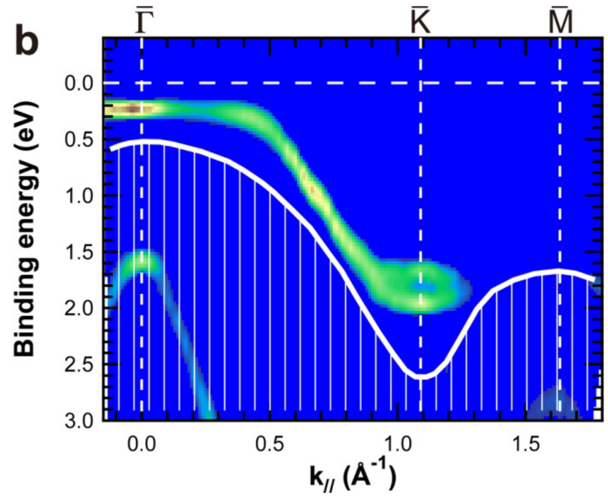

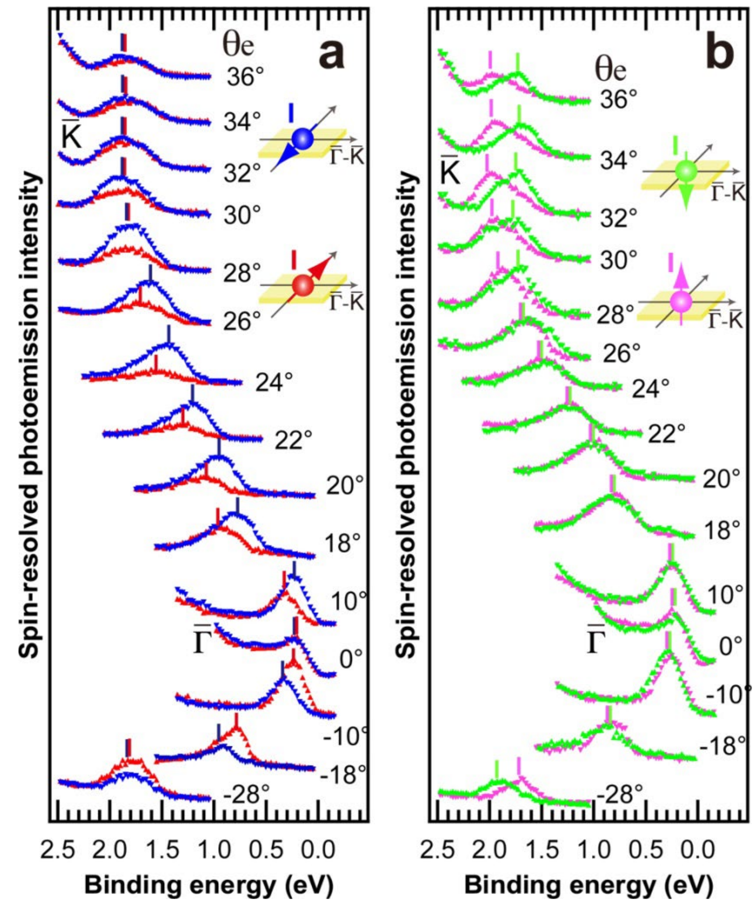

Spin splitting along Rashba direction

Normal to Rashba direction

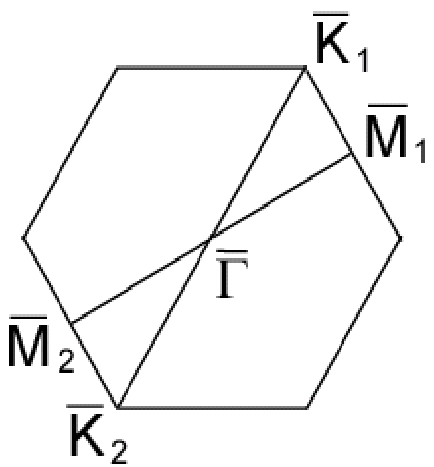

Clear splitting of electron levels in spin states at K̄

Sakamoto, Oda, Kimura *et al*., Phys.Rev. Lett., 102 (2009) 096805.

Wave vector dependence of spin direction : Voltical spin polarization

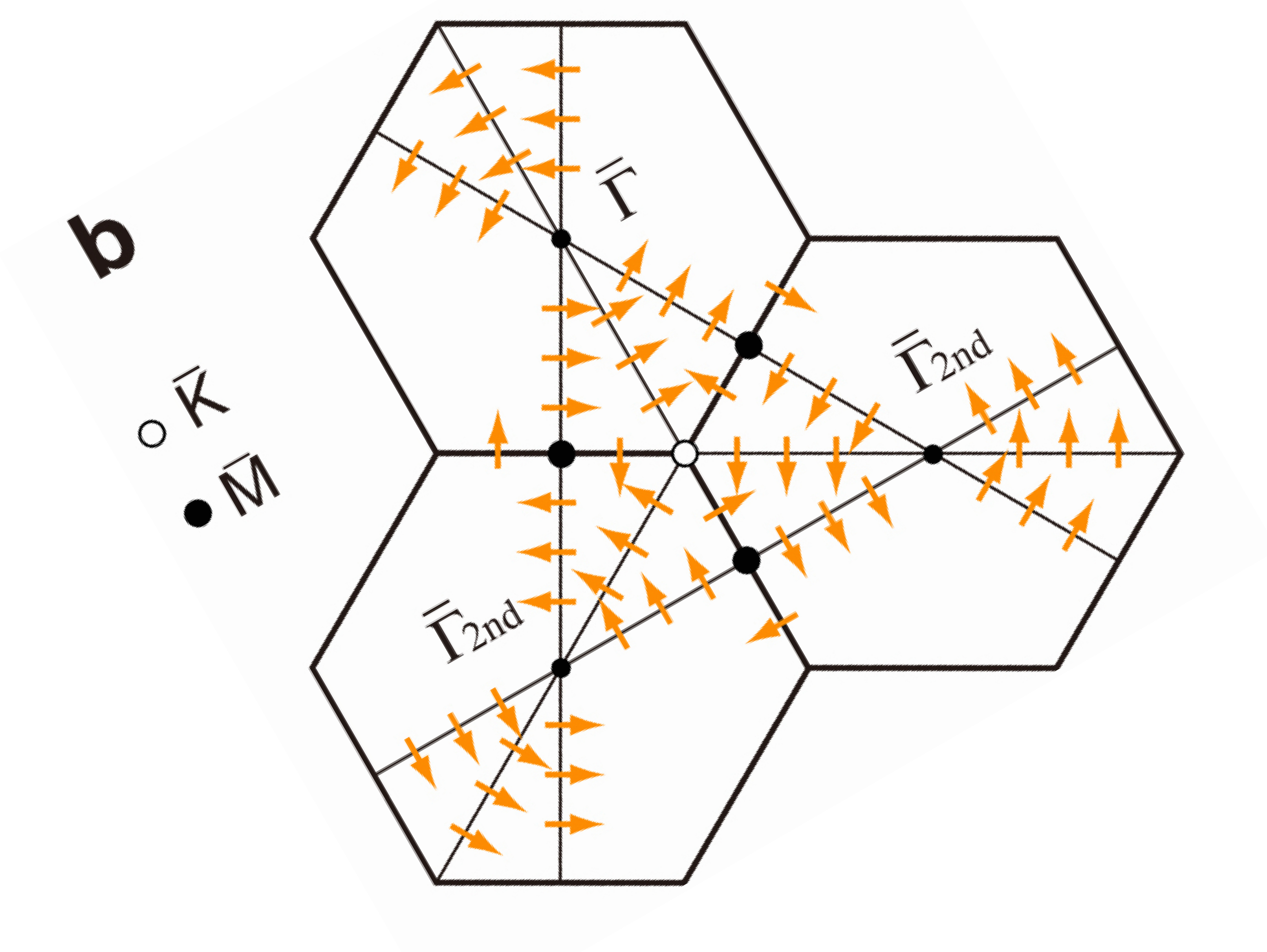

Wave vector dependence of electron spin direction : Tl site

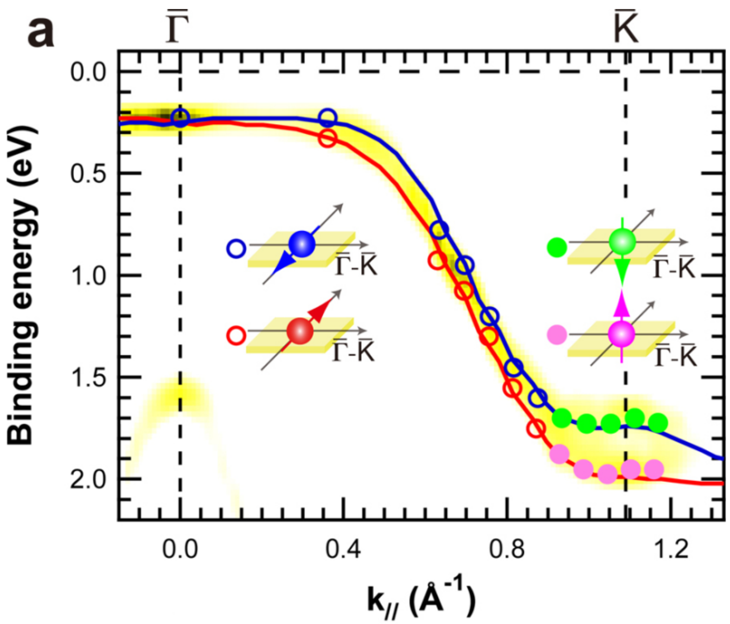

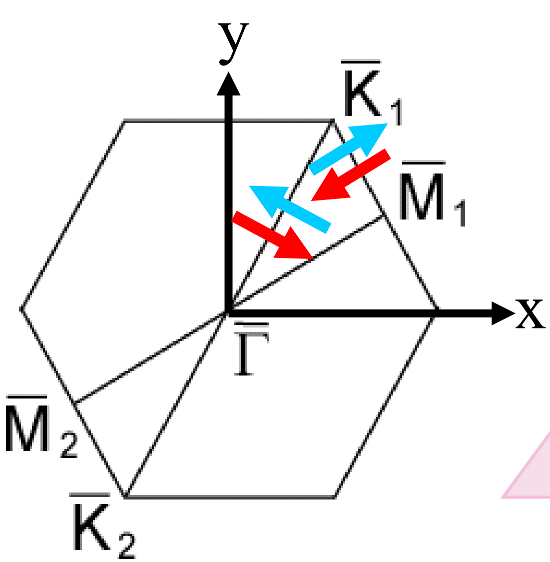

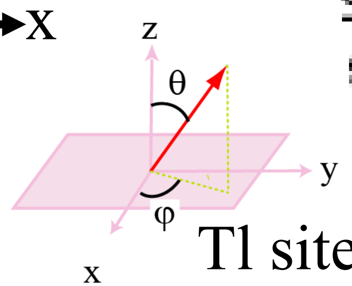

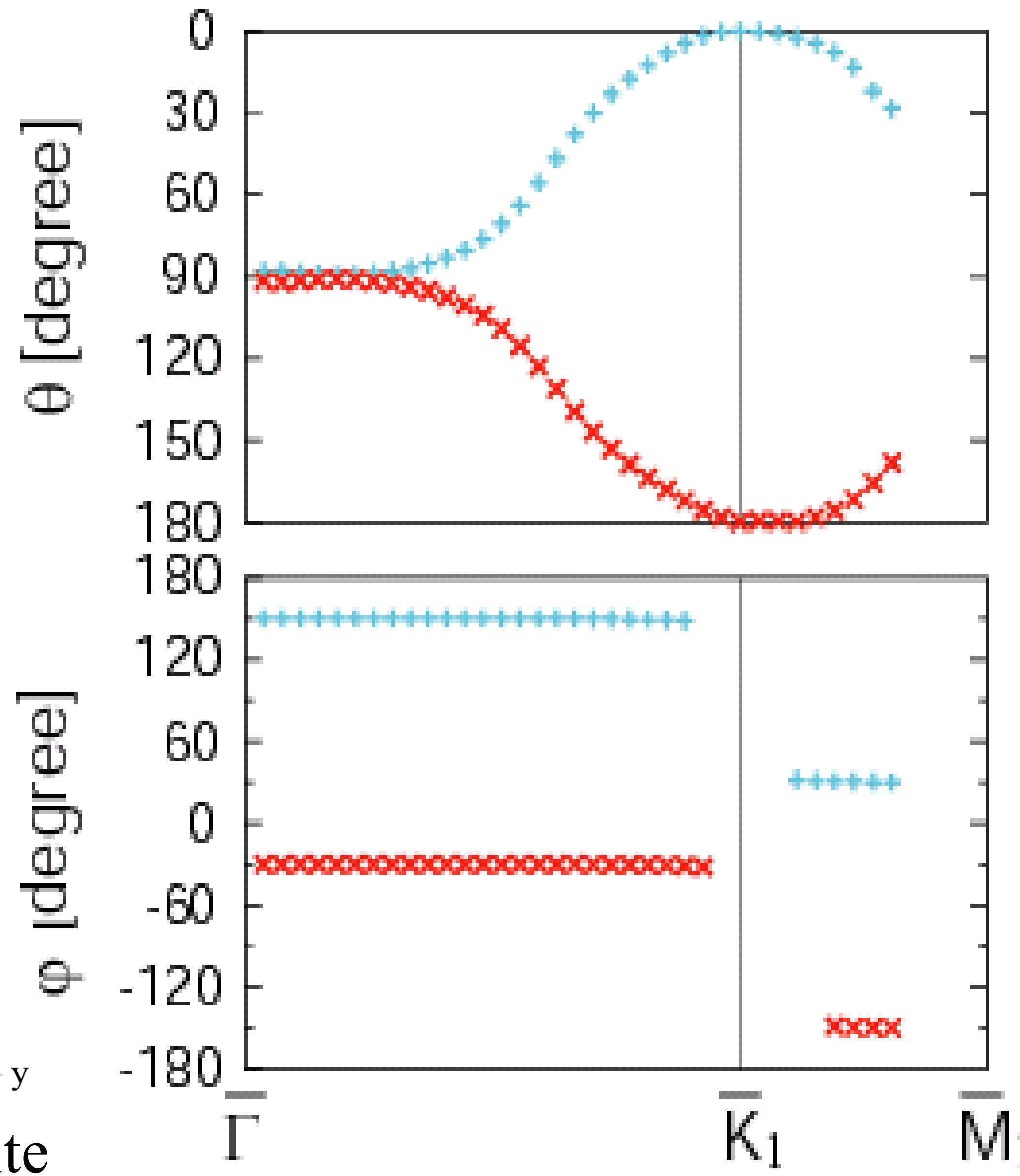

Atomic orbital components in the eigenstates at $\overline{\mathrm{K}}$

$\overline{\mathrm{K}}$ point	$\langle \ell_z \rangle_{\mathrm{Tl}}$	Tl(p_x,p_y)	(p_z)	Si(1)(p_x,p_y)	(p_z)	Si(2)(p_x,p_y)	(p_z)
Γ_6 -1.53eV	-0.047	↓0.060	---	---	↓0.105	↓0.028	---
Γ_5 -1.73eV	-0.068	↑0.090	↓0.002	---	↑0.090	↑0.024	↓0.002

C_3 double group $\langle \ell_z \rangle_{\mathrm{Si(2)}} = -0.023$

Good quantum state of ℓ_z

$$\mathrm{Tl} : p_x - i\, p_y$$

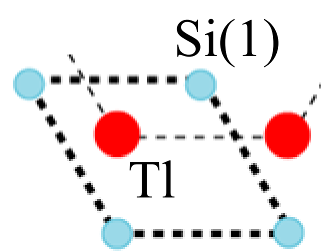

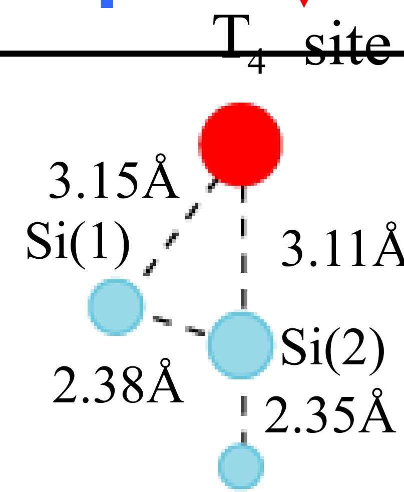

basis function of atomic orbital

	Tl site, Si(2)	Si(1) site
Γ_6 :	$\{(x+iy)\alpha,\ (x-iy)\beta\}$	$\{(x-iy)\alpha,\ z\beta\}$
Γ_5 :	$\{(x-iy)\alpha,\ z\beta\}$	$\{z\alpha,\ (x+iy)\beta\}$
Γ_4 :	$\{z\alpha,\ (x+iy)\beta\}$	$\{(x+iy)\alpha,\ (x-iy)\beta\}$

A. Araki, T. Nishijima, M. Tsujikawa and TO, J. Phys.: Conf. Ser., 200 (2010) 062001.

Single spin-state valley with vertical spin direction

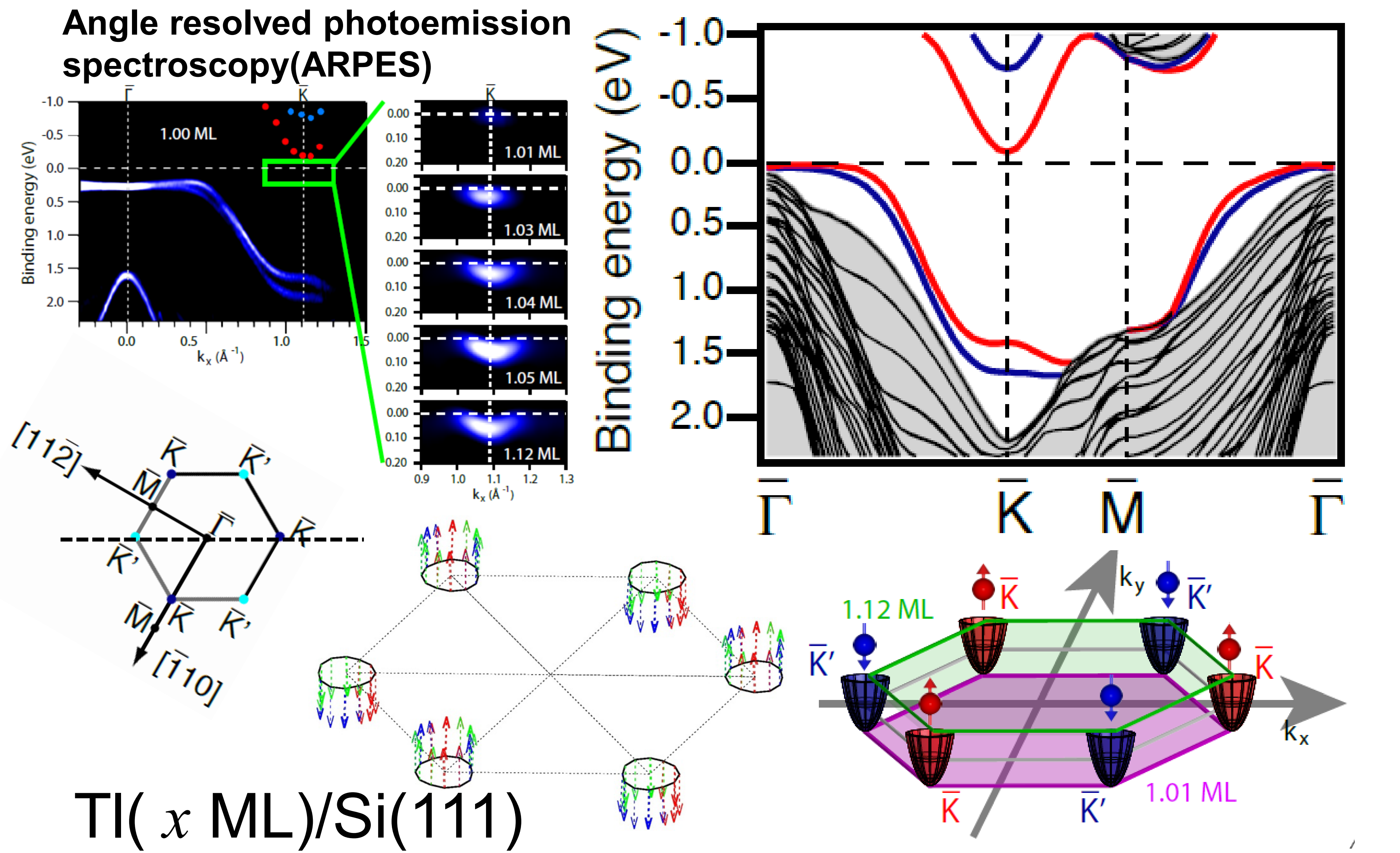

K. Sakamoto et al., Nat. Commun., 4, 2073, doi: 10.1038/ncomms3073, (2013)

Spin-splitting of the surface Tl/Si(110)

Structure

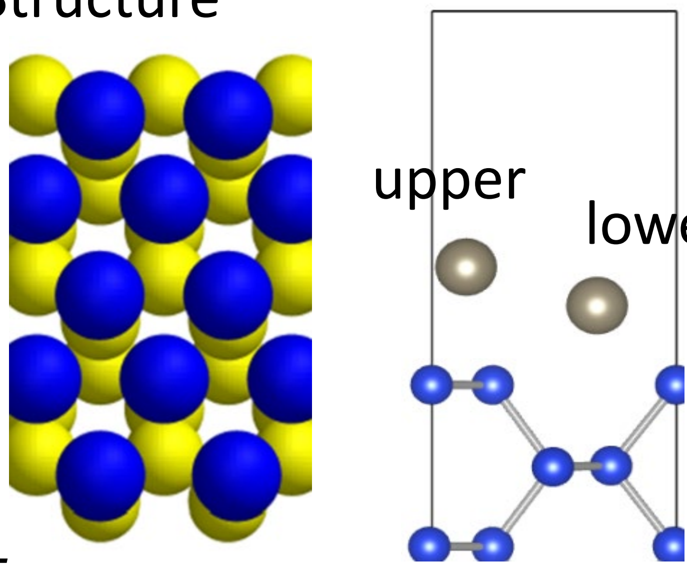

ARPES

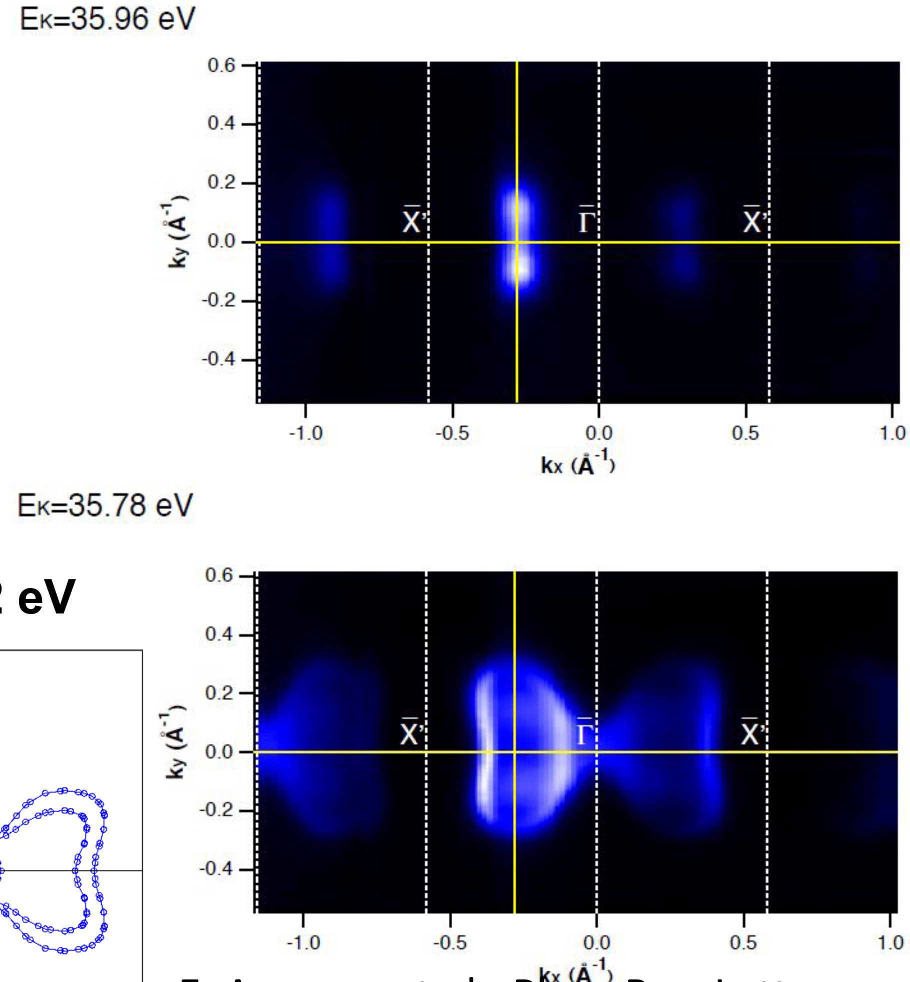

E-E_F

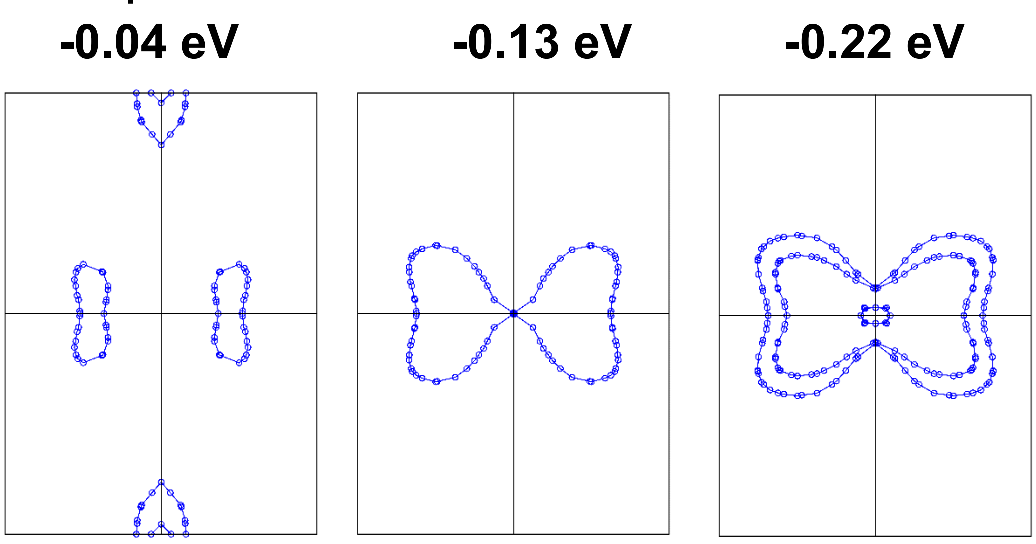

E. Annese, et al., Phys. Rev. Lett., 117, 16803(2016)

Band dispersion and Spin texture

Tl/Si(110)

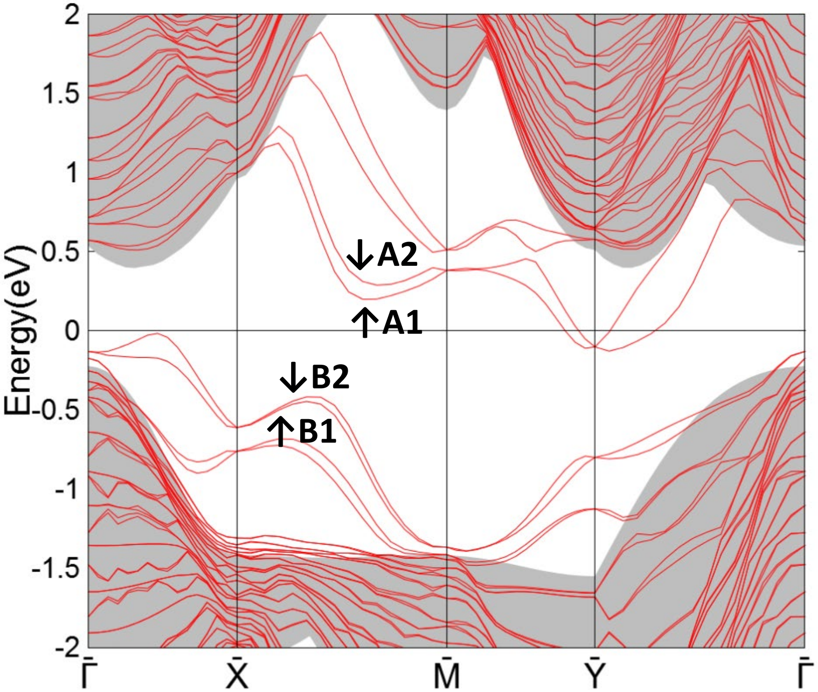

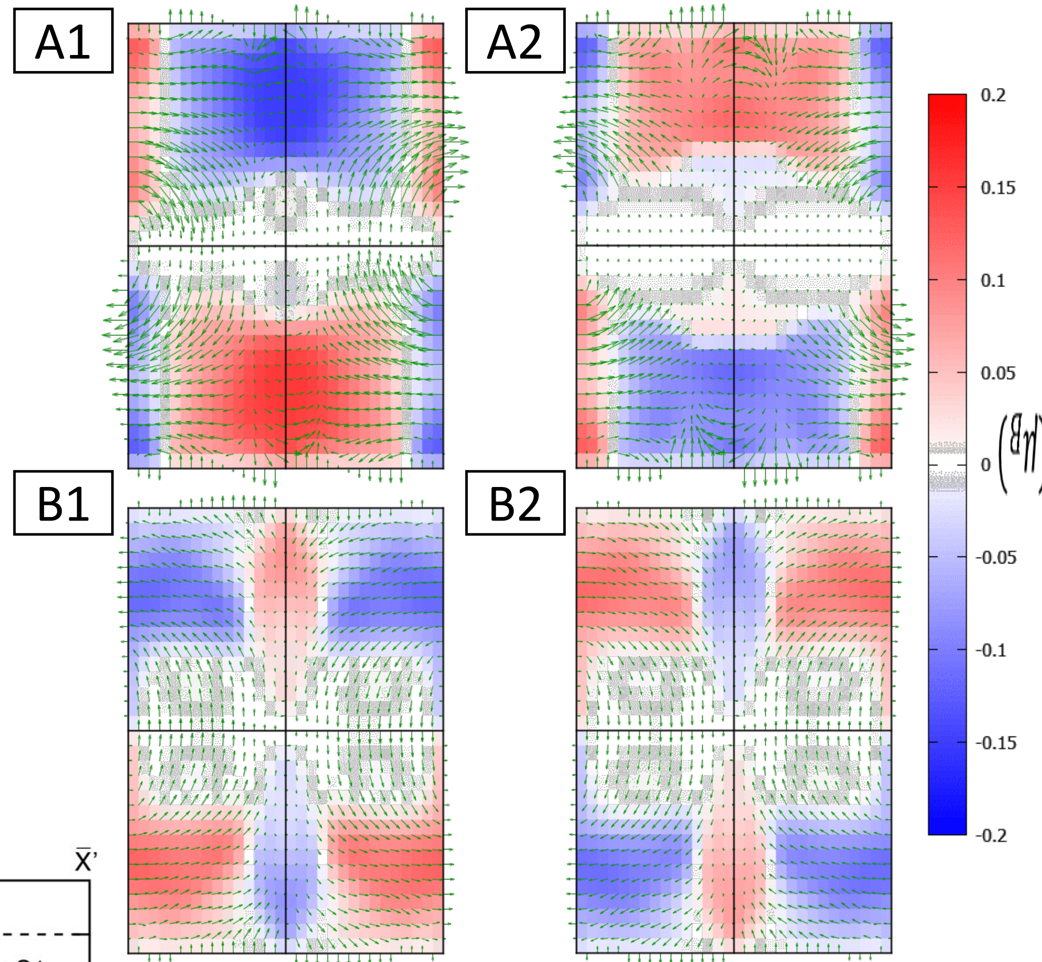

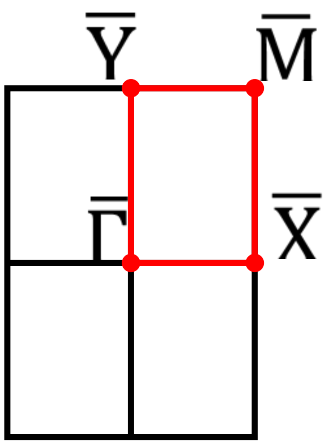

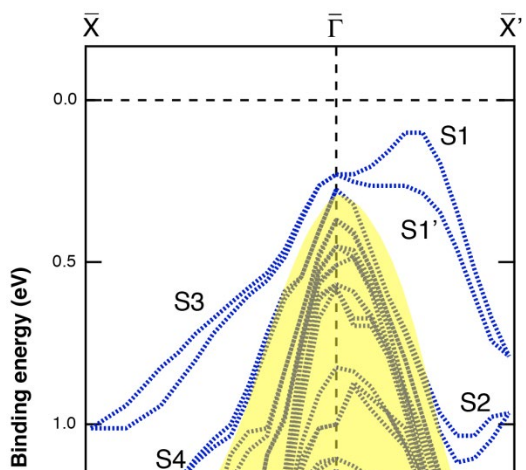

- The electron spins at

B2

$$\mathbf{K} = \alpha_{\mathrm{K}}\mathbf{K} + \mathbf{G}$$

Vortical

C_{1h}

The **mirror plane** requires the spin parallel to y-direction.

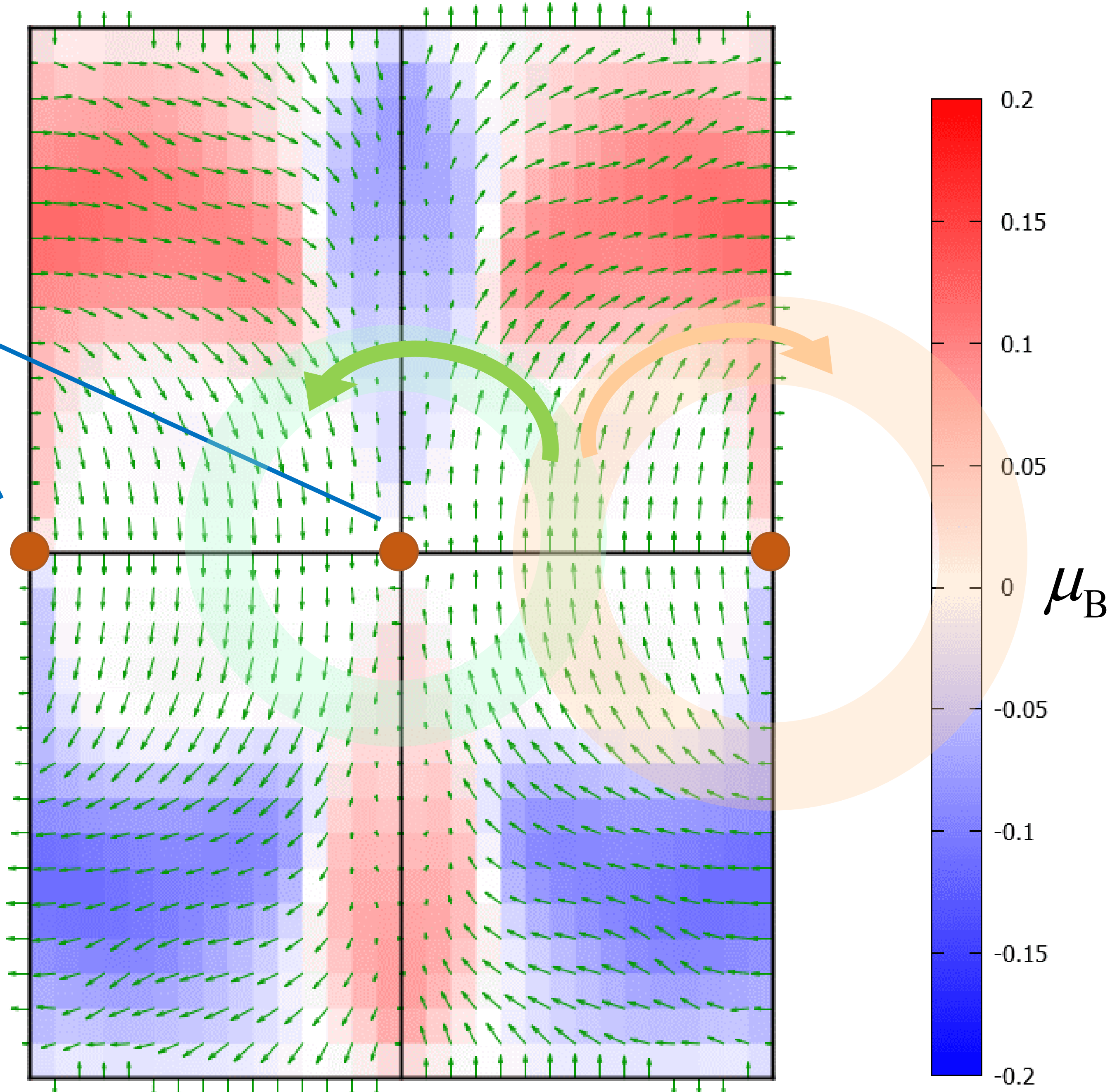

Discussion on group theory, see the paper, Nagano, Kodama, Shishido, Oguchi, JPCM,2009.

Single spin-state valley with in-pane spin direction in Tl/Si(110)

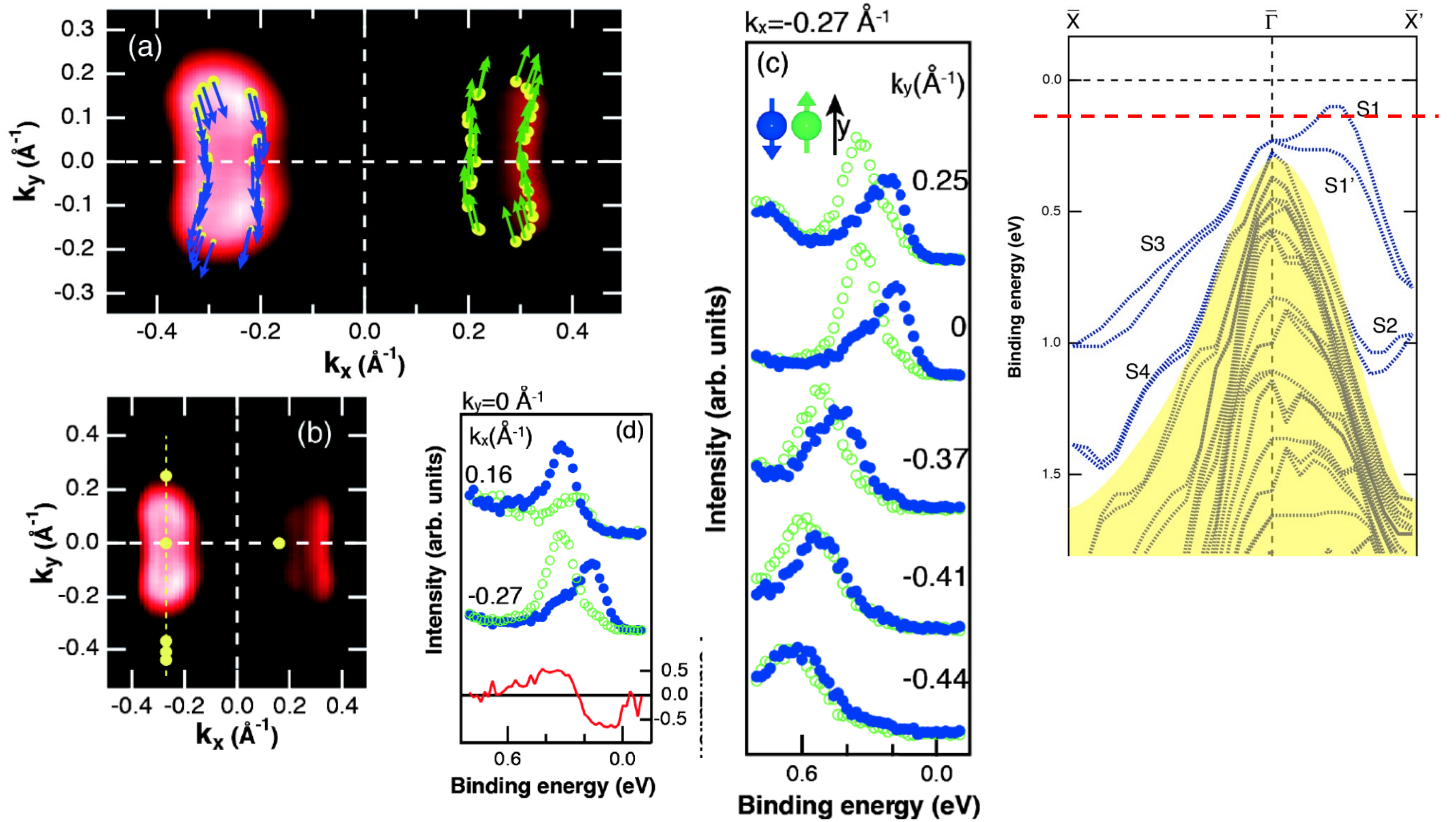

E. Annese et al., Phys. Rev. Lett., 117, 16803(2016)

Interpretation of Spin-orbit interaction

$$H_{\mathrm{SOI}} = \frac{\hbar}{4m^2c^2}\vec{\sigma}\cdot\left\{\left(\vec{\nabla}V(\vec{r})\right)\times\vec{p}\right\}$$

$$H_{\mathrm{SOI}} = 2\frac{\hbar e}{2mc}\frac{\vec{\sigma}}{2}\cdot\left\{\frac{1}{2mce}\left(\vec{\nabla}V(\vec{r})\right)\times\vec{p}\right\} = 2\mu_{\mathrm{B}}\frac{\vec{\sigma}}{2}\cdot\left\{\frac{1}{2mce}\left(\vec{\nabla}V(\vec{r})\right)\times\vec{p}\right\}$$

Bohr magneton

Effective magnetic field

$$H_{\mathrm{SOI}} = \frac{\hbar}{4m^2c^2}\left\{\vec{\sigma}\times\vec{\nabla}V(\vec{r})\right\}\cdot\vec{p} = \frac{\hbar}{m}\frac{1}{4mc^2}\left\{\vec{\sigma}\times\vec{\nabla}V(\vec{r})\right\}\cdot\vec{p}$$

Effective wave number

$$H_{\mathrm{SOI}} = -e\frac{\hbar}{4m^2c^2}\left(\vec{\sigma}\times\vec{p}\right)\cdot\frac{1}{e}\vec{\nabla}V(\vec{r})$$

Effective electric dipole **Electric field**

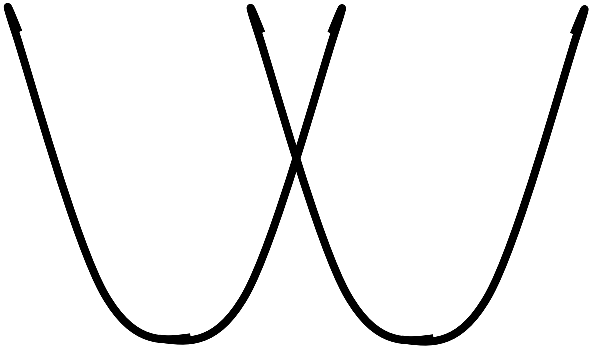

(Appendix 3)
Spin and orbital magnetic moments in an electronic structure calculation

Spin and orbital magnetic moments

spin magnetic moment

$$m^I_{spin,k} = -\mu_B \left\langle m_k(\vec{r}) \right\rangle_I$$

orbital magnetic moment

$$m^I_{orb,k} = -\mu_B \left\langle \ell_k \right\rangle_I$$

expansion with the local basis

$$\Psi_{i\alpha}(\vec{r}) = \sum_{\ell m} Y_{\ell m}(\hat{r}_I) R_{\ell m, i\alpha}(r)$$

$$\left\langle \ell_k \right\rangle_I = \left\langle \ell_k \right\rangle_{I,PW} + \left\langle \ell_k \right\rangle_{I,VB}$$

$$\left\langle \ell_k \right\rangle_{I,PW} = \sum_i f_i \left\langle \Psi_i \middle| \ell_k \middle| \Psi_i \right\rangle_I$$

$$\left\langle \ell_k \right\rangle_{I,VB} = \sum_{ipq} f_i \left\langle \Psi_i \middle| \beta^I_q \right\rangle \ell^I_{k,pq} \left\langle \beta^I_p \middle| \Psi_i \right\rangle$$

$$\ell^I_{k,pq} = \int_0^{r_c} \phi_p(r_I)\phi_q(r_I) r_I{}^2 dr_I \left\langle \mathrm{Y}^{\mathrm{sgn}(\kappa_q)}_{j_q \mu_q} \middle| \ell_k \middle| \mathrm{Y}^{\mathrm{sgn}(\kappa_p)}_{j_p \mu_p} \right\rangle$$

T. Oda and A. Hosokawa, Phys. Rev. B, 72, 224428 (2005)

Atomic magnetic moments in CoPt and FePt

r_c=2.5 a.u.		spin (μ_B)		orbital(μ_B)	
		USPP	AE	USPP	AE
CoPt [001]	Co	1.926	1.91 1.803	0.102	0.11 0.089
	Pt	0.377	0.38 0.394	0.061	0.07 0.056
CoPt [110]	Co	1.929	1.809	0.069	0.057
	Pt	0.377	0.398	0.078	0.073
FePt [001]	Fe	3.016	2.93 2.891	0.067	0.08 0.067
	Pt	0.338	0.33 0.353	0.046	0.05 0.042
FePt [110]	Fe	3.020	2.893	0.062	0.061
	Pt	0.340	0.355	0.059	0.055

AE: Sakuma,JPSJ(1994), Ravindran *et al.*,PRB(2001)

(Appendix 4)
Approximation in Dirac equation

Dirac equation (part 2)

(eq. in stationary-state)

$$p_0 = i\hbar \frac{\partial}{\partial(ct)} \longrightarrow p_0 = \frac{\varepsilon}{c}$$

Coupled equations for the large and small components;

$$\left(\varepsilon - mc^2 + eA_0\right)\varphi_L = c\left(\vec{\sigma}, \vec{p} + \frac{e}{c}\vec{A}\right)\varphi_S$$

$$\left(\varepsilon + mc^2 + eA_0\right)\varphi_S = c\left(\vec{\sigma}, \vec{p} + \frac{e}{c}\vec{A}\right)\varphi_L$$

Eliminate the small component;

$$\left(\varepsilon - mc^2 + eA_0\right)\varphi_L = c^2 \underline{\left(\vec{\sigma}, \vec{p} + \frac{e}{c}\vec{A}\right)} \underline{\left(\varepsilon + mc^2 + eA_0\right)}^{-1}\left(\vec{\sigma}, \vec{p} + \frac{e}{c}\vec{A}\right)\varphi_L$$

Commute the parts with underline:

Dirac equation (part 3)

$$\left(\varepsilon - mc^2 + eA_0\right)\phi_L = c^2\left[\underline{\left(\varepsilon + mc^2 + eA_0\right)^{-1}}\left(\vec{\sigma}, \vec{p} + \frac{e}{c}\vec{A}\right)^2\right.$$

$$\left. + c^2\underline{\left(\varepsilon + mc^2 + eA_0\right)^{-2}}\left(\vec{\sigma}, (-e\vec{p}A_0)\right)\left(\vec{\sigma}, \vec{p} + \frac{e}{c}\vec{A}\right)\right]\phi_L$$

For not heavy elements, the eigenvalue at valence electrons is larger than the rest energy by a small value. Therefore, we cant take a following approximation;

$$\varepsilon' = \varepsilon - mc^2, \quad \frac{\varepsilon' + eV_0}{mc^2} <<< 1$$

$$\varepsilon + mc^2 + eV_0 \approx 2mc^2$$

Using this approximation, the equation for the large component;

Formula 1

$\left(\vec{a},\vec{b}\right)$: Scalar product

Using following general properties;

$$\left(\vec{\sigma},\vec{B}\right)\left(\vec{\sigma},\vec{C}\right)=\left(\vec{B},\vec{C}\right)+i\left(\vec{\sigma},\vec{B}\times\vec{C}\right)$$

$$\vec{H}=\vec{\nabla}\times\overline{A}$$

We obtain the following formula related with Zeeman term;

$$\left(\vec{\sigma},\vec{p}+\frac{e}{c}\vec{A}\right)^2=\left(\vec{p}+\frac{e}{c}\vec{A}\right)^2+\frac{\hbar e}{c}\left(\vec{\sigma},\vec{H}\right)$$

$$(\vec{\sigma},(-e\vec{p}A_0))\left(\vec{\sigma},\vec{p}+\frac{e}{c}\vec{A}\right)=\left((-e\vec{p}A_0),\vec{p}+\frac{e}{c}\vec{A}\right)+i\left(\vec{\sigma},(-e\vec{p}A_0)\times(\vec{p}+\frac{e}{c}\vec{A})\right)$$

$$=\left((-e\vec{p}A_0),\vec{p}+\frac{e}{c}\vec{A}\right)+\left(i\vec{\sigma}\times(-e\vec{p}A_0),\vec{p}+\frac{e}{c}\vec{A}\right)$$

$$c^2\left(\varepsilon+mc^2+eA_0\right)^{-1}=\frac{1}{2m}\left(1+\frac{\varepsilon'+eA_0}{2mc^2}\right)^{-1}=\frac{1}{2m}\left(1-\frac{\varepsilon'+eA_0}{2mc^2}+.....\right)$$

$$c^2\left(\varepsilon+mc^2+eA_0\right)^{-2}=\frac{1}{4m^2c^2}\left(1+\frac{\varepsilon'+eA_0}{2mc^2}\right)^{-2}=\frac{1}{4m^2c^2}\left(1-\frac{\varepsilon'+eA_0}{mc^2}+.....\right)$$

Formula 2

$$
\left(\varepsilon' + eA_0\right)\varphi_L =
$$

$$
\left(1 - \frac{\varepsilon' + eA_0}{2mc^2} + \ldots\ldots\right)\left\{\frac{1}{2m}\left(\vec{p} + \frac{e}{c}\vec{A}\right)^2 + \frac{\hbar e}{2mc}\left(\vec{\sigma}, \vec{H}\right)\right\}\varphi_L +
$$

$$
\left(1 - \frac{\varepsilon' + eA_0}{mc^2} + \ldots\ldots\right)\times
$$

$$
\left\{\frac{1}{4m^2c^2}\left((-e\vec{p}A_0), \vec{p} + \frac{e}{c}\vec{A}\right) + \frac{1}{4m^2c^2}\left(i\vec{\sigma}\times(-e\vec{p}A_0), \vec{p} + \frac{e}{c}\vec{A}\right)\right\}\varphi_L
$$

Taking the leading terms in the approximation;

the approximation formula in (5-3).

(Appendix 5)
Spin-orbit splitting in the heavy element

$$E_{\mathrm{SO}}^{j} = \lambda\,\vec{\ell}\cdot\vec{s} = \frac{\lambda}{2}\{j(j+1) - s(s+1) - \ell(\ell+1)\}$$

$$\left.\begin{array}{r} s, s_z = s, s-1, \ldots, -s \\ \\ \ell,\;\; m = \ell, \ell-1, \ldots\ldots, -\ell \end{array}\right\} j = \ell + s, \ldots\ldots, |\,\ell - s\,|$$

$$s = \frac{1}{2},\;\; s_z = \frac{1}{2}, -\frac{1}{2}$$

$$\ell = 1 \longrightarrow j = \frac{3}{2}, \frac{1}{2} \qquad\qquad \ell = 2 \longrightarrow j = \frac{5}{2}, \frac{3}{2}$$

$\boxed{\lambda > 0}$

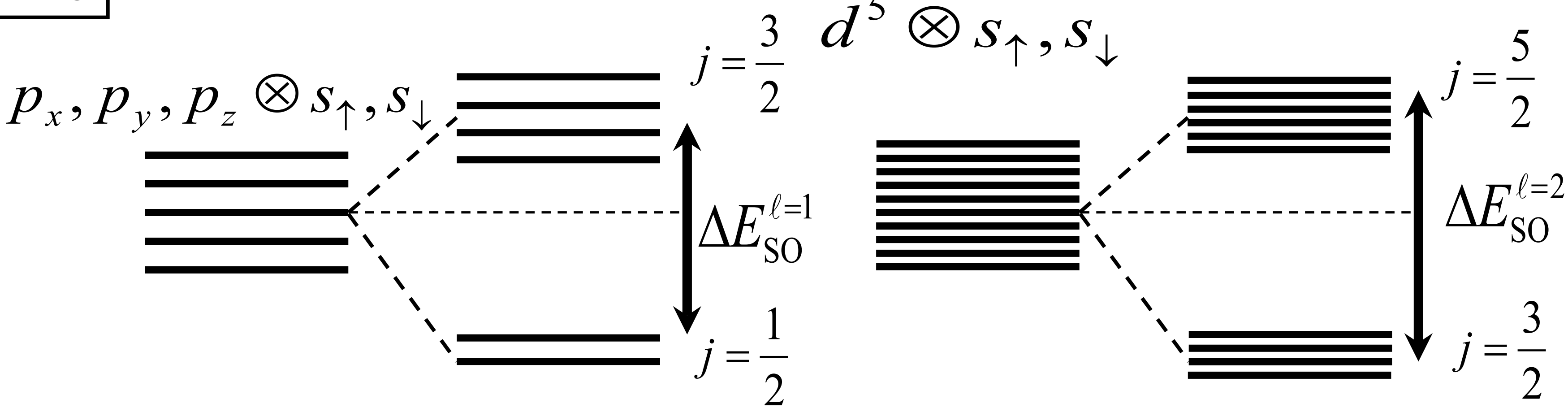

Eigenvalues of Pb atom

(in Ry energy unit)

Ref. State:
(Kr Core)$(5d)^{10}(6s)^2(6p)^2$

$n\ell$	j	all electron	pseudo (ΔE)
$5d$	3/2	-1.6734	-1.6733 (+0.0001)
$5d$	5/2	-1.4823	-1.4821 (+0.0002)
$6s$	1/2	-0.9016	-0.9014 (+0.0002)
$6p$	1/2	-0.3547	-0.3545 (+0.0002)
$6p$	3/2	-0.2440	-0.2439 (+0.0001)

$\Delta E_{so}(d)$
0.1912
2.601 eV

$\Delta E_{so}(p)$
0.1106
1.505 eV

These values are in good agreement with the previous data.

$$\Delta E_{\mathrm{SO}}^{\ell} = E_{\mathrm{SO}}^{\ell+1/2} - E_{\mathrm{SO}}^{\ell-1/2} = \frac{\lambda}{2}\left(2\ell+1\right) \quad \lambda = \frac{2}{2\ell+1}\Delta E_{SO}^{\ell}$$

$$\lambda_{\ell=2}^{\mathrm{Pb}} = 1.04\,\mathrm{eV}$$

$$\lambda_{\ell=1}^{\mathrm{Pb}} = 1.00\,\mathrm{eV}$$

Band dispersion of fcc Pb

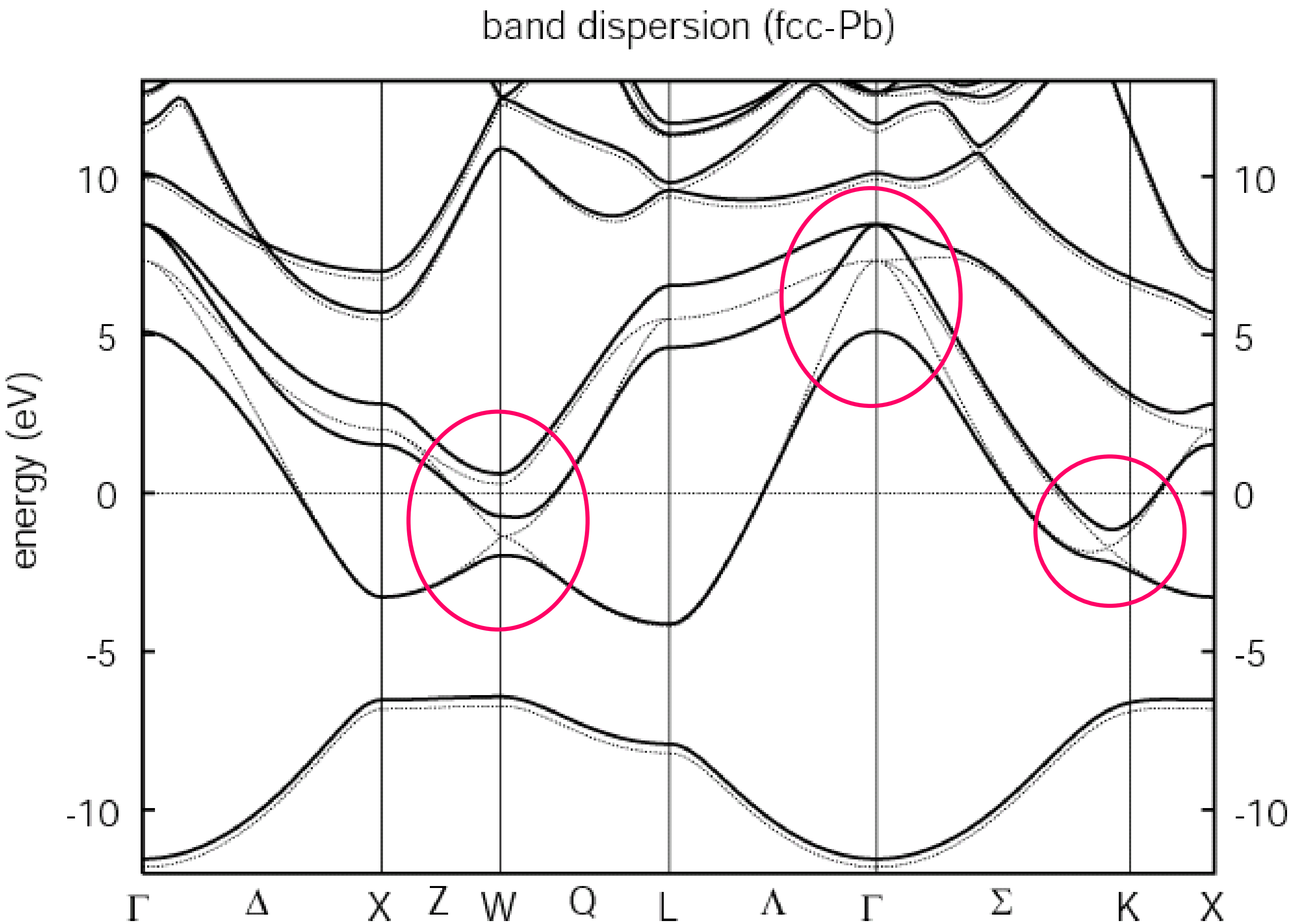

Thick lines : Fully-Relativistic
Thin lines : Scalar-Relativistic

a=9.35 a.u.(exp.)

	USPP	(RAPW)
Γ:	-11.55	(-11.4)
L:	-7.92	(-8.2)
	-4.13	(-4.5)
K:	-6.61	(-6.7)
	-2.44	(-2.8)
	-0.93	(-1.2)
W:	-6.43	(-7.2)
X:	-6.52	(-6.7)
	-3.28	(-3.6)

At Γ point, ΔE_{so}
5*d*: 2.50 eV
6*p*: 3.38 eV

Band dispersion of fcc noble metals, Au

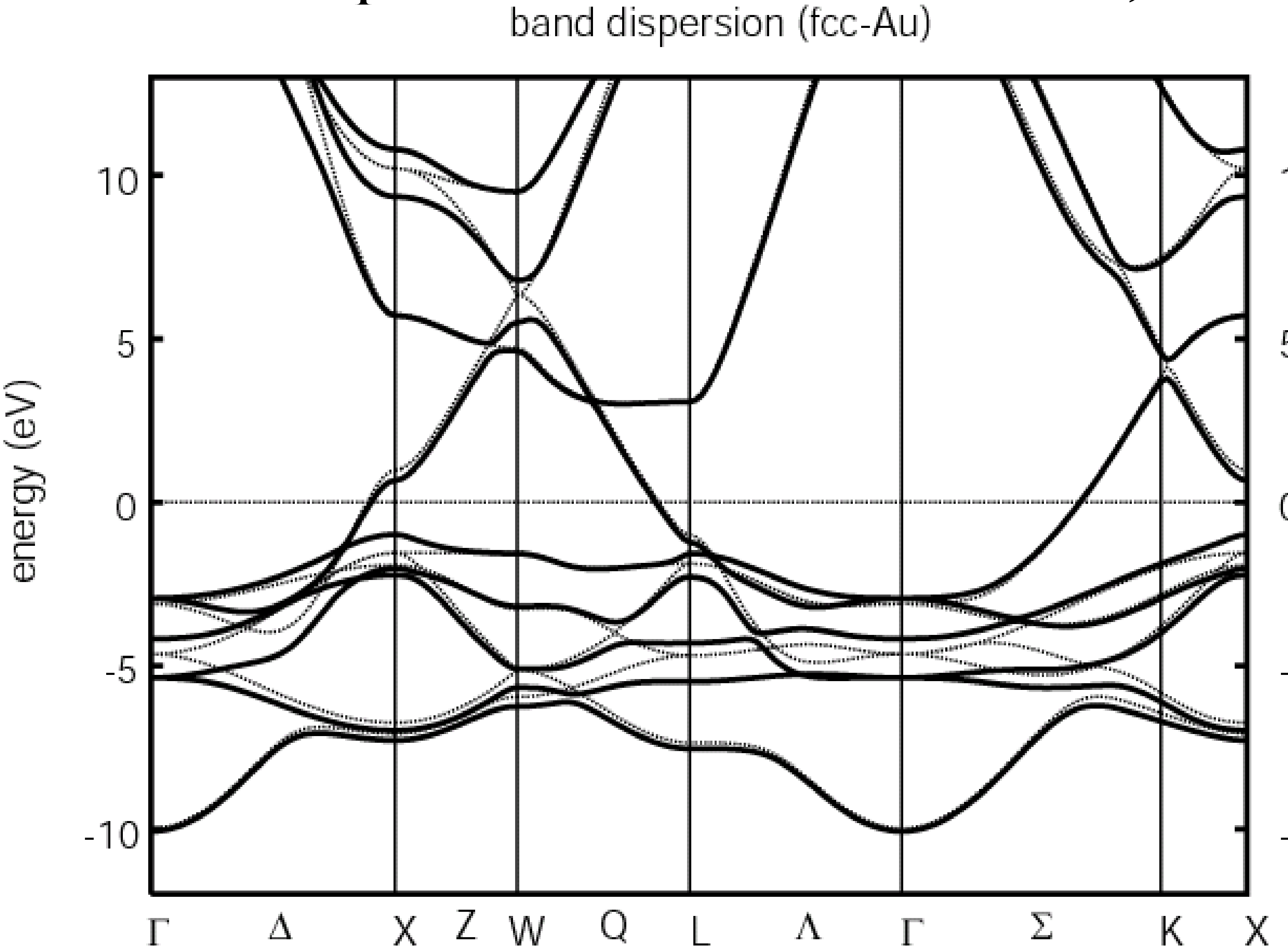

Au: a=7.71 a.u.(exp.)

Band dispersion of fcc noble metals, Pt

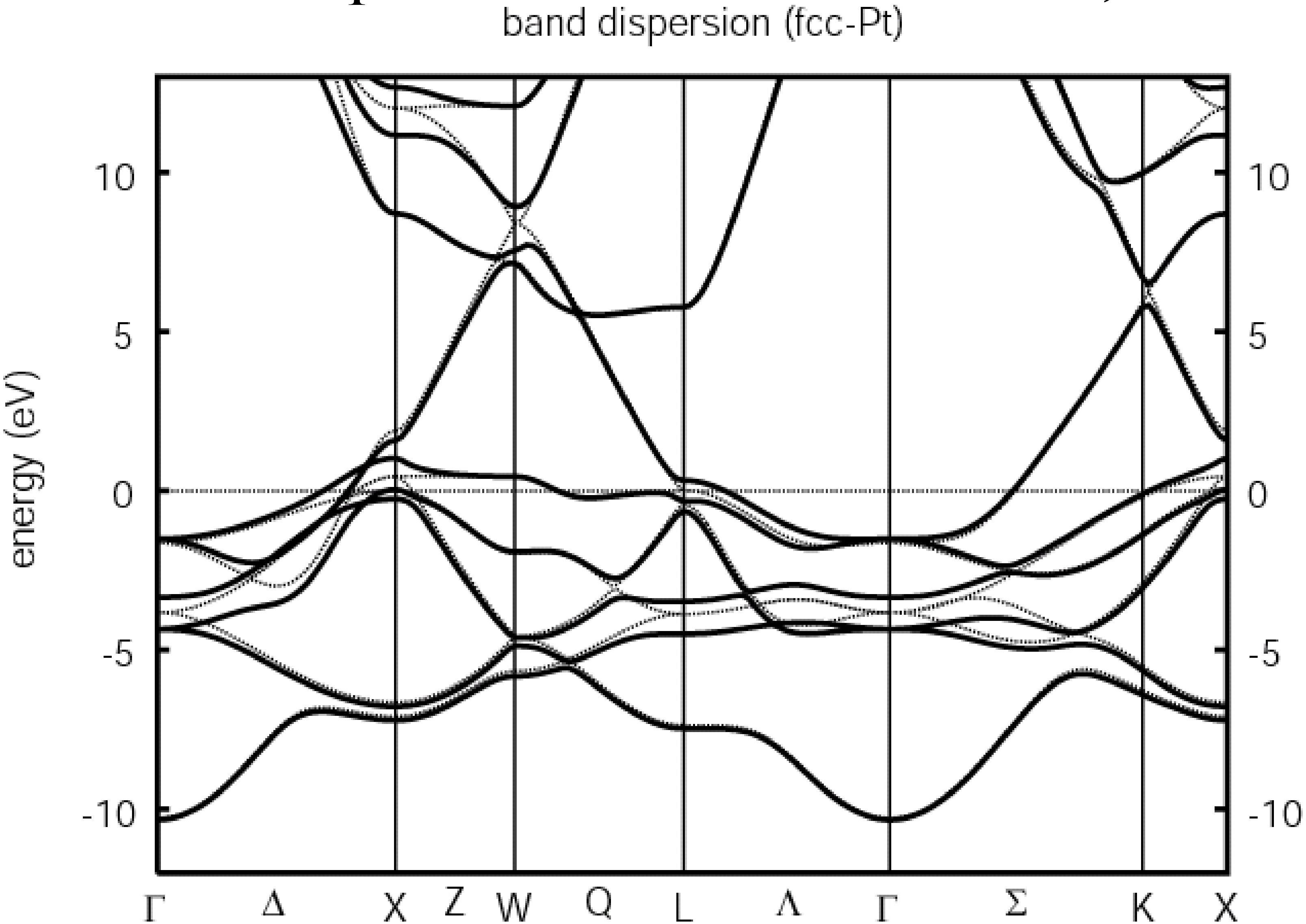

Pt: a=7.41 a.u.(exp.)

(Appendix 6)
Kohn-Sham equation, variational principles, Car-Parrinello molecular dynamics, fully relativistic pseudo potential

Density functional theory: Kohn&Sham eqution

Variational principles

$$\widetilde{E}[n(\mathbf{r})] = E[n(\mathbf{r})] - \mu\left(\int n(\mathbf{r})d\mathbf{r} - N_\mathrm{e}\right)$$

$$\frac{\delta \widetilde{E}}{\delta n(\mathbf{r})} = 0$$

Kohn&Sham equation → Electron density

$$\left\{-\frac{1}{2}\nabla^2 + V_\mathrm{eff}(\mathbf{r})\right\}\Psi_i(\mathbf{r}) = \varepsilon_i \Psi_i(\mathbf{r})$$

$$n(\mathbf{r}) = \sum_i^{\mathrm{occ.}} \left|\Psi_i(\mathbf{r})\right|^2$$

Electron potential ← Poisson equation

$$V_\mathrm{eff}(\mathbf{r}) = V_\mathrm{ext}(\mathbf{r}) + \frac{1}{2}\int \frac{n(\mathbf{r}')}{|\mathbf{r}-\mathbf{r}'|}d\mathbf{r}' + \frac{\delta E_\mathrm{xc}}{\delta n(\mathbf{r})}$$

Car-Parrinello Molecular Dynamics for Noncollinear Magnetism

- Bispinor Wave Functions for Single Electron States

$$\Phi_k(r) = \begin{pmatrix} \phi_{k1}(r) \\ \phi_{k2}(r) \end{pmatrix}$$

Soft part

Augmented part (hard part)

- Density Matrix

$$\rho_{\alpha\beta}(r) = \sum_k f_k \{\phi_{k\alpha}(r)\, \phi^*_{k\beta}(r) + \sum_{Inm} Q^I_{nm}(r) \langle \beta^I_n \mid \phi_{k\alpha} \rangle \langle \phi_{k\beta} \mid \beta^I_m \rangle\}$$

$$= \frac{1}{2}(n(r)\sigma_0 + m_x(r)\sigma_x + m_y(r)\sigma_y + m_z(r)\sigma_z)_{\alpha\beta}$$

unit matrix $\sigma_0 = \begin{pmatrix} 1 & 0 \\ 0 & 1 \end{pmatrix}$

Charge density $n(r)$

Spin density vector $m_\alpha(r)$

Pauli matrix $\sigma_x = \begin{pmatrix} 0 & 1 \\ 1 & 0 \end{pmatrix}$ $\sigma_y = \begin{pmatrix} 0 & -i \\ i & 0 \end{pmatrix}$ $\sigma_z = \begin{pmatrix} 1 & 0 \\ 0 & -1 \end{pmatrix}$

$$n(r) = \rho_{11} + \rho_{22}$$

$$m_x(r) = 2\,\mathrm{Re}\,\rho_{12} \quad m_y(r) = -2\,\mathrm{Im}\,\rho_{12} \quad m_z(r) = \rho_{11} - \rho_{22}$$

- Total Energy(Energy Functional)

$$E_{tot}\left[\{\Phi_k\},\{R_I\}\right]=\sum_k f_k \langle \Phi_k \mid (-\frac{1}{2}\nabla^2 \ \sigma_0 + V_{NL}) \mid \Phi_k \rangle + \frac{1}{2}\iint \frac{n(r)n(r')}{|r-r'|}drdr'$$

$$+\int V_{loc}^{ion}(r)\,n(r)\,dr + \underline{E_{XC}\left[n(r),m(r)\right]} + U_{ion}\left[\{R_I\}\right]$$

$$V_{loc}^{ion}(r) = \sum_I V_{loc}^I(r-R\ ) \qquad V_{NL} = \left(\sum_{Inm} |\beta_m^I\rangle D_{nm}^{(0)I} \langle \beta_n^I|\right)\sigma_0$$

$$U_{ion}\left[\{R_I\}\right] = \frac{1}{2}\sum_{IJ}\frac{Z_I Z_J}{|R_I - R_J|} \qquad \underline{m(r) = |\vec{m}(r)|}$$

$$\beta_n^I(r) \quad D_{nm}^{(0)I} \quad Q_{nm}^I(r) \quad V_{loc}^I(r)$$

These quantities are transferred from an atomic reference configuration. The pseudo potential is the ultra-soft type.

- Density Functional for the Exchange-Correlation Term.
  Local spin density approximation(LDA),
  Generalized gradient approximation（GGA,PW91)
  Van der Waals density functional (vdW-DF)

- Lagrangian (Car-Parrinello Molecular Dynamics)

$$L = m_\Phi \sum_k f_k \langle \dot{\Phi}_k | \dot{\Phi}_k \rangle + \frac{1}{2} \sum_I M_I \dot{R}_I^2 - E_{tot}\left[\{\Phi_k\},\{R_I\}\right] + \sum_{k\ell} \Lambda_{k\ell} \left(\langle \Phi_k | S | \Phi_\ell \rangle - \delta_{k\ell} \right)$$

- Molecular Dynamics (Euler-Lagrange equation)

$$m_\Phi \ddot{\Phi}_k(r) = -H\Phi_k(r) + \sum_\ell \frac{1}{f_k} \Lambda_{k\ell} S \Phi_\ell(r)$$

$$\begin{pmatrix} \bar{\phi}_{k1}(r) \\ \bar{\phi}_{k2}(r) \end{pmatrix} = -\begin{pmatrix} H11 & H12 \\ H21 & H22 \end{pmatrix} \begin{pmatrix} \phi_{k1}(r) \\ \phi_{k2}(r) \end{pmatrix}$$

$$M_I \ddot{R}_I = F_I + \sum_{k\ell} \Lambda_{k\ell} \langle \Phi_k | \frac{\partial S}{\partial R_I} | \Phi_\ell \rangle$$

$$H = \frac{1}{f_k} \frac{\delta E_{tot}}{\delta \Phi_k}$$

$$F_I = -\frac{\partial E_{tot}}{\partial R_I}$$

Install to the plane wave method (I)

spinor wave function

$$\Phi_k(r) = \begin{pmatrix} \phi_{k1}(r) \\ \phi_{k2}(r) \end{pmatrix}$$

density matrix

$$\rho_{\alpha\beta}(r) = \sum_k f_k \{\phi_{k\alpha}(r)\phi^*_{k\beta}(r) \quad + \sum_{Ipq} \underline{Q^I_{pq,\alpha\beta}(r)} \langle \beta^I_p | \Phi_k \rangle \langle \Phi_k | \beta^I_q \rangle \}$$

spinor type projector function

$$\beta^I_p(r) = b^I_{j\kappa\tau}(r) \mathrm{Y}^{\mathrm{sgn}(\kappa)}_{j\mu}(r_I) \qquad p = \{j\mu\kappa\tau\}$$

$$j = \ell + \frac{1}{2}, \mu = m + \frac{1}{2} \quad \mathrm{Y}^{(-)}_{j,\mu} = \left(\frac{l+m+1}{2l+1}\right)^{1/2} Y_{l,m} \begin{pmatrix} 1 \\ 0 \end{pmatrix} + \left(\frac{l-m}{2l+1}\right)^{\frac{1}{2}} Y_{l,m+1} \begin{pmatrix} 0 \\ 1 \end{pmatrix}$$

$$\kappa = -\ell - 1 < 0$$

$$j = \ell - \frac{1}{2}, \mu = m - \frac{1}{2} \quad \mathrm{Y}^{(+)}_{j,\mu} = \left(\frac{l-m+1}{2l+1}\right)^{1/2} Y_{l,m-1} \begin{pmatrix} 1 \\ 0 \end{pmatrix} - \left(\frac{l+m}{2l+1}\right)^{\frac{1}{2}} Y_{l,m} \begin{pmatrix} 0 \\ 1 \end{pmatrix}$$

$$\kappa = \ell > 0$$

TO and A. Hosokawa, PRB, **72**, 224428 (2005)

Install to the plane wave method (II)

nonlocal potential

$$V_{NL} = \sum_{Ipq} |\beta_q^I\rangle D_{pq}^{(0)I} \langle \beta_p^I |$$

transfer from the atomic generation code

$$\beta_p^I(r) \quad D_{pq}^{(0)I} \quad Q_{pq,\alpha\beta}^I(r) \quad V_{loc}^I(r)$$

Kohn-Sham equation

$$H\ \Phi_k(r) = \varepsilon_k\ S\ \Phi_k(r)$$

$$H = \left(-\frac{1}{2}\nabla^2\right)\sigma_0 + \overline{V}_{eff} + \sum_{Ipq} |\beta_p^I\rangle D_{pq}^I \langle \beta_q^I | \qquad S = 1 + \sum_{Ipq} |\beta_q^I\rangle q_{pq}^I \langle \beta_p^I |$$

$$\overline{V}_{eff}(r) = \left(V_{loc}^{ion}(r) + \int \frac{n(r')}{|r-r'|} dr' + V_{xc}^N(r) \right)\sigma_0 + V_{xc}^M(r) \frac{1}{m(r)} \vec{m}(r)\cdot\vec{\sigma}$$

$$D_{pq}^I = D_{pq}^{(0)I} + \sum_{\alpha\beta} \int Q_{pq,\alpha\beta}^I(r) \left(V_{eff}(r)\right)_{\alpha\beta} dr \quad V_{xc}^N(r) = \frac{\delta E_{XC}}{\delta n(r)} \quad V_{xc}^M(r) = \frac{\delta E_{XC}}{\delta m(r)}$$

TO and A. Hosokawa, PRB, **72**, 224428 (2005)

(Appendix 7)
Magnetic anisotropy:
shape magnetic anisotropy
and
magnetocrystalline anisotropy

Method: Density functional calculation

Pseudopotential : fully relativistic ultrasoft

Wave function : two component spinor form

Exchange correlation

generalized gradient approximation (GGA)

Energy cut-off : wave function 30 Ry, density 300 Ry

TO, A. Pasquarello, and R. Car, Phys. Rev. Lett. 80, 3622 (1998);
TO and A. Pasquarello, Phys. Rev. B 70, 134402 (2004);
TO and A. Hosokawa, Phys. Rev. B, 72, 224428 (2005).

Magnetic Anisotropy Energy（MAE）

From
the total energies

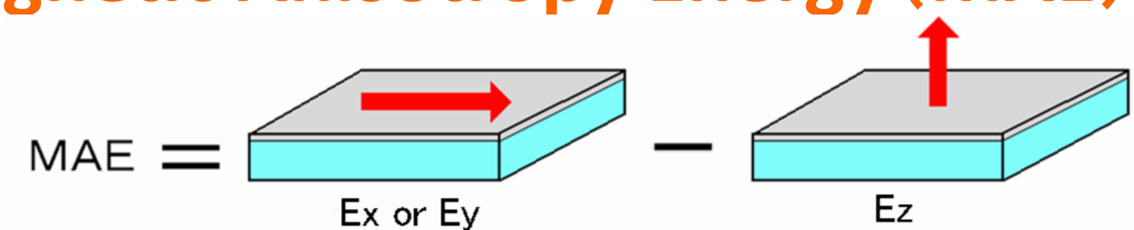

TOTAL ENERGY (density functional calculations)

MAE > 0 : perpendicular anisotropy

Quadrupole atomic spin density distribution at interface/surface

MgO(5ML)/Fe(xML)/MgO(5ML)-lcMgO(1x1)

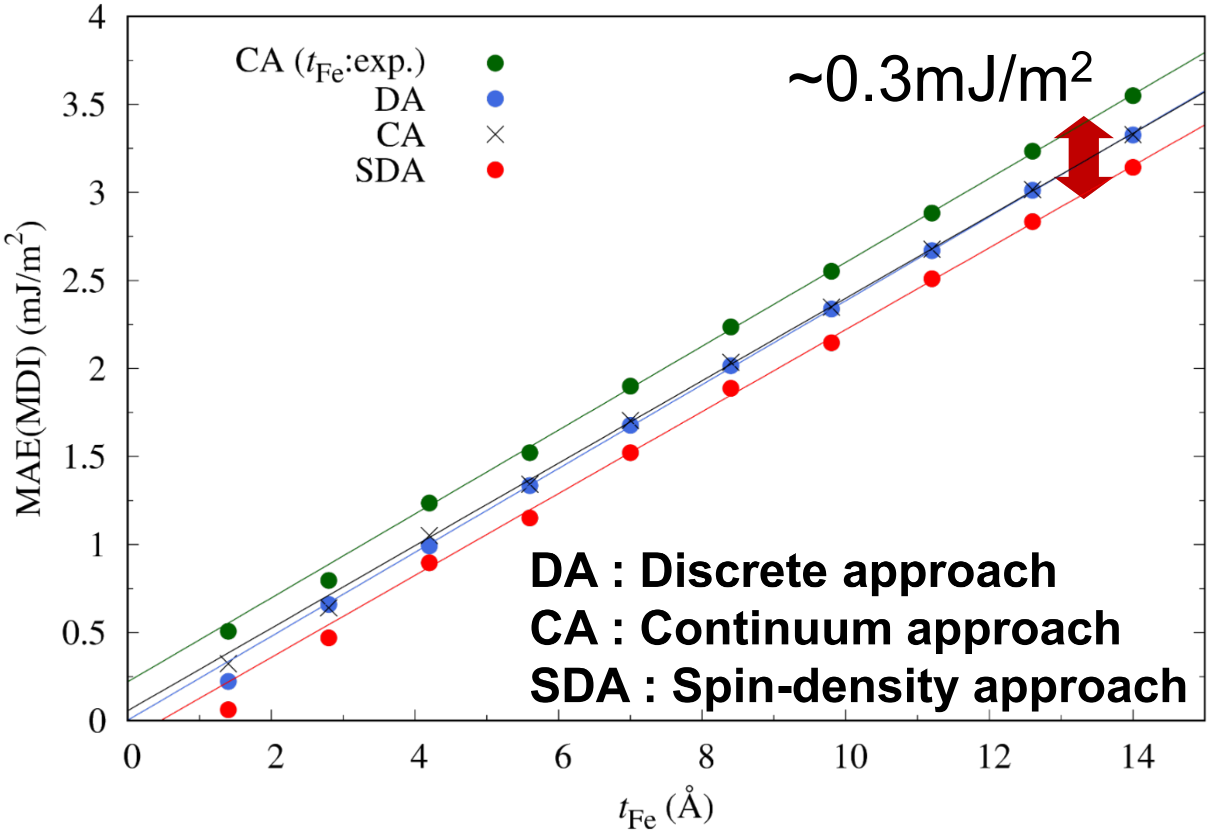

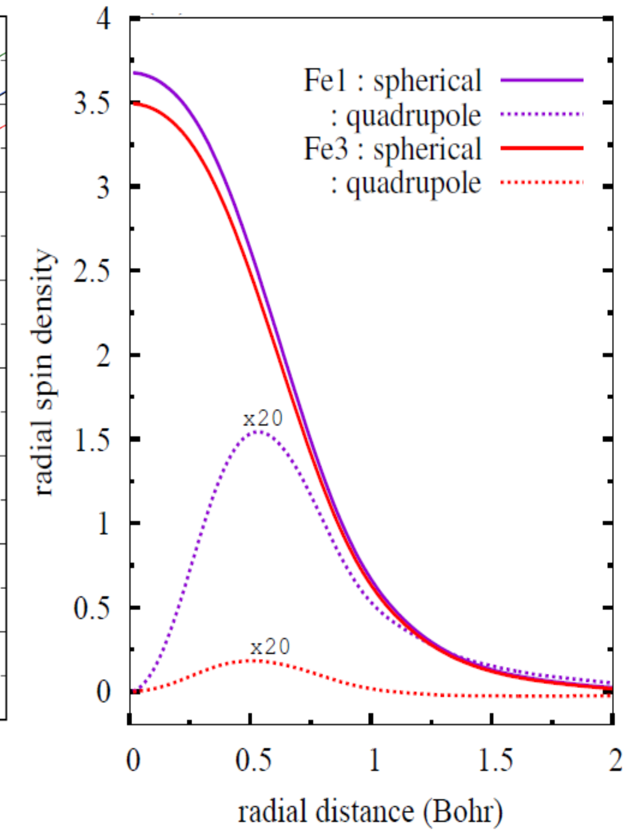

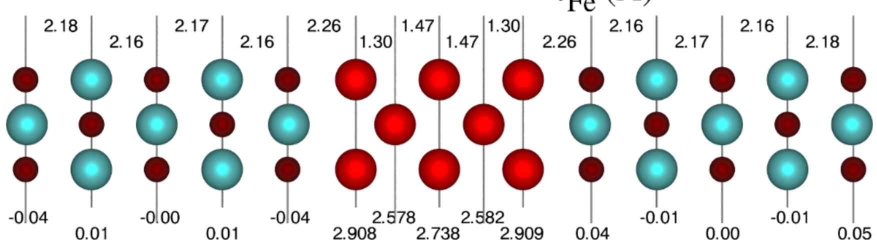

Interface Fe/MgO supresses

Interface: quadrupole: Large

Inside : quadrupole: Small

TO, I. Pardede, et al., IEEE Trans. Magn. **55**, 1300104 (2018).

(Appendix 8)
Spin-orbit interaction:
Rashba effects

(5-5) Spin-orbit interaction

$$H_{\mathrm{SOI}} = \frac{\hbar}{4m^2c^2}\vec{\sigma}\cdot\left(\mathrm{grad}\ V(\vec{r})\times\vec{p}\right)$$

$\vec{\sigma}$ Pauli's matrix

$$V(\mathbf{r}) \approx -\frac{Ze^2}{r} \qquad \mathrm{grad}\,V(r) \approx \frac{dV}{dr}\frac{\mathbf{r}}{r}$$

The effect is emphasized at surface/interface: becoming not spherical.

$$H_{SOI} = \xi\vec{\ell}\cdot\vec{\sigma} = \xi(\ell_x\sigma_x + \ell_y\sigma_y + \ell_z\sigma_z)$$

connects orbital and spin spaces

$$\xi(r) = \frac{\hbar^2}{4m^2c^2r}\frac{dV}{dr}$$

2

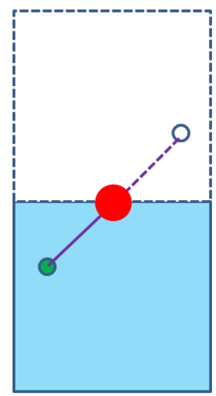

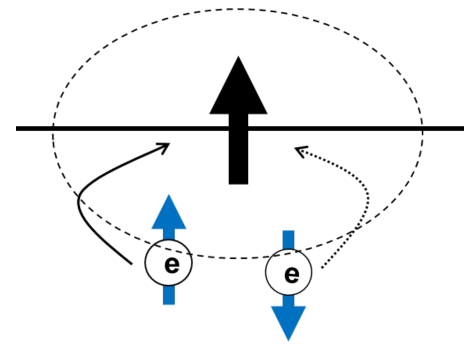

Biot-Savart law in the classical electromagnetics

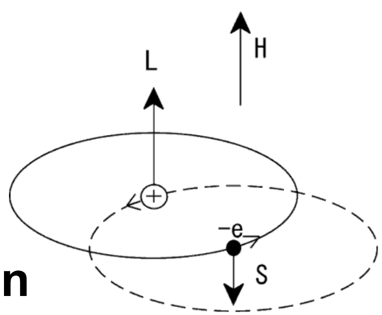

spin-orbit interaction

$$E_{\mathrm{SO}}^{j} = \lambda\vec{\ell}\cdot\vec{s} = \frac{\lambda}{2}\left\{j(j+1) - s(s+1) - \ell(\ell+1)\right\}$$

Due to the surface/interface the inversion symmetry breaks.

→ Rashba effect, etc.

(5-5-2) Spin-texture in the reciprocal space: Rashba effect 1

2 dimensional free electron with spin-orbit interaction

$$H = -\frac{\hbar^2}{2m}\nabla^2 + \vec{\sigma}\cdot\left(\vec{\alpha}\times\vec{p}\right)$$

$$\vec{\alpha} \propto \left\langle \text{grad } V(r) = \frac{1}{r}\frac{dV(r)}{dr}\mathbf{r} \right\rangle$$

$$\propto \vec{e}_z$$

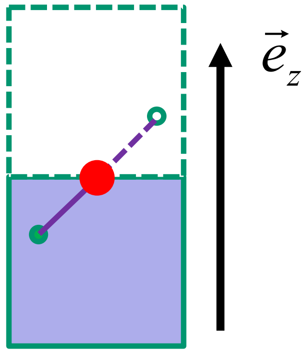

Plane wave $$\varphi_{\vec{k}} = \frac{1}{\sqrt{\Omega}}e^{i\vec{k}\cdot\vec{r}}\begin{pmatrix} u_1 \\ u_2 \end{pmatrix}$$

$$H = \frac{\hbar^2 k^2}{2m} + \vec{\sigma}\cdot\left(\vec{\alpha}\times\vec{k}\right) = \frac{\hbar^2 k^2}{2m} + \alpha_z\left(\vec{k}\times\vec{\sigma}\right)_z$$

$$= \frac{\hbar^2 k^2}{2m} + \alpha_z\left(k_x\sigma_y - k_y\sigma_x\right)$$

$$\vec{k} = (k_x, k_y) \qquad k = \sqrt{k_x^2 + k_y^2}$$

$$E_+ = \frac{\hbar^2 k^2}{2m} + \alpha_z k \qquad \varphi_{\vec{k}}^{+} = \frac{1}{\sqrt{\Omega}}e^{i\vec{k}\cdot\vec{r}}\frac{1}{\sqrt{2}}\begin{pmatrix} -1 \\ -ie^{i\theta_k} \end{pmatrix} \propto \frac{1}{\sqrt{2}}\begin{pmatrix} e^{-i(\theta_k+\pi/2)/2} \\ e^{i(\theta_k+\pi/2)/2} \end{pmatrix}$$

$$E_- = \frac{\hbar^2 k^2}{2m} - \alpha_z k \qquad \varphi_{\vec{k}}^{-} = \frac{1}{\sqrt{\Omega}}e^{i\vec{k}\cdot\vec{r}}\frac{1}{\sqrt{2}}\begin{pmatrix} 1 \\ -ie^{i\theta_k} \end{pmatrix} \propto \frac{1}{\sqrt{2}}\begin{pmatrix} -e^{-i(\theta_k+\pi/2)/2} \\ e^{i(\theta_k+\pi/2)/2} \end{pmatrix}$$

(5-5-3) Spin-texture in the reciprocal space: Rashba effect 2

$$\left\langle \varphi_{\vec{k}}^{+} \middle| \vec{\sigma} \middle| \varphi_{\vec{k}}^{+} \right\rangle = (-\sin\theta_k, \cos\theta_k, 0)$$

$$\left\langle \varphi_{\vec{k}}^{-} \middle| \vec{\sigma} \middle| \varphi_{\vec{k}}^{-} \right\rangle = (\sin\theta_k, -\cos\theta_k, 0)$$

$$E_{\pm} = \frac{\hbar^2}{2m}\left(k \pm \frac{m\alpha_z}{\hbar^2}\right)^2 - \frac{\hbar^2}{2m}\left(\frac{m\alpha_z}{\hbar^2}\right)^2$$

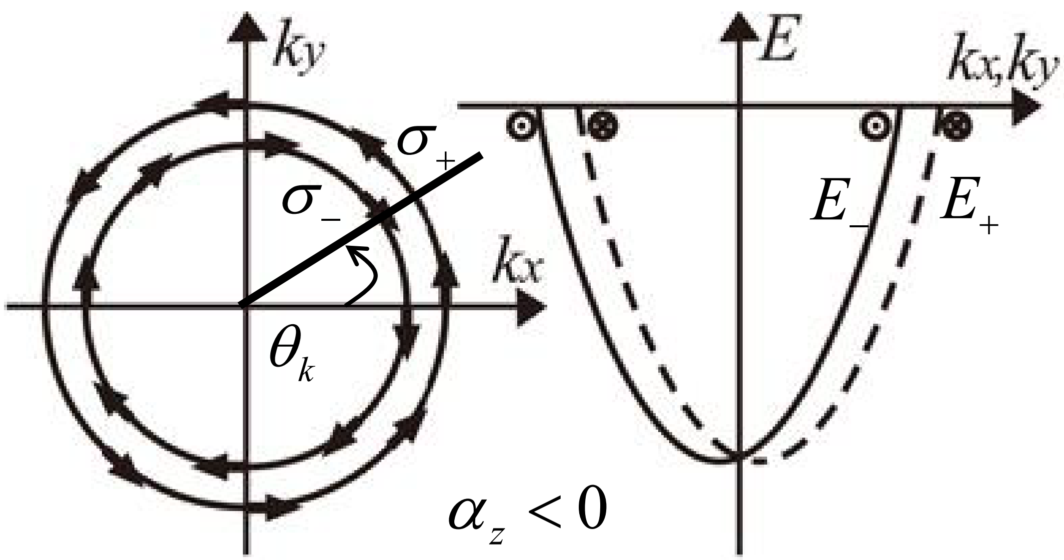

Au(111) surface: ARPES

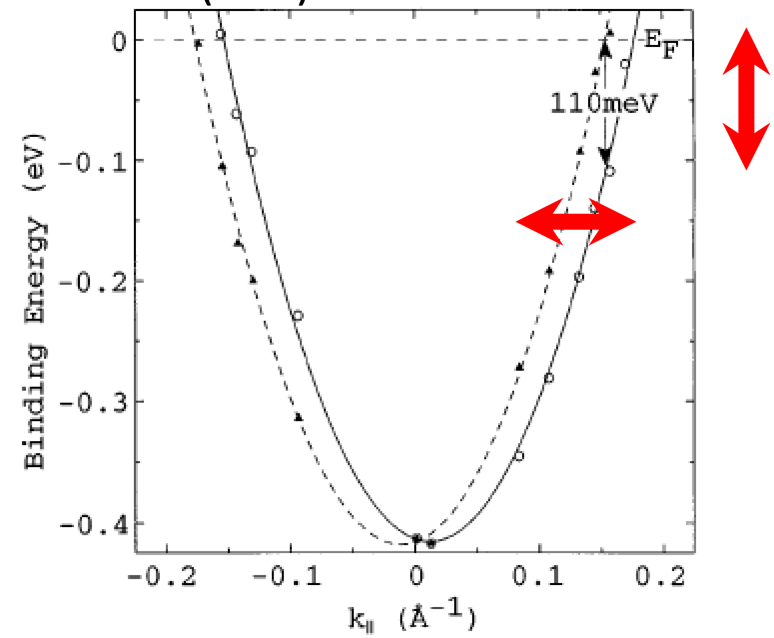

- High resolution

Lashell et al., Phys. Rev. Lett. 77, 3419 (1996)

PES: Angle Resolved Photoelectron Spectroscopy

(5-5-4) Spin-orbit interaction 2

$$H_{\mathrm{SOI}} = \frac{\hbar}{4m^2c^2}\vec{\sigma}\cdot\left\{\left(\vec{\nabla}V(\vec{r})\right)\times\vec{p}\right\}$$

$$= \frac{\hbar}{4m^2c^2}\left\{\left(-\frac{\partial V}{\partial z}\right)\left(\sigma_x p_y - \sigma_y p_x\right) + \sigma_z\left(\frac{\partial V}{\partial x}p_y - \frac{\partial V}{\partial y}p_x\right) + \left(\sigma_x\frac{\partial V}{\partial y} - \sigma_y\frac{\partial V}{\partial x}\right)p_z\right\}$$

Normal Rashba term

General Rashba term **Effective in-plane potential gradient**

Spin-orbit interaction (Rashba term + damping rate term)

(5-5-5) Electric field effects in electronic structures of the surface/interface

- Stark effect

$$H_{\mathrm{ED}} = -e\vec{r} \cdot \vec{E}_{\mathrm{ext}}$$

Electric dipole

Orbital coupling between the states of different angular quantum number $\Delta\ell = \pm 1$.

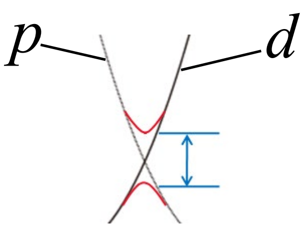

- Rashba (SOI) effect

$$H_{\mathrm{SOI}} = -e\frac{\hbar}{4m^2c^2}\left(\vec{\sigma} \times \vec{p}\right) \cdot \vec{E}_{\mathrm{ext}}$$

Modification of the Rashba effect.

- Electron depletion (accumulation)

When imposing the EF, for PDOS ~ 1 states/eV

Induced change in the number of electrons ~0.01 ~0.01 eV

Induced change in the number of electrons ~0.1 ~0.1 eV

by lattice constant, or modification surface/interface, etc.

(Appendix 9)
The other handouts 1: involving the dynamical control of magnetization

Trade-off property in magnetic memory

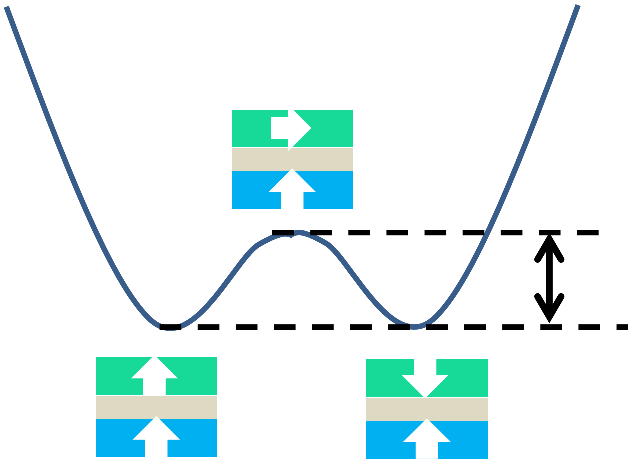

$K_U V$

- $K_U V$ becomes small, loosing memory
  = small thermo-stability
- $K_U V$ Becomes large, increasing the barrier for magnetization reverse
  = large threshold of magnetization reverse

Trade-off

One of necessary condition

Non-volatile

$$\Delta \geq 60$$ (ten years)

$$\Delta = \frac{K_U V}{k_B T}$$

$K_U V$: Magnetic anisotropy energy of magnetic memory

$k_B T$: Heat energy

- K_U Magnetic anisotropy energy per volume
- V Volume of magnet

Driving forces in dynamical control of magnetization

- **External magnetic field (by current)**
- **Injection of spin polarized current**

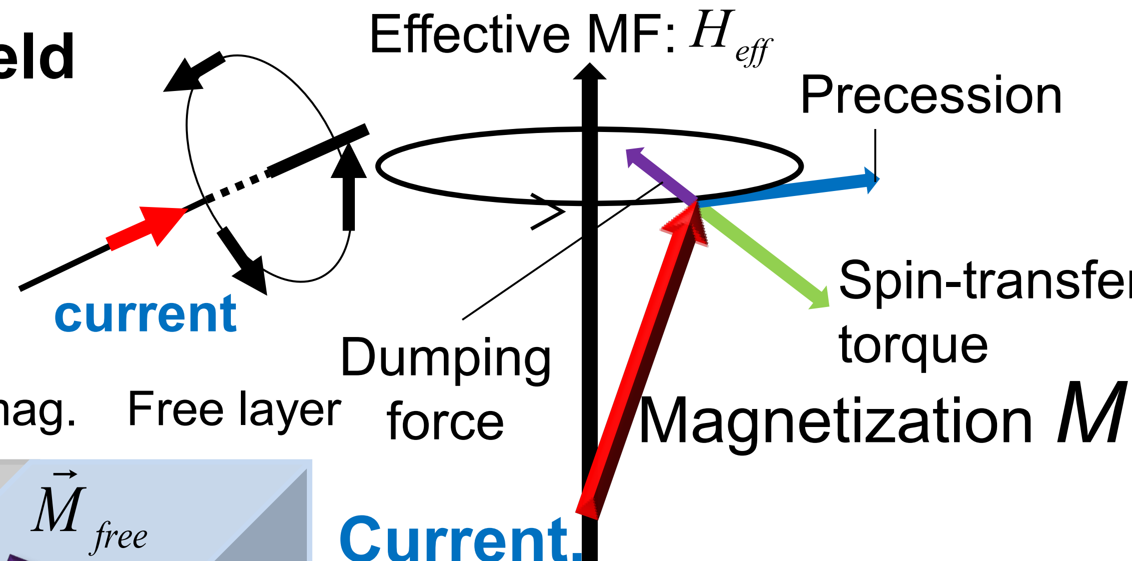

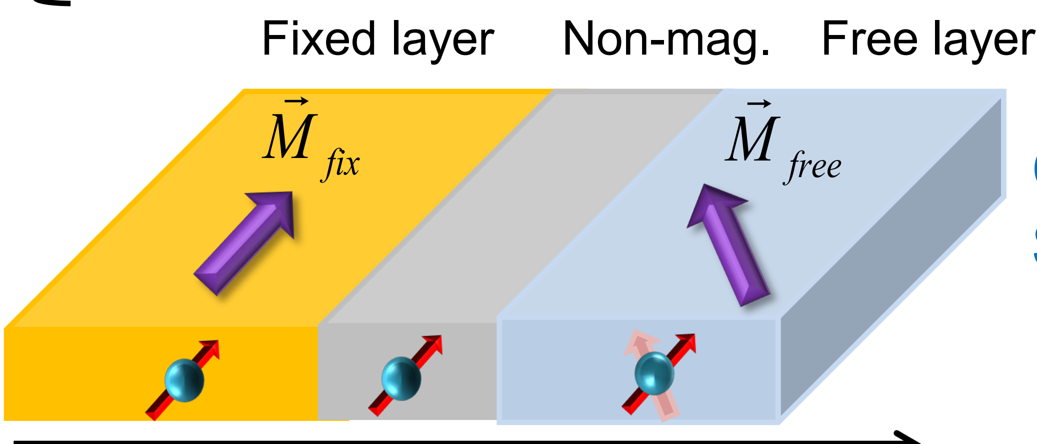

Spin polarized current

Conservation law of (spin) angular momenta

Current, Spin polarized current

Problem: Disturbing compactness, energy consumption, Joule heating, etc.

↓

Electric field (Voltage)

$$\vec{H}_{eff} = \vec{H}_{ext} + \vec{H}_{stt} + \vec{H}_{shape} + \vec{H}_{aniso}$$

Expectation: ultra-low energy consumption, non-volatile property, compactness(high density memory), enough high speed in reading&writing

Schematic diagram of magnetization reversal in imposing electric field

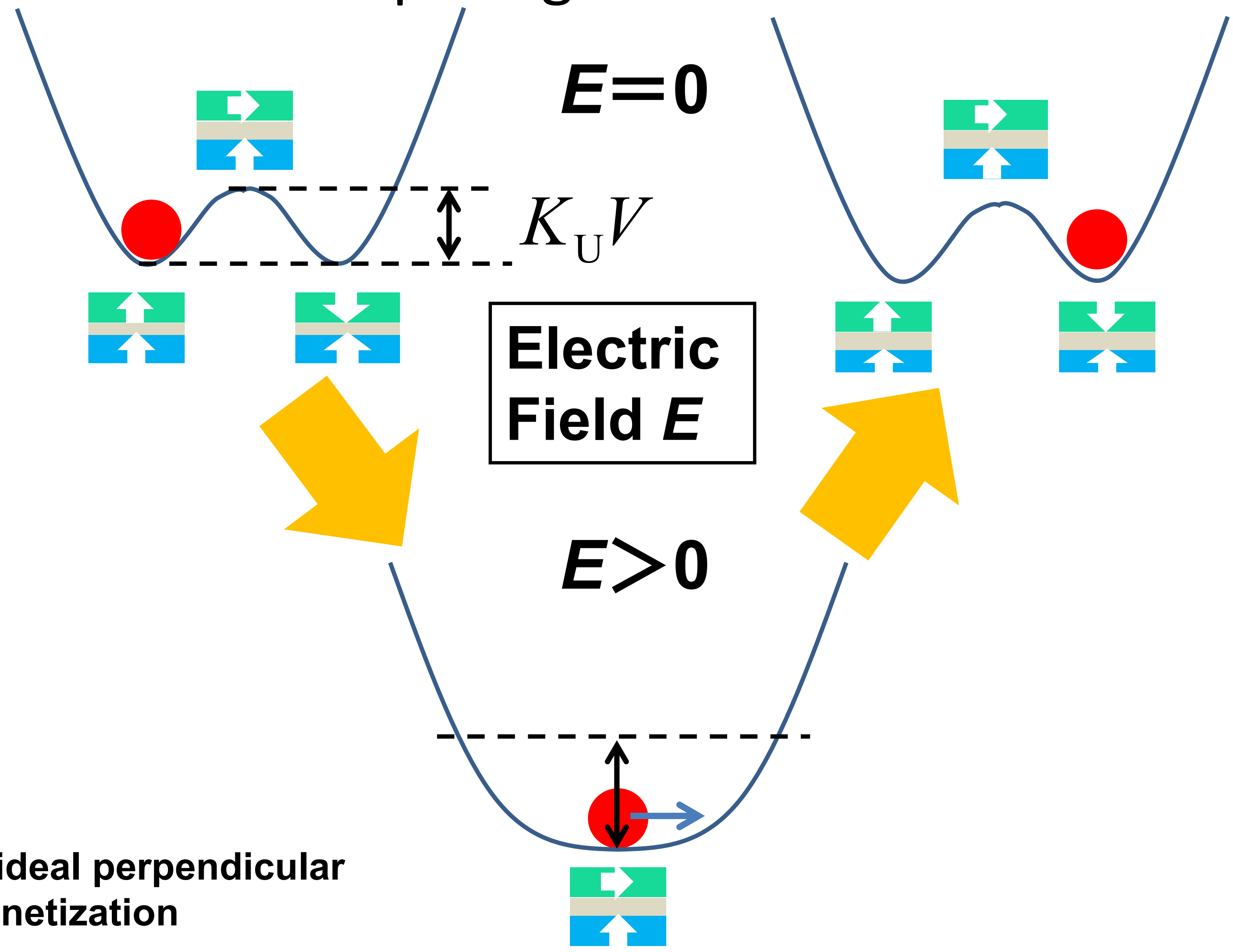

For ideal perpendicular magnetization

(5-9) Voltage-induced spin torque

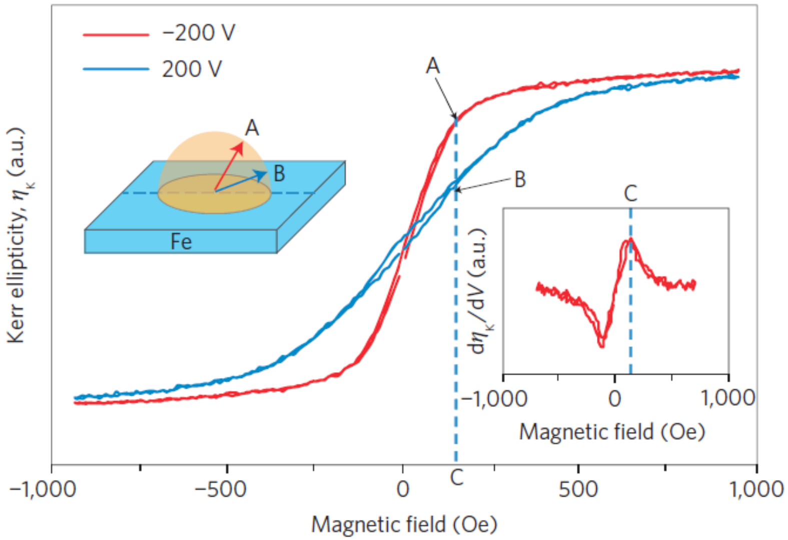

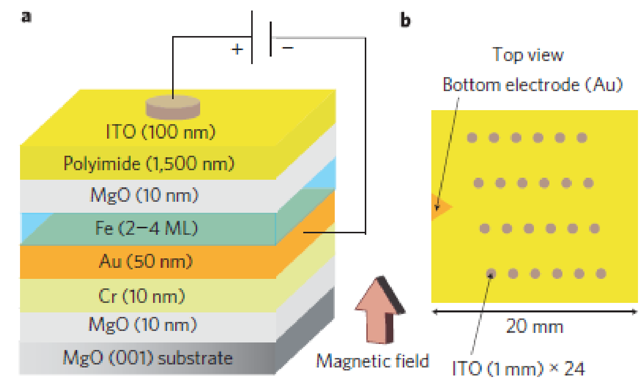

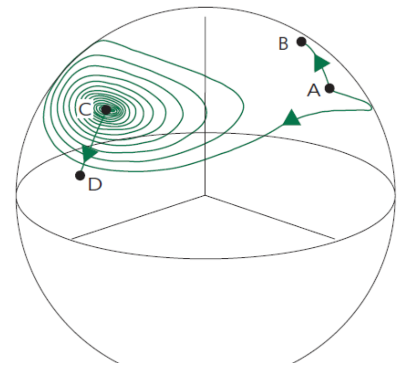

MgO/Fe/Au(001)

$$\frac{d\vec{M}}{dt} = \gamma\vec{M} \times \vec{H}_{eff} + \frac{\alpha\vec{M}}{M_s} \times \frac{d\vec{M}}{dt} \qquad \vec{H}_{eff} = -\frac{1}{\mu_0 M_s}\vec{\nabla}E_{mag}$$

$$E_{mag} = -\mu_0 M_z H_{ext} + \frac{1}{2}\underline{K_u(V)}\left(\frac{M_z}{M_s}\right)^2 + \frac{1}{2}K_{//}\left(\frac{M_x}{M_s}\right)^2$$

T. Maruyama et. al., Nature Nanotech. 4, 158 (2009)

(5-6) Spin transfer torque

Spin current produced in fixed layer → **Spin torque** provided to free layer

$$N_{\mathrm{stt}} = \frac{d\vec{M}_{\mathrm{free}}}{dt} \propto -I_{\mathrm{s}} \vec{M}_{\mathrm{free}} \times \left(\vec{M}_{\mathrm{free}} \times \vec{M}_{\mathrm{fix}} \right)$$

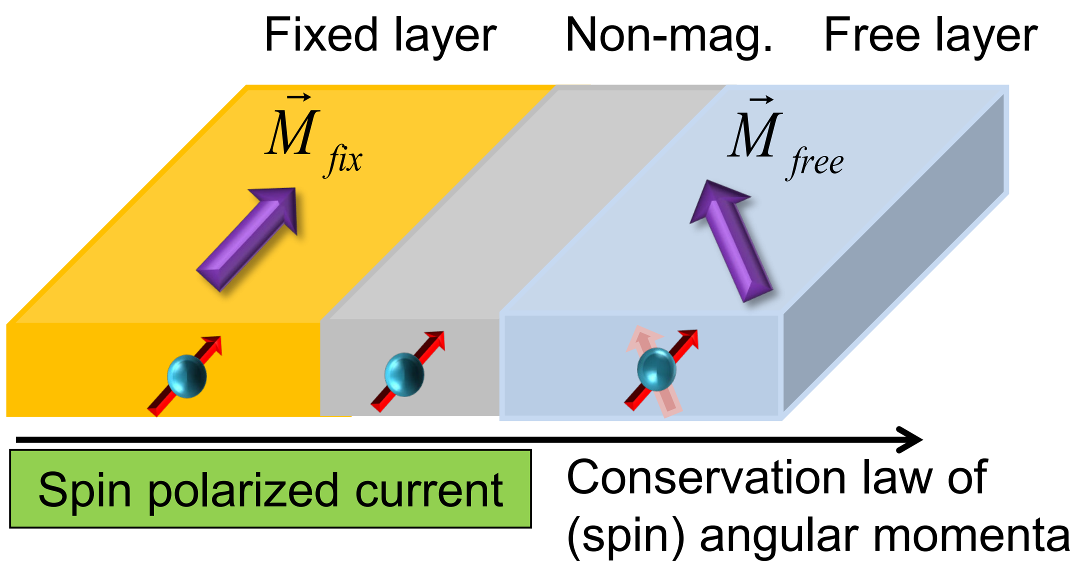

J.C. Slonczewski, J. Magn. Magn. Mater. 159, L1 (1996).

Dynamics of the magnetization on the free layer

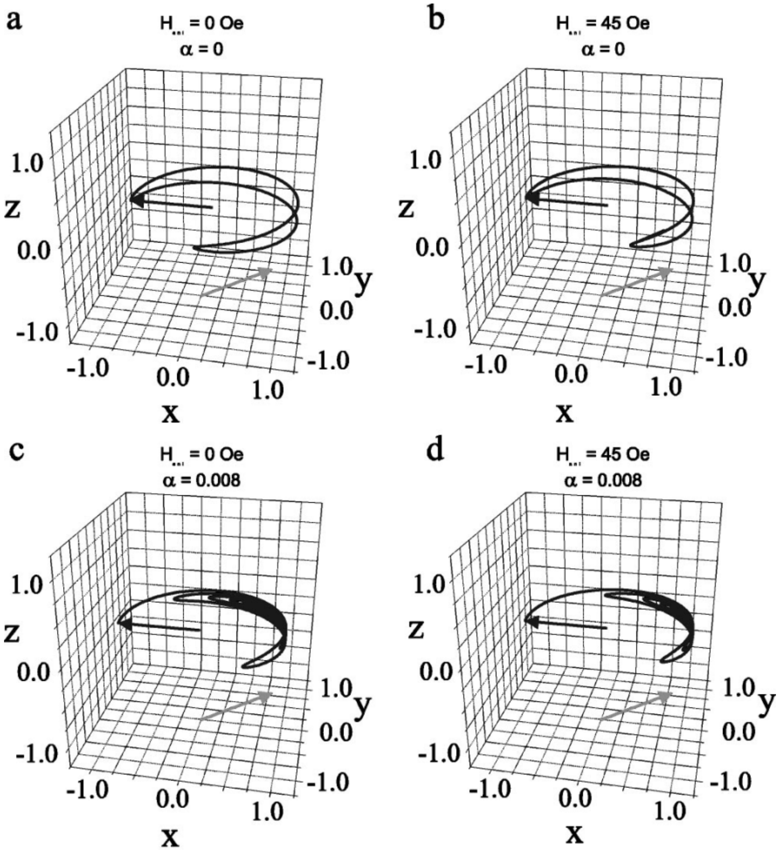

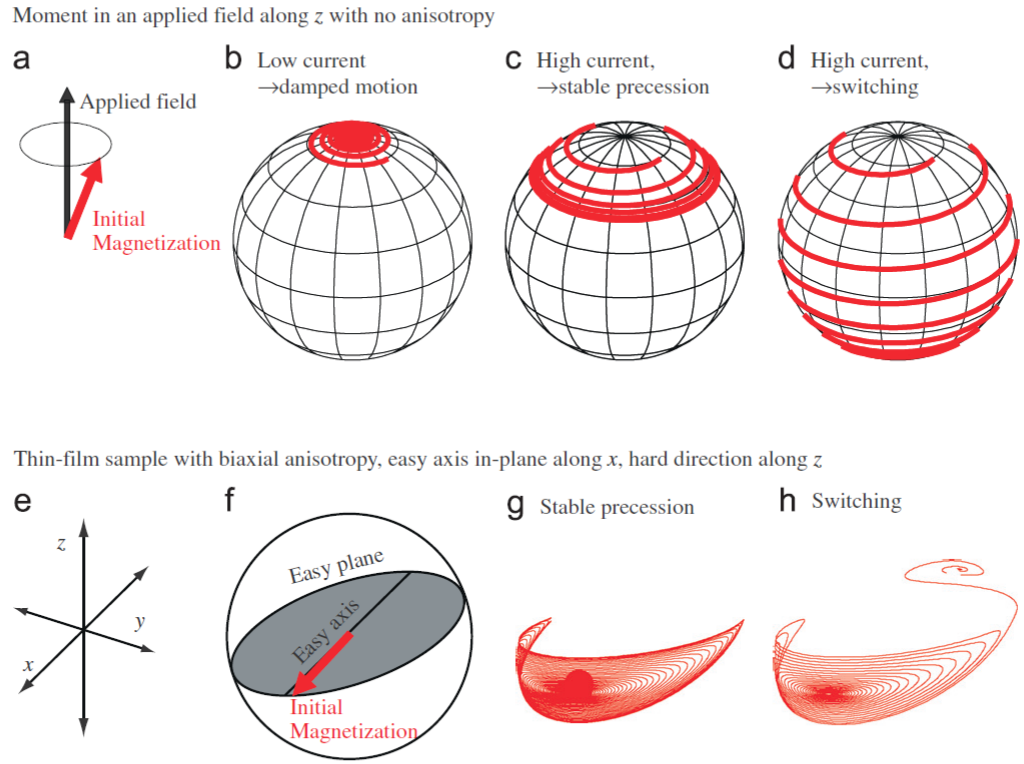

M. Bauer et al., Phy. Rev . B**61**, 3410-3416(2000)

D.C. Ralph, M.D. Stiles, J. Magn. Magn. Materials 320, 1190 (2008)

Shreshold current (derived from LLG equation）

$$I_c = \frac{2e}{\hbar}\frac{\alpha}{\eta(0)} V \mu_0 M_s \left(H + H_k + \frac{M_s}{2} \right) \propto \frac{\alpha}{\eta(0)} M_s$$

external anisotropy diamagnetism

V Free layer volume

α about 0.01

$$\eta(\theta) = \frac{q}{A + B\cos\theta}$$ Anisotropy function

θ : the angle between the directions of spin current and fixed magnetization M_s

D.C. Ralph, M.D. Stiles, J. Magn. Magn. Materials **320**, 1190 (2008)

(Appendix 10)
The other handouts

Elements for controlling the MAE and EF variation in thin magnetic layers

Magnetic materials and interfaces.

Fe　Fe/Pt　Fe/Pd　Fe/Au　MgO/Fe　Fe/Ni

MgO/FeCo　MgO/Co2FeAl (Huesler alloy)

Mn3Ga　Mn3Ge

L1-0 MnGa: K. Z. Suzuki et al., Scientific Reports, 6, 30249 (2016).

Number of magnetic layers, layer-stacking alignment, etc.

$(Fe_n/Ni_m)_\ell$

Ref.) K. Hotta et al., Phys. Rev. Lett., **110**, 267206 (2013).

Insulating materials: larger dielectric constant : ε_r

insulator/Fe

$\varepsilon_r(MgO) = 9.8 \approx 10$

Magnetic interaction with neighboring layers.

Exchange bias between ferro- and antiferr-magnets.

Threshold to magnetic anisotropy transition

Films	E_b (mJ/m^2)	E_s (mJ/m^2)	E_b+E_s (mJ/m^2)	MAE slope γ (fJ/Vm)	spin rotation EF (V/nm)
MgO/Fe/Pd(001)	0.36	-0.34	0.02	130	-0.2
MgO/Fe/Pt(001)	-1.18	-0.32	-1.50	615	2.4
MgO/Fe/Au(001)	0.96	-0.25	0.71	18	-40.2
MgO/Fe(2ML)/Au(001)	2.11	-0.57	1.54	-114	13.5
MgO/Pd/Fe/Au(001)	-0.68	-0.28	-0.96	-388	-2.5
MgO/Pt/Fe/Au(001)	1.52	-0.28	1.24	846	-1.5
MgO/Au/Fe/Au(001)	2.06	-0.26	1.80	-196	9.2
MgO/Pt/Fe(3ML)/Au(001)	0.69	-1.17	-0.48	633	0.8

$$\mathrm{MAE}(\varepsilon) \approx E_{\mathrm{b}} + E_{\mathrm{s}} + \gamma \Delta\varepsilon$$

$$\varepsilon_{\mathrm{c}} = -\left(E_{\mathrm{b}} + E_{\mathrm{s}}\right)/\gamma$$

M. Tsujikawa et al., JAP, **111**, 083910 (2012).

(5-1) Electronics structure: Ferromagnetism, Anti-ferromagnetism

One electron approx.

$$\left\{-\frac{\hbar^2}{2m}\nabla^2 + V(\mathbf{r})\right\}\Psi_{n\mathbf{k}\sigma}(\mathbf{r}) = \varepsilon_{n\mathbf{k}\sigma}\Psi_{n\mathbf{k}\sigma}(\mathbf{r})$$

$(n\mathbf{k}\sigma)$: quantum number

$\Psi_{n\mathbf{k}\sigma}(\mathbf{r})$: wave function

$\varepsilon_{n\mathbf{k}\sigma}$: eigenvalue

n : band index

$\mathbf{k}$: wave number

σ : spin index $(\sigma = \uparrow, \downarrow)$

Band dispersion

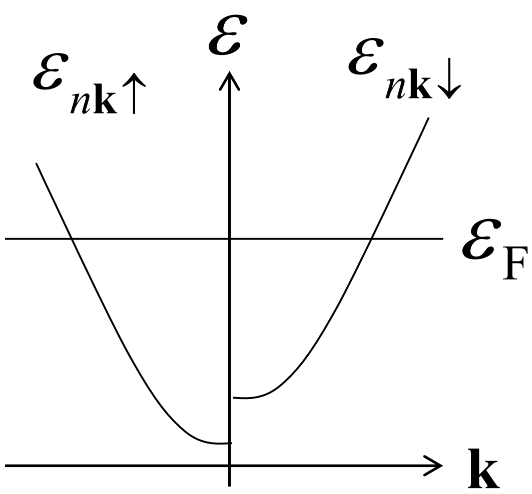

<u>Ferromagnet(F)</u>

$$\varepsilon_{n\mathbf{k}\uparrow} \neq \varepsilon_{n\mathbf{k}\downarrow}$$

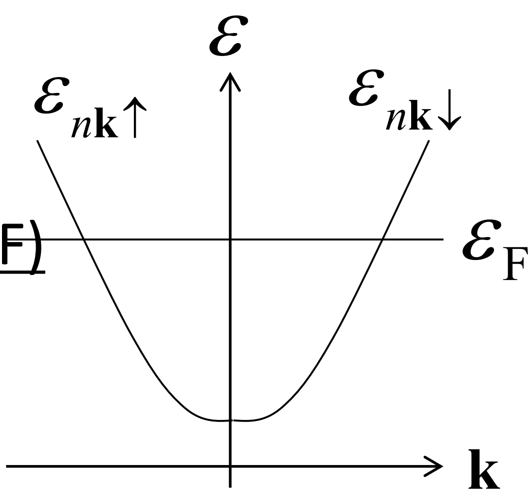

<u>Anti-Ferromagnet(AF)</u>

$$\varepsilon_{n\mathbf{k}\uparrow} = \varepsilon_{n\mathbf{k}\downarrow}$$

(5-1-2) Electronics structure: Density of states

Density of states(DOS)

$$n(\varepsilon) = \sum_{\sigma} \sum_{n\mathbf{k}} \delta(\varepsilon - \varepsilon_{n\mathbf{k}\sigma})$$

$$n_{\sigma}(\varepsilon) = \sum_{n\mathbf{k}} \delta(\varepsilon - \varepsilon_{n\mathbf{k}\sigma})$$

σ : spin index $\left(\sigma = \uparrow, \downarrow\right)$

Spin-up state   Spin-down state

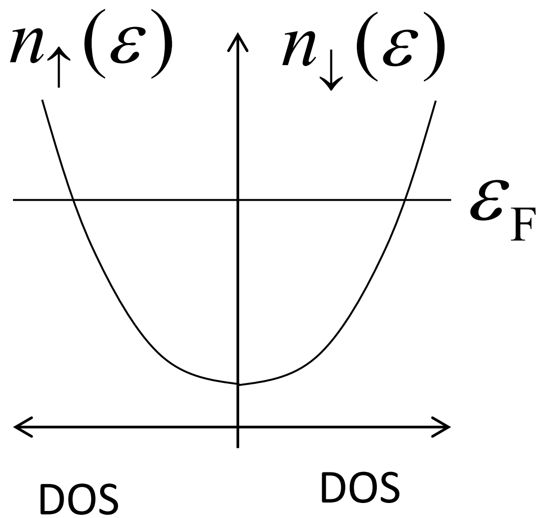

[states/(energy unit)/cell]

Ferromagnet(F)

Majority spin state   Minority spin state

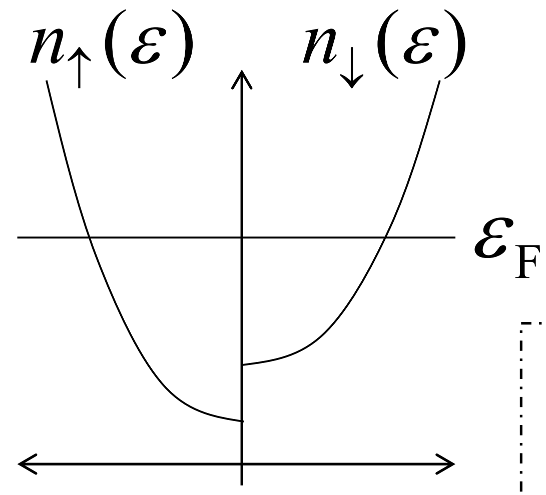

Effective potential $V(\mathbf{r})$

Anti-Ferromagnet(AF)

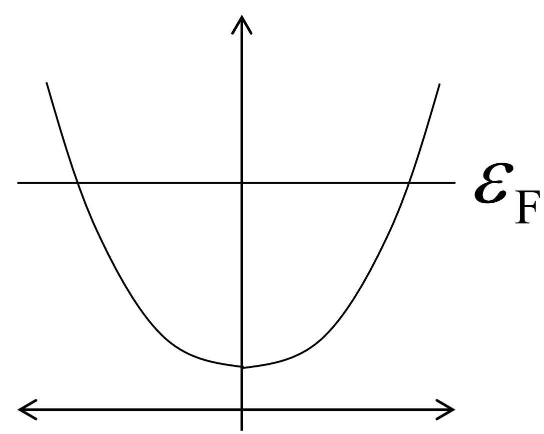

Design on magnetic anisotropy in magnetic materials

- **Parameters for controlling MAE and its EF effect**

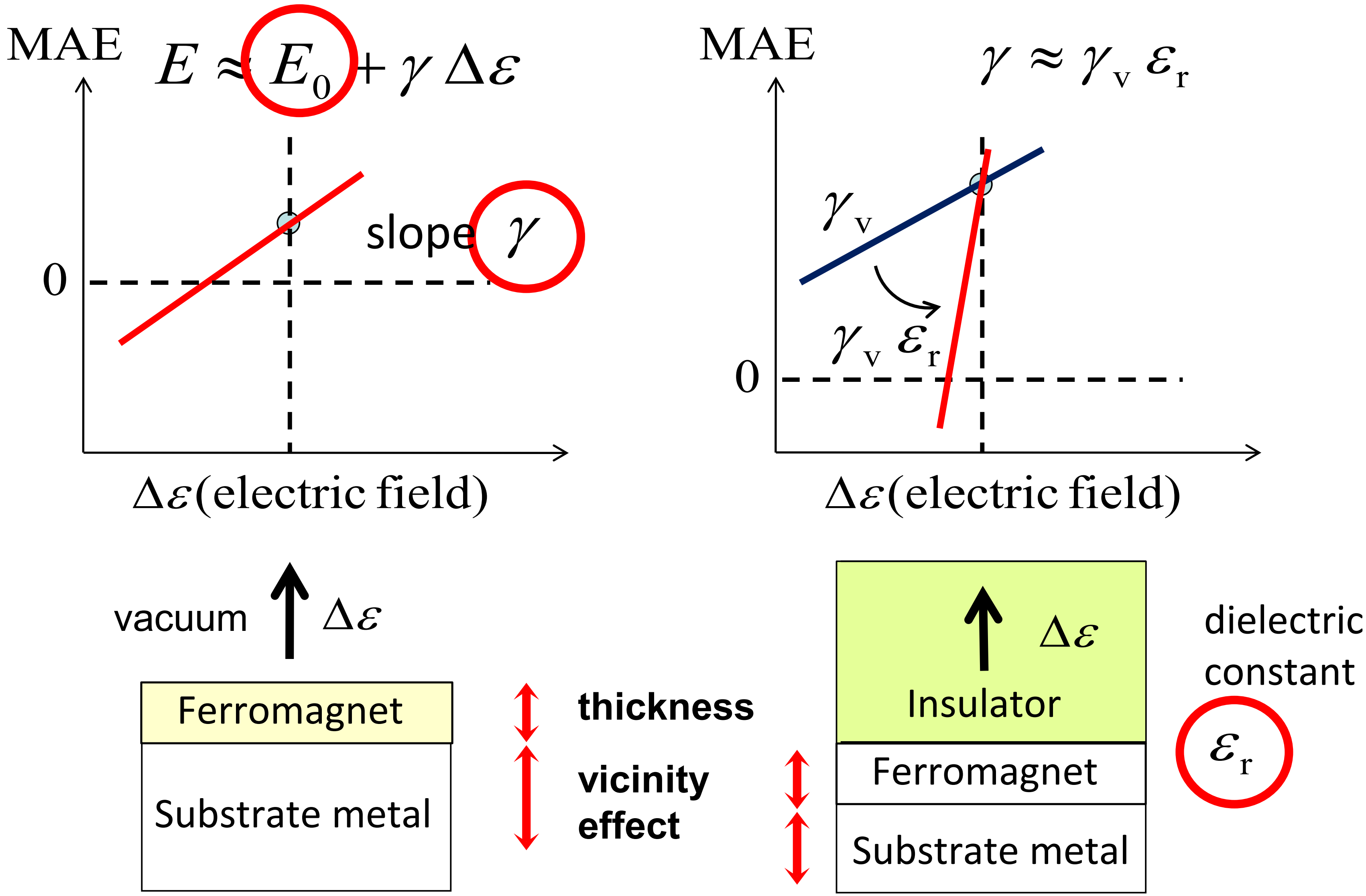

Proto-type of the magnetic device for a voltage driven MRAM

Magnetization switching using voltage pulse

Y. Shiota, T. Nozaki, F. Bonell, S. Murakami, T. Shinio and Y. Suzuki. Nat. Mat.. **11**. 39(2012)

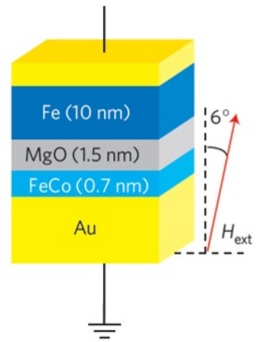

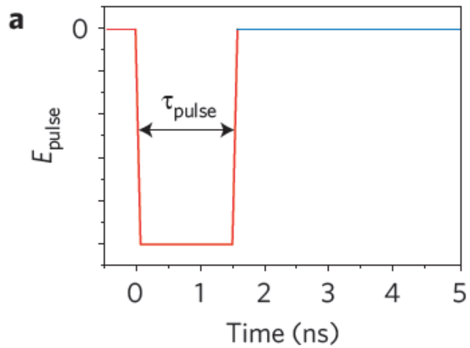

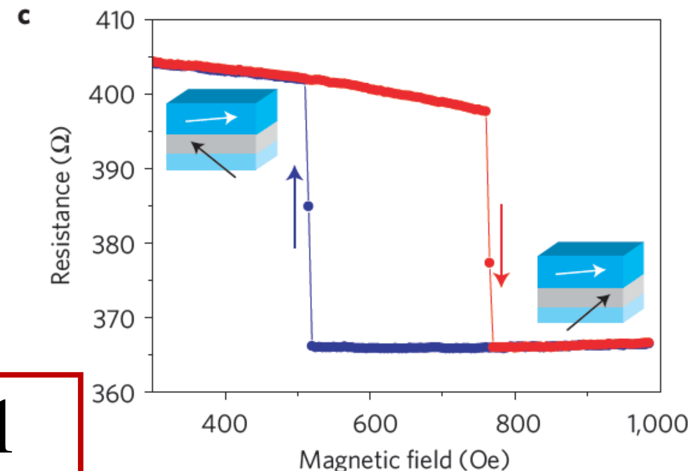

Consumption energy ratio with respect to a typical device of spin-transfer-torque driven MRAM(similar scale)

$$\frac{1}{500}$$

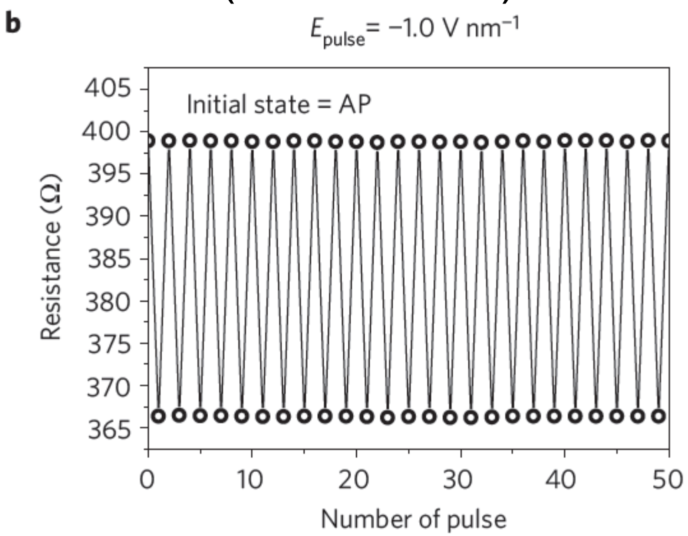

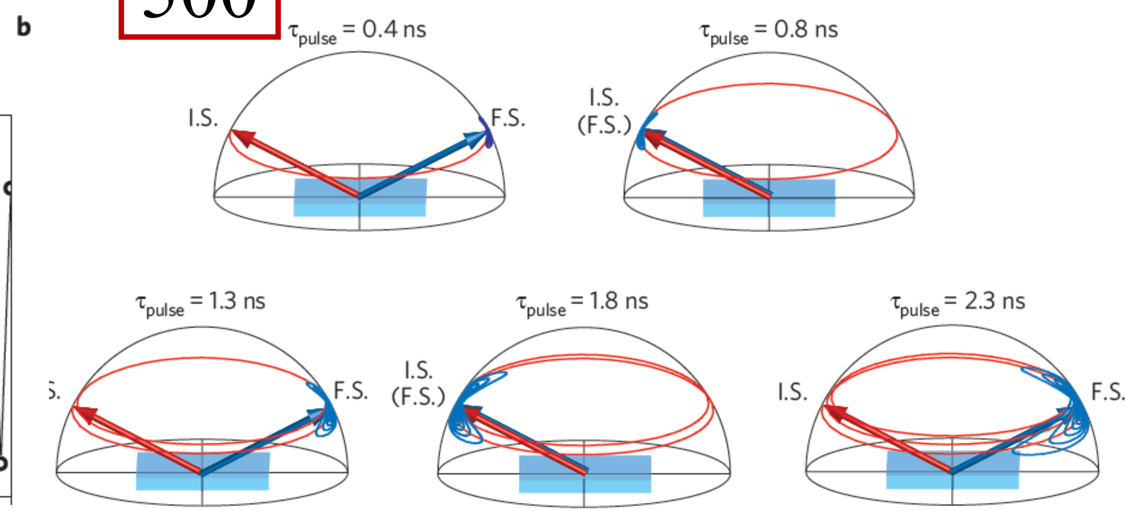

Macro-spin model simulation

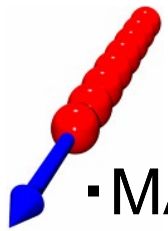

example: Isolated iron chain

- MAE=3.23 meV/Fe

red: mag. perpendicular to the axis

blue: mag. parallel to the axis

- Easy axis: parallel to the chain-axis (z direction).

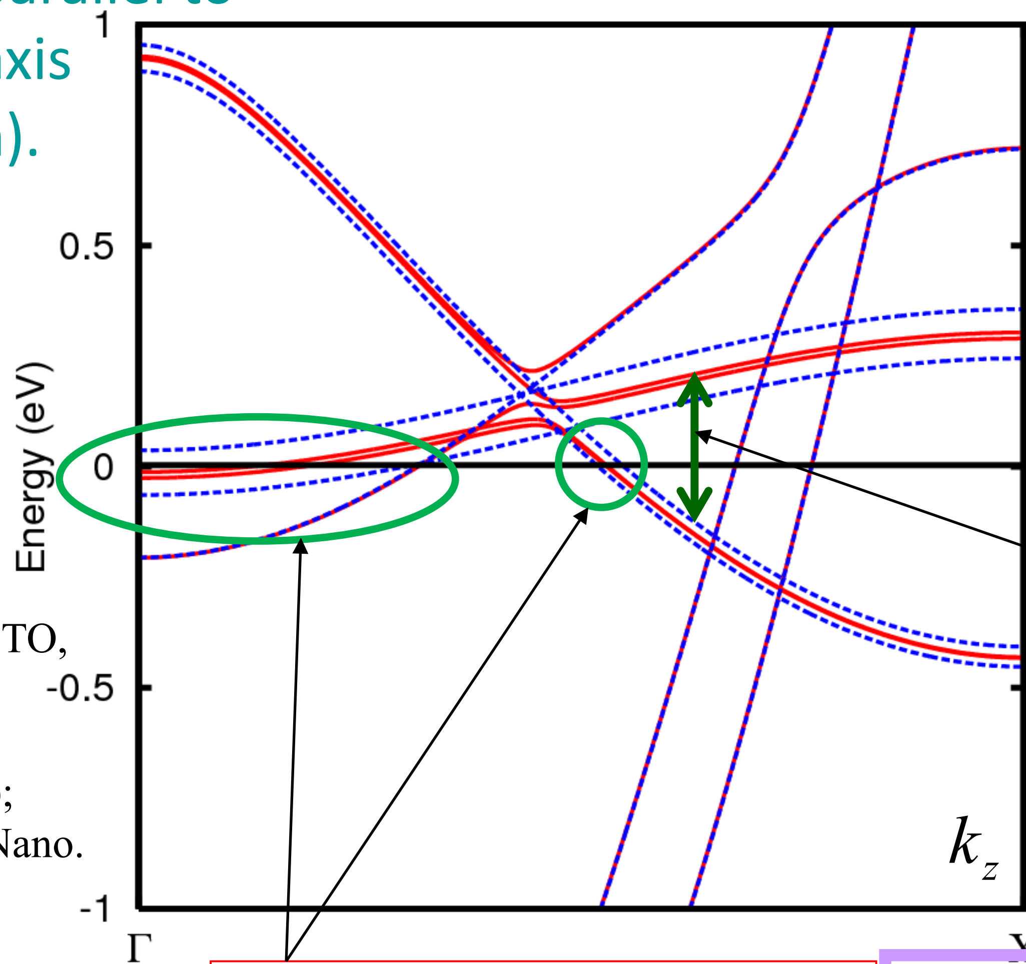

$3z^2-r^2$ $(m=0)$

xy, x^2-y^2 $(m=\pm 2)$

xz, yz $(m=\pm 1)$

contribution to the perpendicular

contribution to the parallel

$\xi m \cos\theta$

ℓ_z $\Delta m = 0$

ℓ_x $\Delta m = \pm 1$

M. Tsujikawa and TO, J. Phys.: Condens. Matter, **21**, 064213 (2009); J. Compt. Theor. Nano. **6**, 2597 (2009).

dipole: 0.05meV/Fe

Magnetic dipole-dipole interaction (MDDI)

Classical magnetic interaction

$$E_{ij}^{\text{dipole}} = \frac{\boldsymbol{\mu}_i \cdot \boldsymbol{\mu}_j - 3(\boldsymbol{\mu}_i \cdot \hat{\mathbf{R}}_{ij})(\boldsymbol{\mu}_j \cdot \hat{\mathbf{R}}_{ij})}{R_{ij}^3}$$

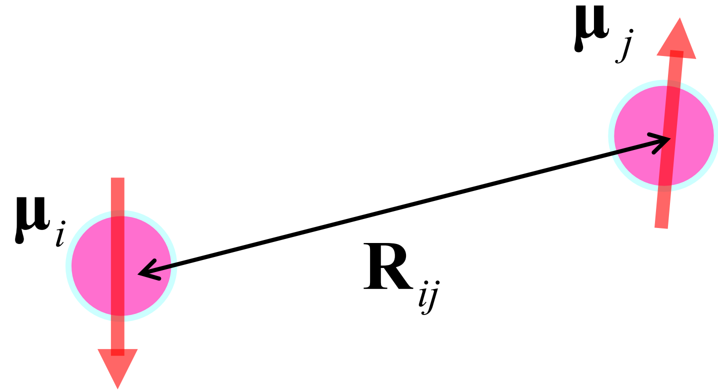

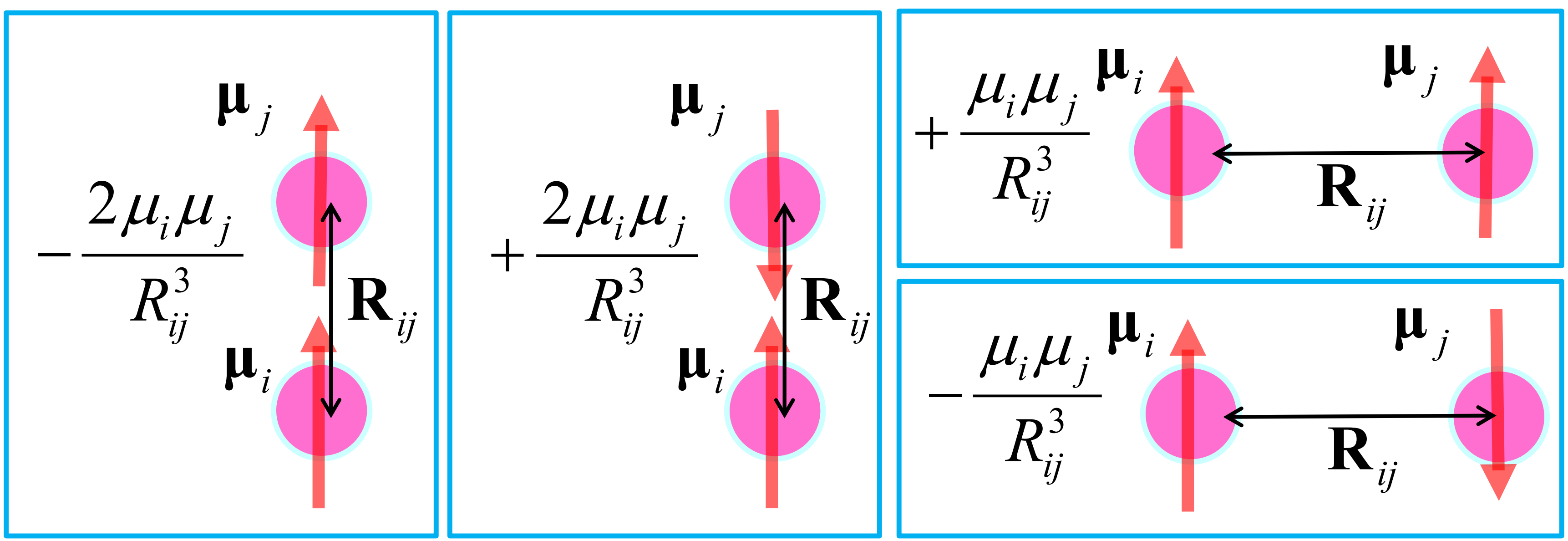

MDDI: Ferromagnetic 1D-chain and 2D-square lattice

- 1D-chain

$$E_{\rm dd}(\theta)=\frac{e^2}{4m^2c^2}\frac{C_{\rm M}\mu^2}{a^3}\left(\frac{3}{2}\cos^2\theta-\frac{1}{2}\right)$$

$C_{\rm M}=4.804$

μ : Magnetic moment in $\mu_{\rm B}$

a : Lattice constant in $a_{\rm B}$

$E_{\rm dd}(\theta)[{\rm Ryd}]$ $\quad m=e=1 \quad c=137.$

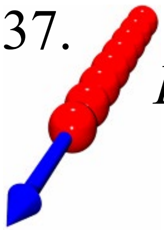

$E_{\rm MAE}^{\rm dd}=0.08\ {\rm meV/Fe}$

$\mu=3\,\mu_{\rm B} \quad a=2.77\ \text{Å}$

- 2D-dimensional case

2D Madelung constant approach

Ref.) L. Szunyogh et al., Phys. Rev. B, **51,** 9552, (1995)

2D square lattice

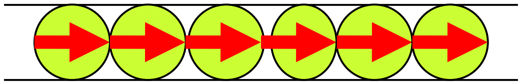

$E_{\rm MAE}^{\rm dd}=0.15\ {\rm meV/Fe}$

$\mu=3.1\mu_{\rm B}$

$a=2.87\ \text{Å}$

$$E_{\rm dd}(\theta)=\frac{e^2}{4m^2c^2}\frac{C_{\rm M}\mu^2}{a^3}\left(\frac{3}{2}\cos^2\theta-\frac{1}{2}\right)$$

$C_{\rm M}=9.03362$

μ : Magnetic moment in $\mu_{\rm B}$

a : Lattice constant in $a_{\rm B}$

$E_{\rm dd}(\theta)[{\rm Ryd}]$ $\quad m=e=1 \quad c=137.$

MDDI: Antiferromagnetic 2D-square lattice

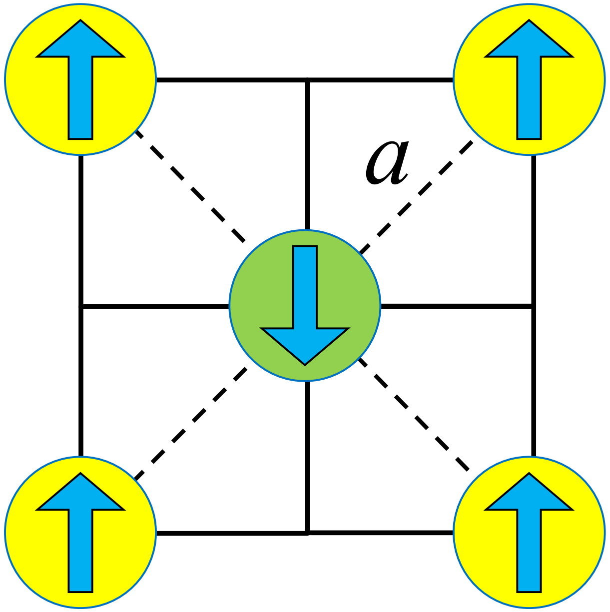

Perpendicular anisotropy

$$E_{\mathrm{MAE}}^{\mathrm{dd}} = -0.082 \text{ meV/Mn}$$

$$\mu = 4.2\mu_{\mathrm{B}}$$

$$a = 2.83 \text{ Å}$$

Note)

$$E_{\mathrm{MAE}}^{\mathrm{dd}} = -0.175 \text{ meV/Mn (SDA)}$$

SDA: Spin density approach (see Appendix 7).

TO, I. Pardede et al, IEEE Trans. Magn., 55(2), Art. Num. 1300104, (2019).

MAE of Fe-chain/Pt(664) surface

-3.23 meV/Fe

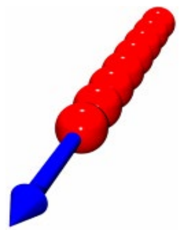

bare Fe-chain

parallel to the chain

-2.25 meV/Fe

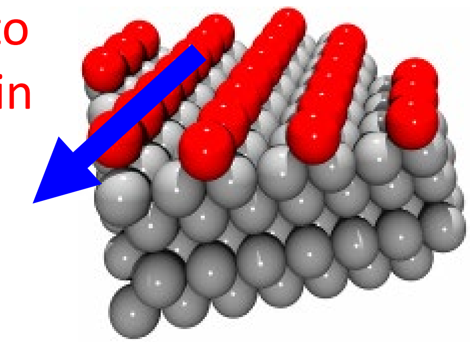

Fe-chain/Pt(111)

1.19 meV/Fe

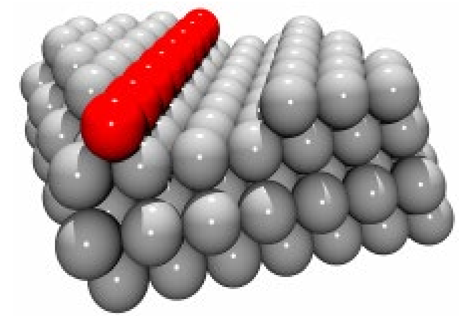

Fe-chain/Pt(664)

perpendicular to the chain

hybridization of 3*d* orbitals between Fe and Pt atoms

yz orbital

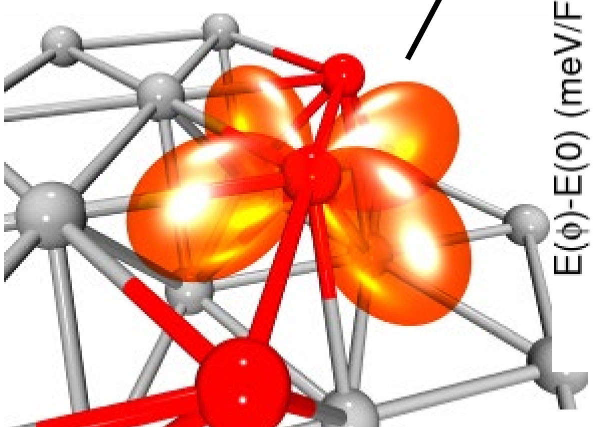

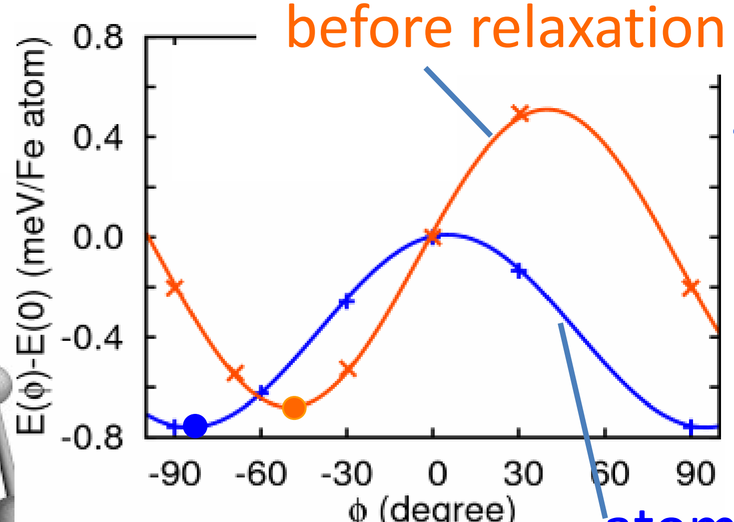

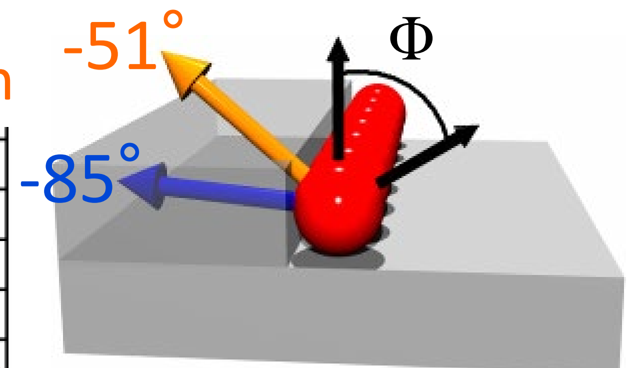

exp. -80°
(Repetto et al., 2006)

M. Tsujikawa A. Hosokawa, and TO, Phys. Rev. B, 77 (2008) 054413

A1-5. Applying the electric field (EF) on iron chain

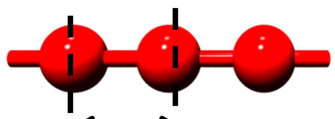

5.23a.u（2.77Å）

Atomic distance in the chain on Pt(111)

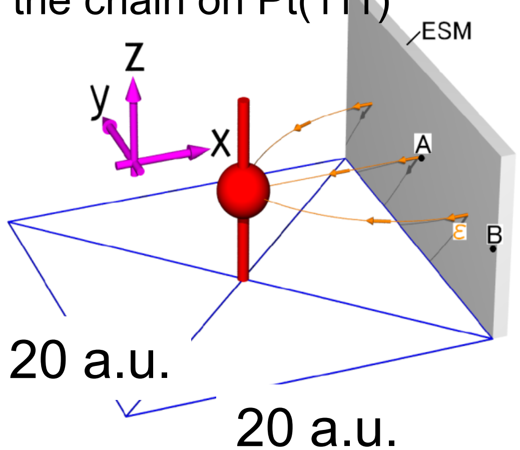

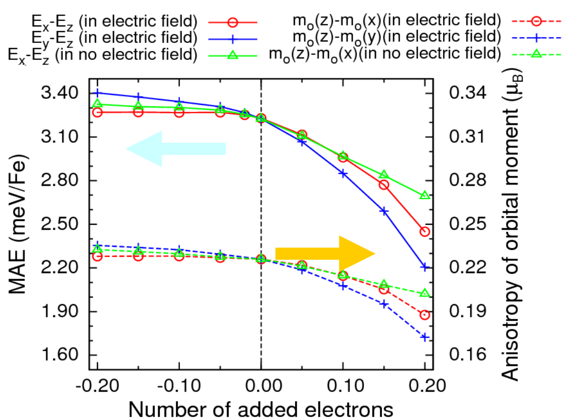

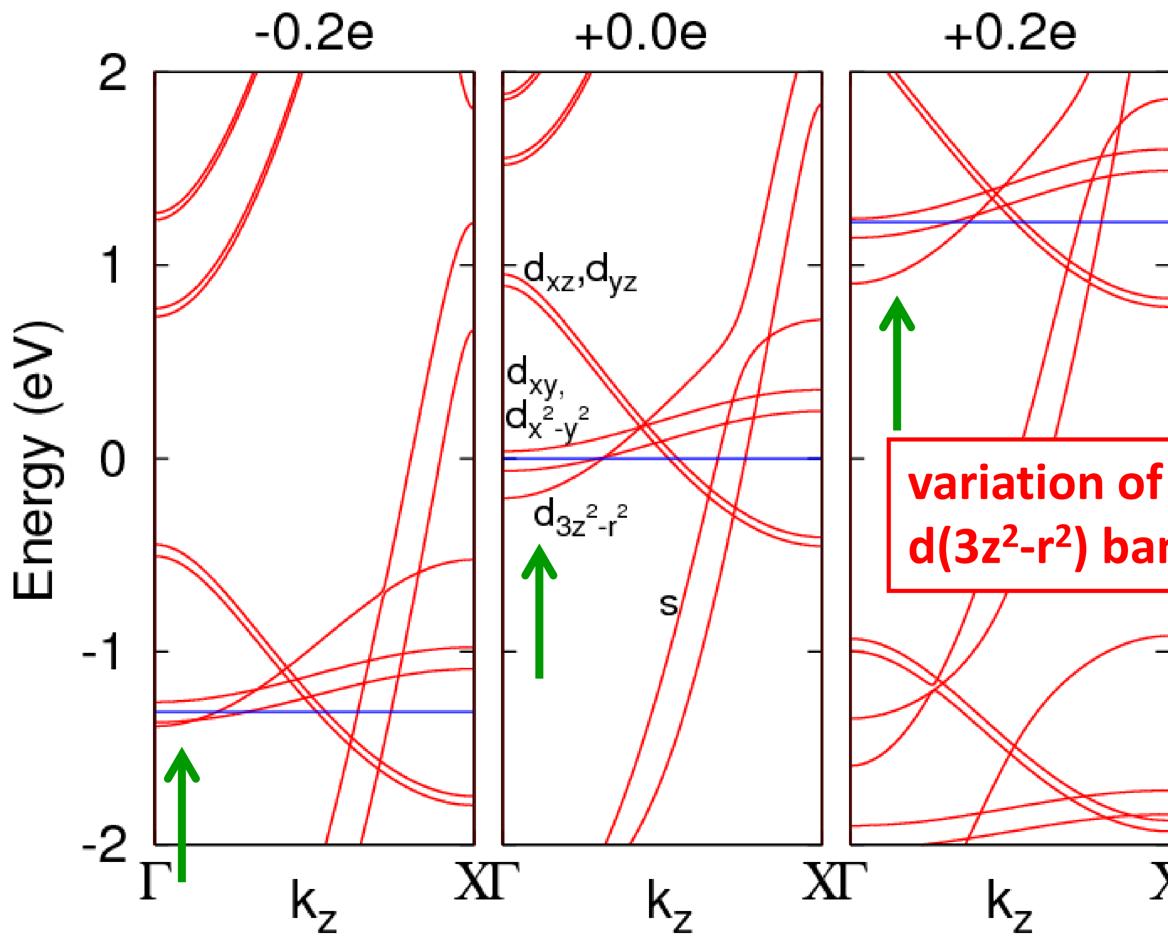

variation of $d(3z^2-r^2)$ band

EF dependence depends on the orbital direction

↓

causes variations of MAE

M. Tsujikawa and TO, J. Phys.: Condens. Matter, **21**, 064213 (2009)

A1-6. Imposing the electric field (EF) on iron chain (part 2)

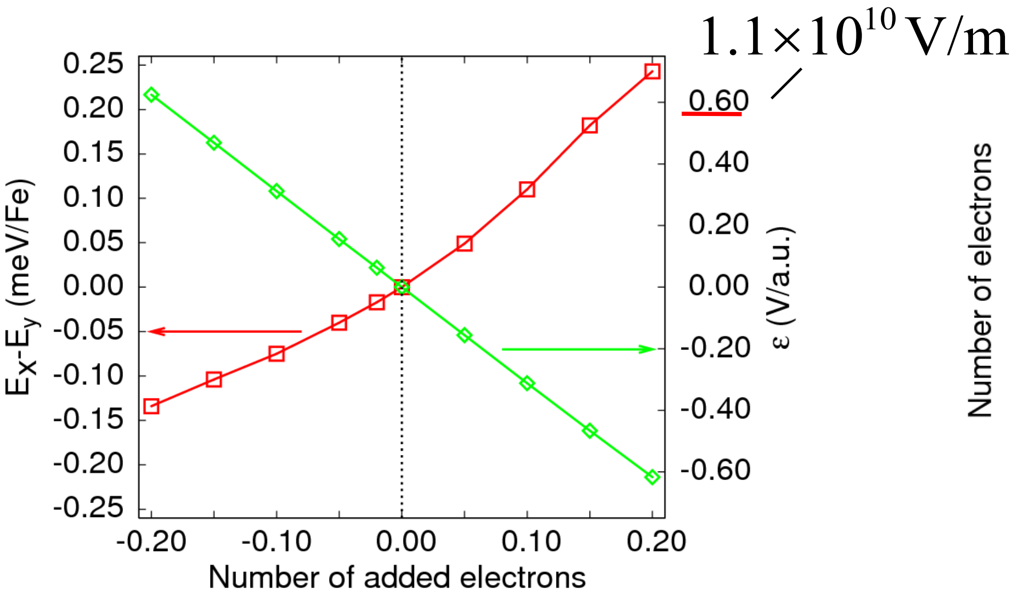

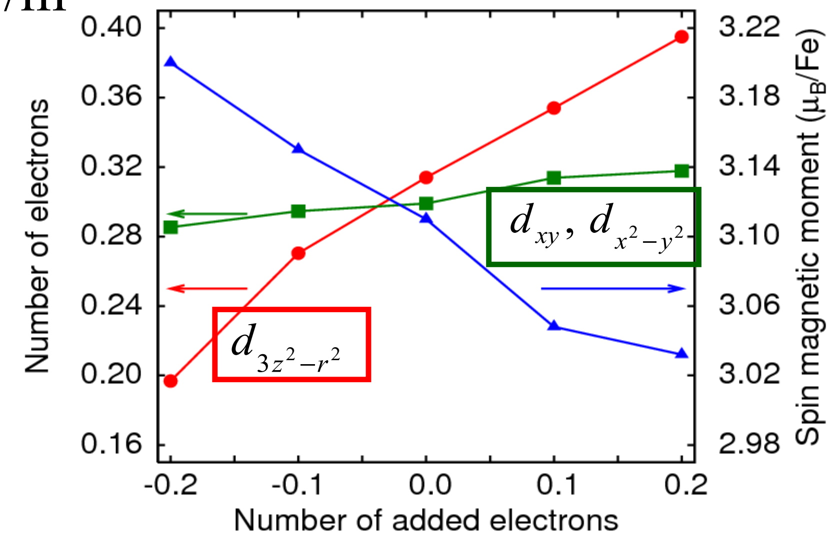

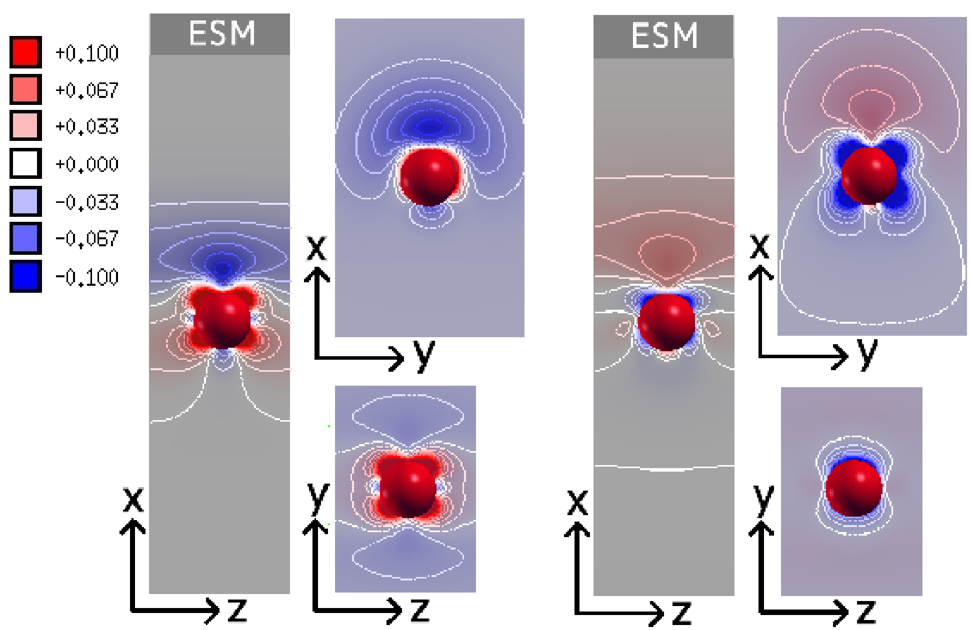

Voltage-Controlled Magnetic Anisotropy:

- **A few examples**

MAE and EF effects(comparison with exp.)

S. Haraguchi et. al., J. Phys. D: Appl. Phys. **44**, 064005 (2011).

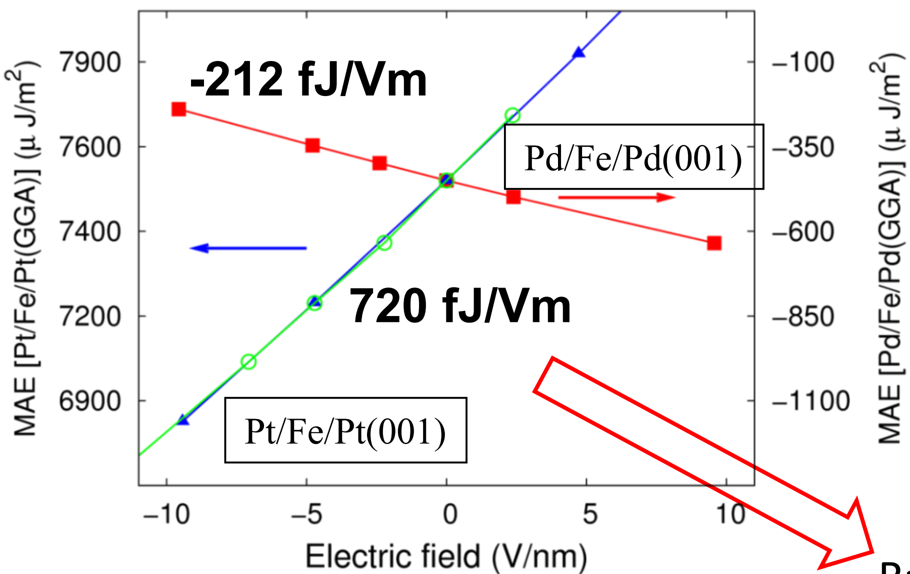

M. Weisheit et. al., Science **315**, 349 (2007).

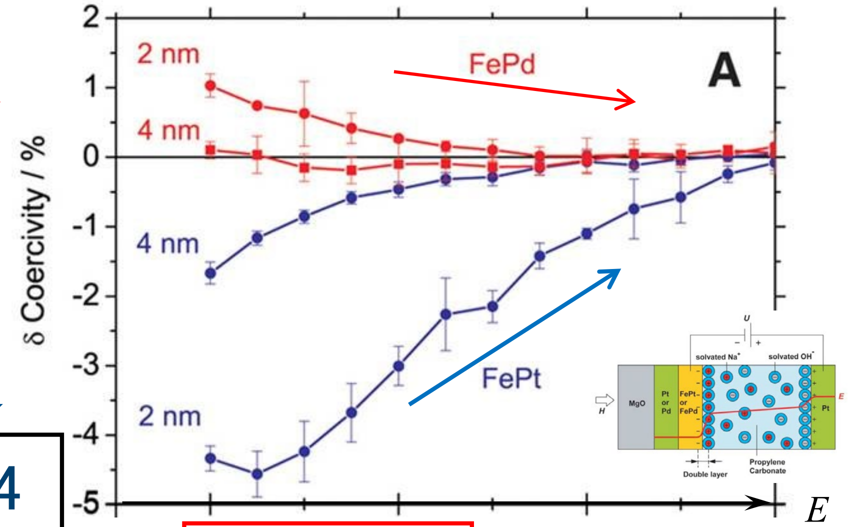

Ratio of slopes $\frac{\gamma_{\mathrm{Pd}}}{\gamma_{\mathrm{Pt}}} \approx -0.27$

➢Pd/Fe/Pd(001)

MAE: -425 μJ/m² (*E*=0.0 V/nm)

EF-effect: -21.2 fJ/Vm

➢experiment

EF-effect: -602 fJ/Vm

F. Bonell et al., APL, **98**, 232510(2011).

MgO $\varepsilon_r \approx 10$ (low frequency limit)

EF-effect=-21.2 × 10 fJ/Vm=-212 fJ/Vm

⇕ **comparable**

-602 fJ/Vm (exp.)

These signs of slopes and the ratio are in good qualitative agreement with the available experimental data.

EF-Induced modulation on density

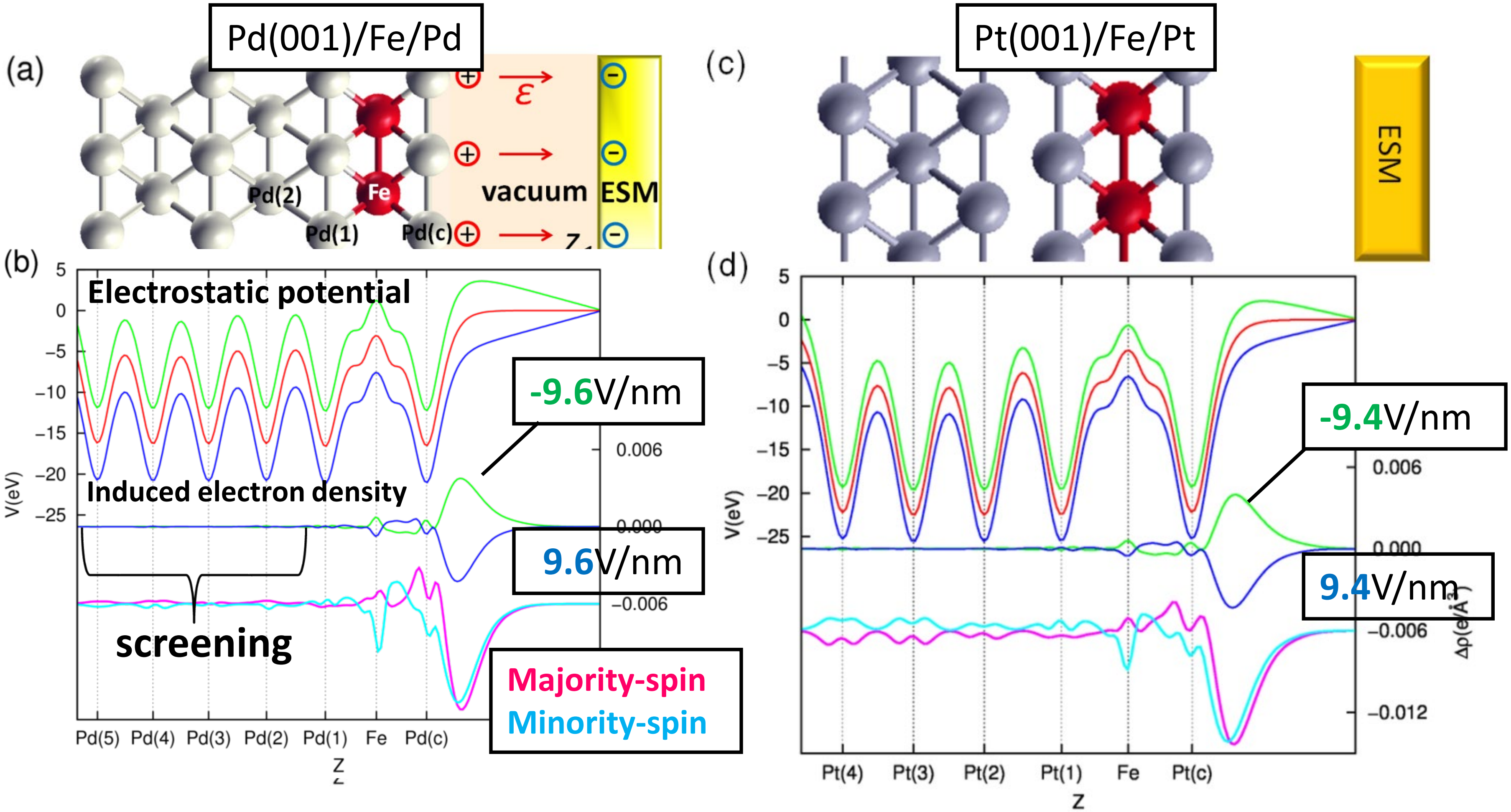

- ➢The electric field is screened in a few number of surface layers.
- ➢In these layers, EF effects are induced.

S. Haraguchi et. al., J. Phys. D: Appl. Phys. **44** (2011) 064005.

Effective Screening Medium(ESM method): Otani et al., PRB **73**,115407 (2006).

Electric field dependence of MAE in Pt(001)/Fe/Pt/MgO film

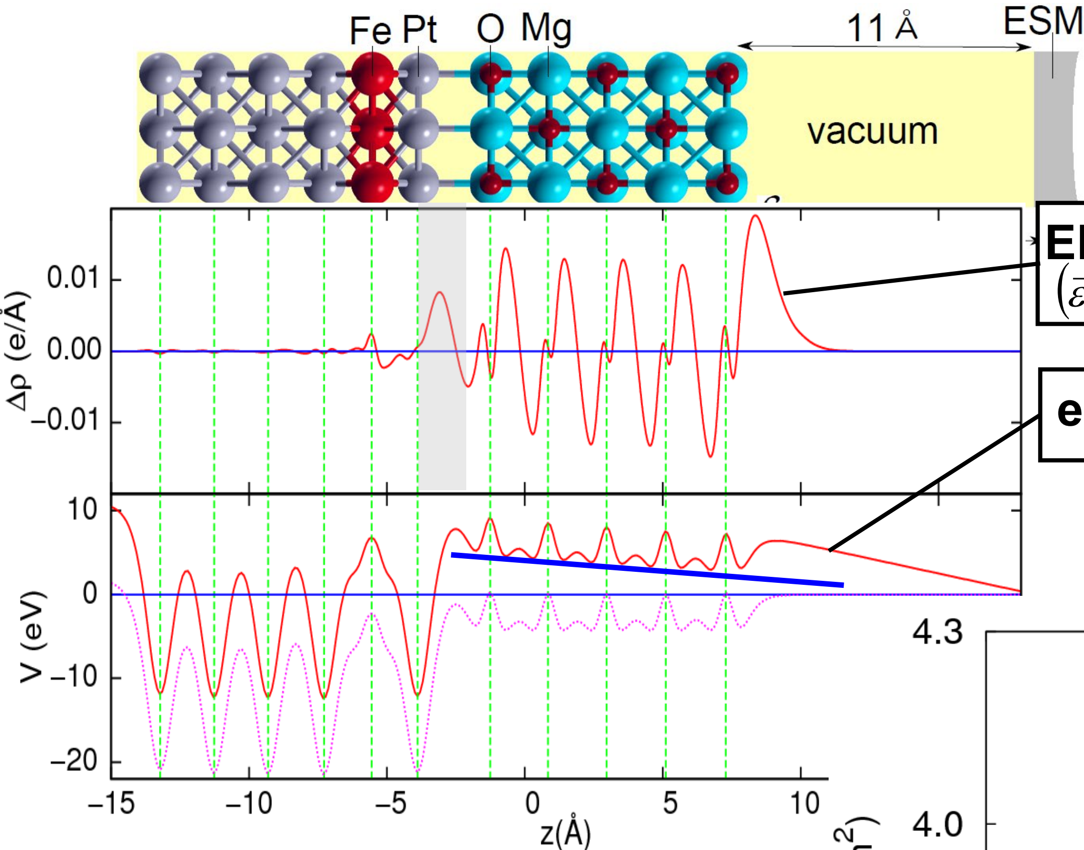

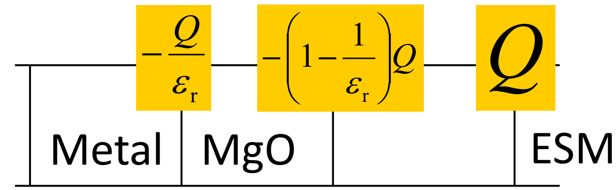

EF-induced electron density
$\left(\vec{\varepsilon} = -0.22\mathrm{V/Å}\right) - \left(\vec{\varepsilon} = 0.00\mathrm{V/Å}\right)$

electrostatic potential $\left(\vec{\varepsilon} = -0.22\mathrm{V/Å}\right)$

In MgO layers, the applied EF 3.3 times smaller than vacuum

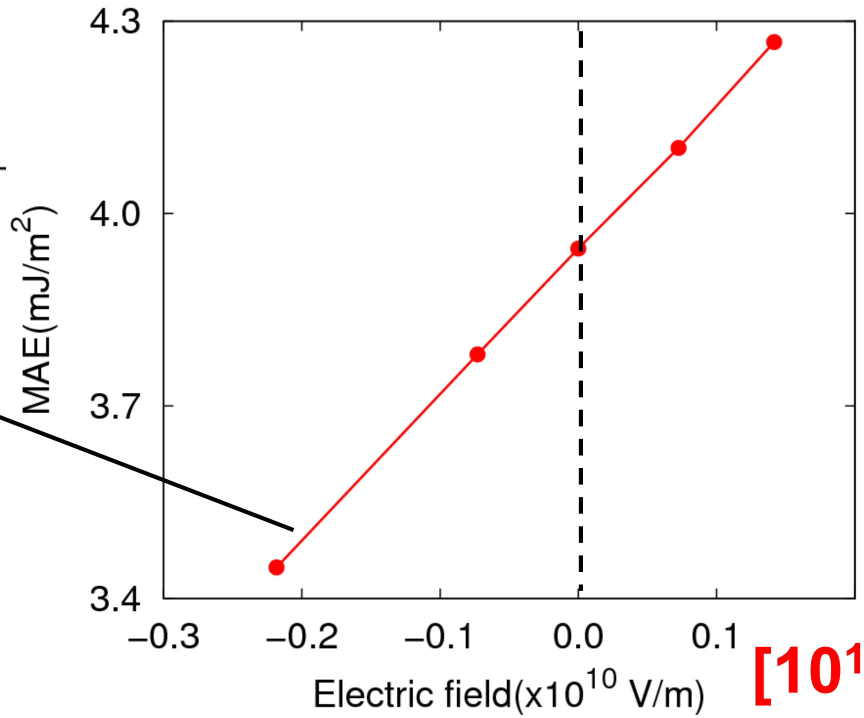

[10^{10} V/m]

slope: 227 fJ/Vm

3.1 times larger than that in Pt/Fe/Pt(001)(GGA) (74 fJ/Vm)

740 fJ/Vm